A DISSERTATION ON

"MYOCARDIAL MAPPING IN EVALUATION OF MYOCARDIAL DISEASES AND ASSESSING NORMATIVE VALUES IN CONTROLS"

Submitted to

THE TAMIL NADU Dr. M.G.R. MEDICAL UNIVERISTY

CHENNAI

In Partial Fulfilment of the Regulations

For the Award of the degree

M.D. DEGREE BRANCH VIII

RADIODIAGNOSIS

MADRAS MEDICAL COLLEGE,

CHENNAI.

MAY - 2019

CERTIFICATE

This is to certify that the dissertation titled **"MYOCARDIAL MAPPING IN EVALUATION OF MYOCARDIAL DISEASES AND ASSESSING NORMATIVE VALUES IN CONTROLS"** submitted by **Dr. VIMAL CHACKO MONDY,** appearing for **M.D.RADIODIAGNOSIS** degree examination in April 2019, is a bonafide record of work done by her under my guidance and supervision in partial fulfillment of requirements of The Tamil Nadu Dr. M.G.R Medical University, Chennai. I forward this to The Tamil Nadu Dr. M.G.R Medical University, Chennai.

PROF.S.BABU PETER, M.D., DNB, MNAMS,
Guide,
Professor,
Barnard institute of Radiology,
Madras Medical College &
Rajiv Gandhi Government General Hospital,
Chennai – 600 003.

PROF.R.RAVI, M.D., D.M.R.D.,
Director & Professor,
Barnard Institute of Radiology,
Madras Medical College &
Rajiv Gandhi Government General Hospital,
Chennai - 600 003.

PROF. R. JAYANTHI, M.D., FRCP (Glasg),
The Dean,
Madras medical college &
Rajiv Gandhi Government General Hospital,
Chennai - 600 003.

DECLARATION

I, **Dr. VIMAL CHACKO MONDY,** certainly declare that this dissertation titled, "**MYOCARDIAL MAPPING IN EVALUATION OF MYOCARDIAL DISEASES AND ASSESSING NORMATIVE VALUES IN CONTROLS**", represent a genuine work of mine, done at the Barnard Institute of Radiology, Madras Medical College and Government General Hospital, under the supervision of **Prof. S. BABU PETER, M.D., DNB, MNAMS**, Professor, Barnard Institute of Radiology, Madras Medical College and Rajiv Gandhi Government General Hospital.

I, also affirm that this bonafide work or part of this work was not submitted by me or any others for any award, degree or diploma to any other university board, neither in India or abroad. This is submitted to The Tamil Nadu Dr. M.G.R. Medical University, Chennai in partial fulfilment of the rules and regulation for the award of Master of Radiodiagnosis Branch VIII

Date :

Place: Chennai **Dr. VIMAL CHACKO MONDY**

ACKNOWLEDGEMENT

I would like to express my deep sense of gratitude to the Dean, **PROF. Dr.R. JAYANTHI, M.D., FRCP (Glasg),** Madras Medical College and **Professor Dr.R.Ravi, M.D.R.D., D.M.R.D., our Director, Barnard Institute of Radiology, MMC & RGGGH,** for allowing me to undertake this study on "**MYOCARDIAL MAPPING IN EVALUATION OF MYOCARDIAL DISEASES AND ASSESSING NORMATIVE VALUES IN CONTROLS"**

I would like to express my deep gratitude and respect to my guide **Professor Dr.S. BABU PETER,** whose advice and insight was invaluable to me. This work would not have been possible without his guidance, support and encouragement.

I was able to carry out my study to my fullest satisfaction, thanks to guidance, encouragement, motivation and constant supervision extended to me, by my beloved **Head of the Department** Professor **Dr.K.Malathi**. Hence my profuse thanks are due for her.

My sincere thanks to **Professor Dr.S.Kalpana** and **Professor Dr.D.Ramesh** for their valuable support.

I am also indebted to my respected **Associate Professors** and **Assistant Professors** for their constant support throughout this study.

I also thank **my past and present fellow postgraduates** who helped me in carrying out my work and preparing this dissertation. I thank **all the Radiology technicians, Staff Nurses and all the Paramedical staff members** in Barnard Institute of Radiology, for their fullest co-operation. I thank my statistician **Mr.Venkatesan**, who rendered his valuable timely help in completing this study.

I thank my **lovable parents and my brothers** for their constant and persistent support for my studies and in all my endeavours.

I would be failing in my duty if I don't place on record my sincere thanks to those **patients and their relatives** who inspite of their sufferings extended their fullest co-operation to the study.

Dr. VIMAL CHACKO MONDY

TABLE OF CONTENTS

"MYOCARDIAL MAPPING IN EVALUATION OF MYOCARDIAL DISEASES AND ASSESSING NORMATIVE VALUES IN CONTROLS"

1. INTRODUCTION

The Extracellular Matrix (ECM) in a normal human heart is composed of collagen fibers, proteoglycans, glycosaminoglycans and fibroblasts. Myocardial fibrosis, defined as a significant increase in collagen volume fraction of myocardial tissue, is a common feature in various myocardial diseases [1]. Myocardial fibrosis is a fundamental process in the development of myocardial dysfunction, leading to myocardial remodelling and poor outcomes [2–6]. It is an independent risk factor for overall mortality.

Several therapeutic strategies aimed at regression of interstitial fibrosis are available. Early identification of this underlying, often diffuse, interstitial myocardial fibrosis is thus important for diagnosis and essential for optimization of reversibility with intervention.

Invasive cardiac imaging is a cornerstone of the diagnosis and it is extremely helpful in numerous cardiovascular pathologies. However, various myocardial diseases like cardiomyopathies, myocarditis, etc. are very difficult to diagnose.

Until recently, myocardial fibrosis was not useful as a clinical marker because the only available method for assessment was invasive endomyocardial biopsy. However, this technique brings with it a risk of serious complications, is prone to sampling error and cannot detect the fibrotic involvement of whole ventricle, and was hence seldom performed.

As such a non-invasive whole-heart method of assessing myocardial fibrosis is required to distinguish fibrotic myocardium from normal myocardium. Multiple non-invasive diagnostic strategies have been trialled for fibrosis assessment including: echocardiographic backscatter [7], nuclear imaging [8], peripheral collagen biomarkers [9] and molecular labelling techniques [10]. Their clinical application has remained limited.

Cardiac imaging, especially cardiac magnetic resonance imaging (CMR), offers unique opportunities for detection and characterization of myocardial pathologies. It is noninvasive and allows accurate assessment of cardiac structure and function with detailed tissue characterisation and great level of accuracy and reproducibility [11].

Late gadolinium enhancement (LGE) imaging, also recognized as scar imaging is currently the primary tool for tissue characterization in CMR detecting focal myocardial fibrosis. Diffuse myocardial fibrosis is, however, more difficult to distinguish using LGE since the myocardial signal intensity may be nearly isointense and may be globally "nulled" thus appearing to be normal tissue. LGE is contraindicated in renal dysfunction as it involves intravenous administration of gadolinium-based contrast agents. Moreover, LGE detects end-stage, irreversible tissue damage with replacement fibrosis. There is, therefore, a need for novel techniques that allow earlier detection of potentially reversible diffuse fibrosis, frequently missed using LGE.

Such early tissue characterisation can be achieved using MRI techniques that allow direct quantification of signal from the myocardium via parametric mapping

techniques - T1 and T2 mapping. All tissues have natural tissue-specific longitudinal (T1) and transverse (T2) relaxation times. These may be altered in disease. Mapping techniques measure these and display the actual values in colour on a pixel-by-pixel basis for regional, and between-patient, comparisons without the need for post-processing. Thus, mapping can noninvasively represent a "sample" of tissue from the entire myocardium and supplement or potentially replace invasive myocardial biopsy [12]. Further, it may help identify the most appropriate location for biopsy, if biopsy is deemed clinically necessary.

2. RATIONALE OF THE STUDY

Cardiac-MRI has been established as the reference standard for the evaluation of cardiac anatomy and function. Late-gadolinium-enhancement also allows myocardial characterization, although the technique possesses limitations in diffuse myocardial fibrosis. In this setting T1 mapping emerges as a promising tool.

Cardiac MR imaging has relied primarily on a qualitative characterization of the myocardium through visual analysis of characteristic enhancement patterns on late gadolinium-enhanced (LGE) MR images. By using a T1-weighted inversion recovery sequence (to null normal myocardium), after gadolinium administration, the signal difference between normal myocardium and focal fibrosis can be identified. Areas of fibrosis demonstrate greater gadolinium accumulation which is represented as a region of high intensity signal with a shorter T1 time than adjacent normal tissue.

Traditional LGE MR images have two main limitations:

1. The identification and characterization of enhancement patterns is subjective, being susceptible to inter- and intraobserver variations.

2. Diffuse fibrosis may go undetected, as normal myocardium is needed as a standard of reference to contrast with a pattern of enhancement.

To surpass these limitations, new tissue characterization strategies have been proposed, including the so-called T1 mapping technique [13].

The native T1 measurement of myocardium can also detect important pathophysiologic processes, related to excess of water as in oedema [14,15], protein deposition [16, 17], and otherT1-altering substances, such as lipid [18, 19] or

iron(haemorrhage, siderosis) [20], without the use of gadolinium, and therefore it can also be applied in patients with severe renal failure. Changes of myocardial native T1 mapping reflect cardiac diseases, such as acute coronary syndromes, infarction, myocarditis, and diffuse fibrosis (that present with high T1) [21], and systemic diseases, such as cardiac amyloid (high T1) [21] Anderson-Fabry disease (low T1) [22], and siderosis (low T1).

The T2 mapping technique can accurately and reliably detect areas of myocardial oedema without the limitations of qualitative T2W imaging namely (a) signal intensity variability caused by phased array coils, (b) high signal from slow-moving ventricular blood that can mimic and mask elevated T2 in subendocardium,(c) motion artefacts, and (d) the subjective nature of T2W image interpretation.

T2 mapping sequences are useful for the detection of myocardial oedema due to acute myocardial infarction [23], myocarditis [24, 25], stress cardiomyopathy [24, 26] , sarcoidosis [27] , and cardiac allograft rejection [28] . T2 mapping is considered superior compared with standard CMR parameters, global myocardial T1 mapping, and ECV for assessing the activity of myocarditis inpatients with recent-onset heart failure and reduced left ventricular function [29]. Furthermore, T2 mapping was proven to be a novel non-invasive tool or transplant monitoring, and in rejection detection [30].

3. ANATOMY AND REVIEW OF LITERATURE

CARDIAC EMBRYOLOGY

ESTABLISHMENT OF THE CARDIOGENIC FIELD

The vascular system appears in the middle of the third week. Cardiac progenitor cells lie in the epiblast, immediately lateral to the primitive streak. From there, they migrate through the streak rostral to the oropharyngeal membrane and neural folds in the splanchnic layer of the lateral plate mesoderm. They are induced by the underlying pharyngeal endoderm to form cardiac myoblasts. Blood islands also appear in this mesoderm, where they will form blood cells and vessels. With time, the islands unite and form a horseshoe-shaped endothelial-lined tube surrounded by myoblasts. This region is known as the cardiogenic field; the intraembryonic cavity over it later develops into the pericardial cavity.

FORMATION AND POSITION OF THE HEART TUBE

Initially, the cardiogenic area is anterior to the oropharyngeal membrane and the neural plate. With closure of the neural tube and formation of the brain vesicles, the central nervous system grows cephalad and extends over the central cardiogenic area. As a result of growth of the brain and cephalic folding of the embryo, the heart and pericardial cavity move to the thorax.

As the embryo folds cephalocaudally, it also folds laterally. As a result, the caudal regions of the paired cardiac primordia merge except at their caudal most ends. Thus, the heart becomes a continuous expanded tube consisting of an inner endothelial

lining and an outer myocardial layer. It receives venous drainage at its caudal pole and begins to pump blood out of the first aortic arch into the dorsal aorta at its cranial pole.

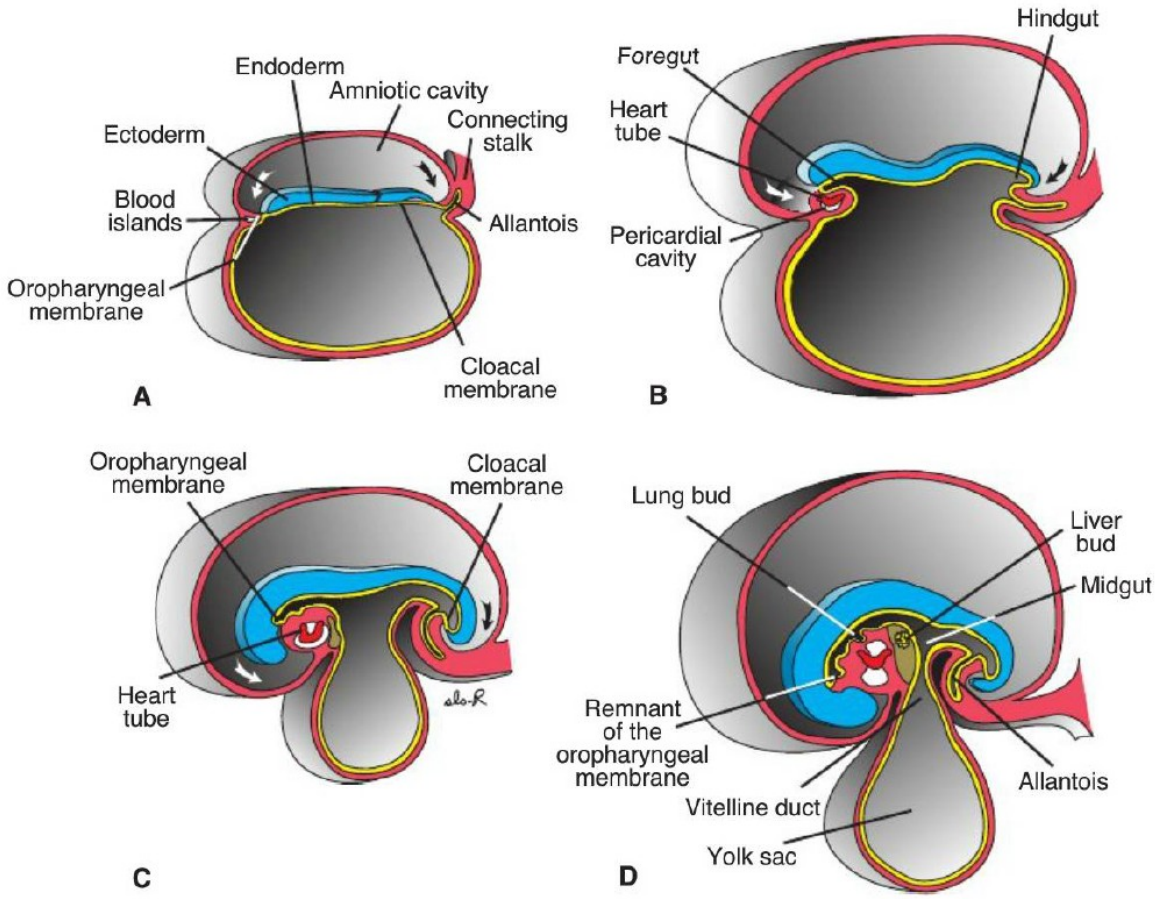

Fig 3.1 Effects of the rapid growth of the brain on positioning of the heart

During these events, the myocardium thickens and secretes a thick layer of extracellular matrix, rich in hyaluronic acid that separates it from the endothelium. Mesothelial cells on the surface of the septum transversum form the proepicardium near the sinus venous and migrate over the heart to form most of the epicardium. Thus, the heart tube consists of three layers: (a) the endocardium, forming the internal endothelial lining of the heart; (b) the myocardium, forming the muscular wall; and (c) the epicardium or visceral pericardium, covering the outside of the tube.

FORMATION OF THE CARDIAC LOOP

The heart tube continues to elongate and bend on day 23. The cephalic portion of the tube bends ventrally, caudally, and to the right; and the atrial (caudal) portion shifts dorsocranially and to the left. This bending creates the cardiac loop. It is complete by day 28. The atrial portion, initially paired, forms a common atrium. The atrioventricular junction remains narrow and forms the atrioventricular canal. The bulbus cordis is narrow except for its proximal third, which forms the trabeculated part of the right ventricle. The midportion, the conus cordis forms the outflow tracts of both ventricles. The distal part of the bulbus, the truncus arteriosus forms the roots and proximal portion of the aorta and pulmonary artery. The junction between the ventricle and the bulbus cordis, remains narrow and is called the primary interventricular foramen.

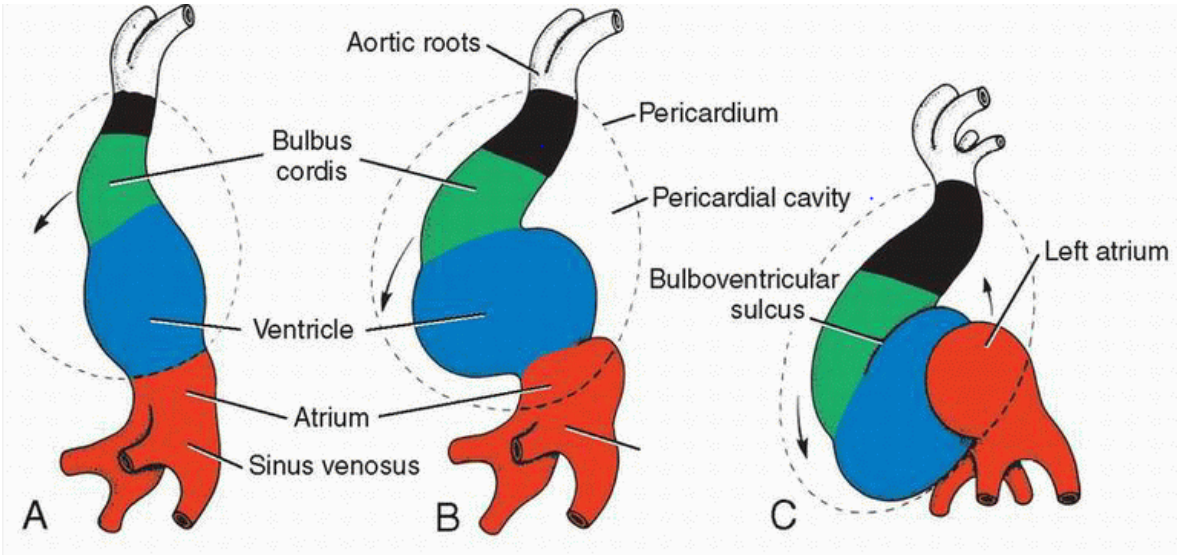

Fig 3.2 Formation of the cardiac loop

At the end of loop formation, the smooth walled heart tube begins to form primitive trabeculae just proximal and distal to the primary interventricular foramen. The primitive ventricle, which is now trabeculated, is called the primitive left

ventricle. The trabeculated proximal third of the bulbus cordis is called the primitive right ventricle.

DEVELOPMENT OF THE SINUS VENOSUS

In the middle of the fourth week, the sinus venosus receives venous blood from the right and left sinus horns. Each horn receives blood from three important veins: (a) the vitelline or omphalomesenteric vein, (b) the umbilical vein, and (c) the common cardinal vein. At first, communication between the sinus and the atrium is wide. Soon, the entrance of the sinus shifts to the right during the fourth and fifth weeks of development.

With obliteration of the right umbilical vein left vitelline vein, left common cardinal vein and the left sinus horn rapidly loses its importance and all that remains is the oblique vein of the left atrium and the coronary sinus.

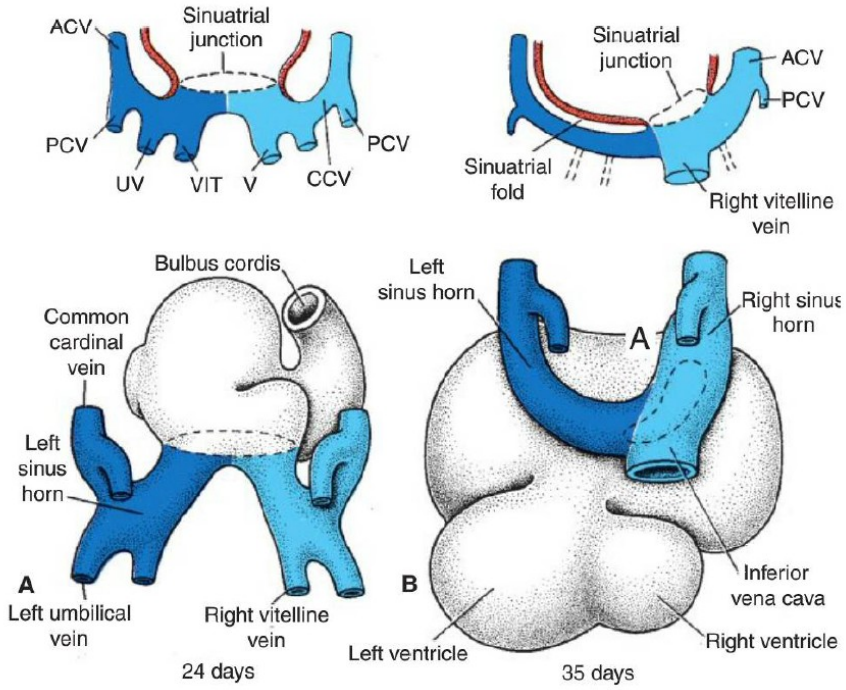

Fig 3.3 Dorsal view of two stages in the development of the sinus venosus at approximately 24 days (A) and 35 days (B). ACV, anterior cardinal vein; PCV, posterior cardinal vein; UV, umbilical vein; VIT V, vitelline vein; CCV, common cardinal vein.

FORMATION OF THE CARDIAC SEPTA

Septum Formation in the Common Atrium

At the end of the fourth week, a sickle-shaped crest grows from the roof of the common atrium into the lumen. This crest is the first portion of the septum primum. The septum extend toward the endocardial cushions in the atrioventricular canal. The opening between the lower rim of the septum primum and the endocardial cushions is the ostium primum. Extensions of the endocardial cushions grow along the edge of the septum primum, closing the ostium primum. Before closure is complete, perforations form in the upper portion of the septum primum which coalesce to form the ostium secundum.

A crescent-shaped fold appears the lumen of the right atrium called the septum secundum which extends downward to the septum in the atrioventricular canal. The free concave edge of the septum secundum overlaps the ostium secundum. The opening left by the septum secundum is called the oval foramen (foramen ovale). The passage between the two atrial cavities consists of an obliquely elongated cleft through which blood from the right atrium flows to the left side. After birth, when lung circulation begins and pressure in the left atrium increases, the valve of the oval foramen is pressed against the septum secundum, obliterating the oval foramen and separating the right and left atria.

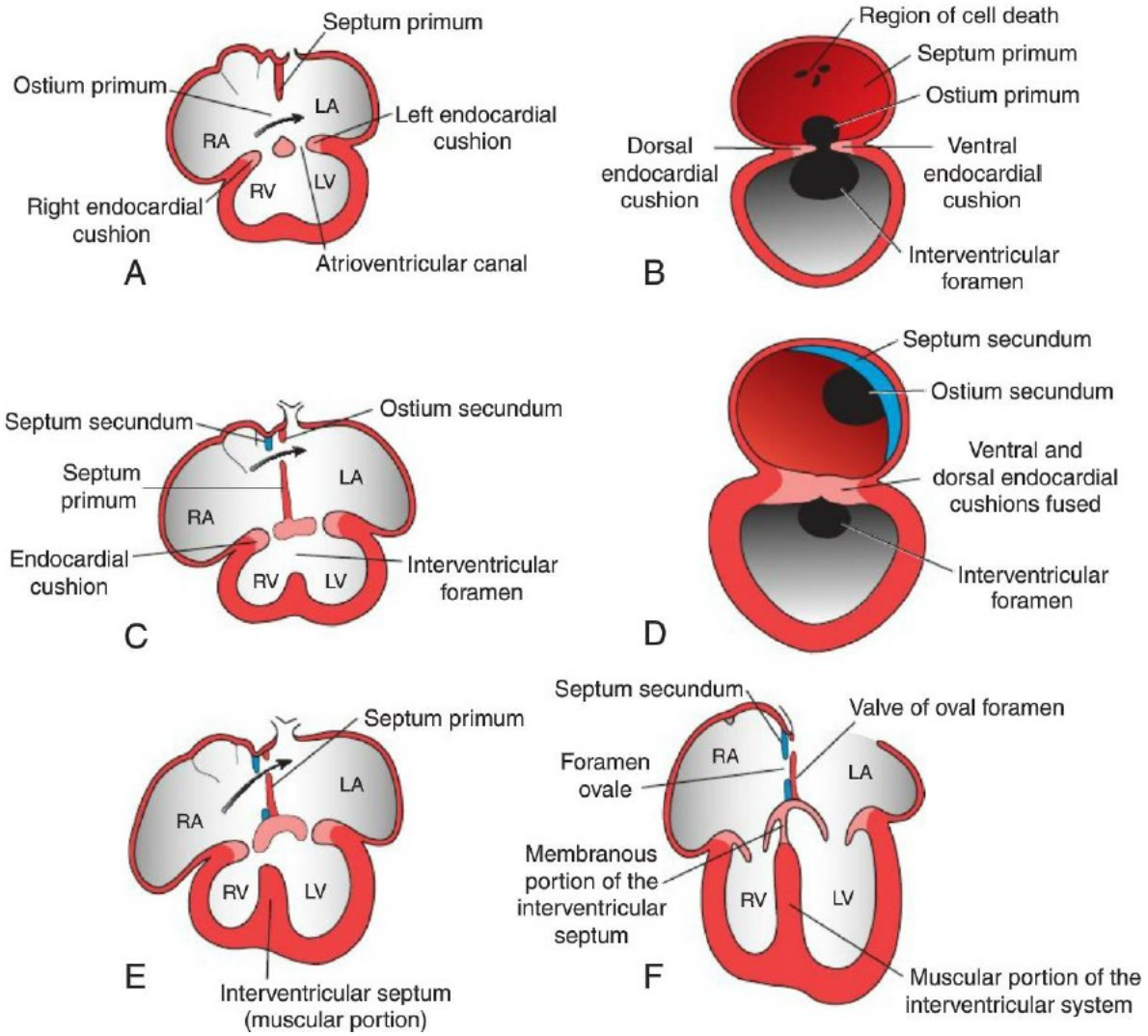

Fig 3.4 Atrial septa at various stages of development

Further Differentiation of the Atria

The primitive right atrium enlarges by incorporation of the right sinus horn. Initially, a single embryonic pulmonary vein develops as an outgrowth of the posterior left atrial wall. This vein gains connection with veins of the developing lung buds. Ultimately, four pulmonary veins are incorporated into the left atrium, forming its smooth walled part. In the fully developed heart, the embryonic left atrium is represented by the trabeculated atrial appendage, while the smooth-walled part originates from the pulmonary veins. The embryonic right atrium becomes the

trabeculated right atrial appendage and the smooth-walled sinus venarum originates from the right horn of the sinus venosus.

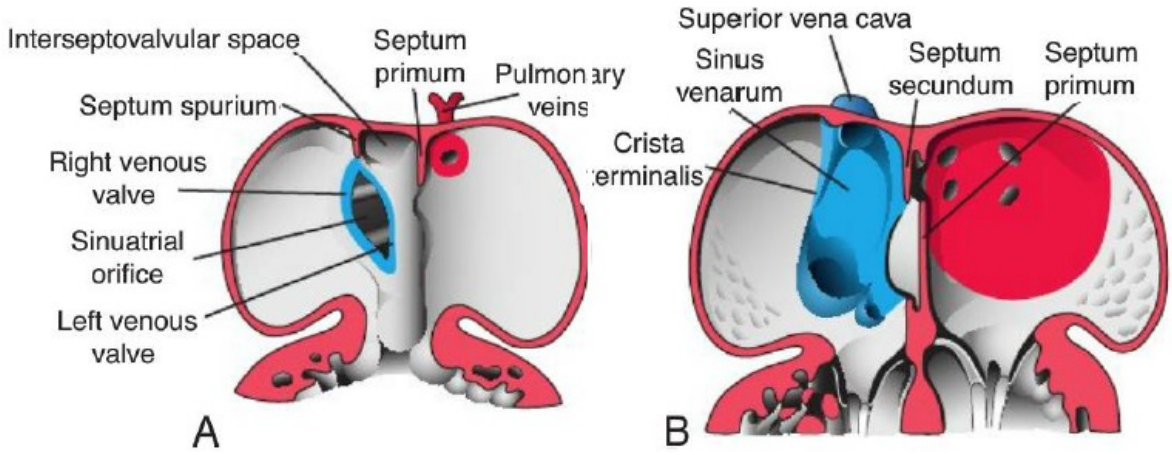

Fig 3.5 Development of the smooth-walled portions of the right and left atriu.

Septum Formation in the Atrioventricular Canal

At the end of the fourth week, two mesenchymal atrioventricular endocardial cushions, appear at the anterior and posterior borders of the atrioventricular canal. In addition to these, the two lateral atrioventricular cushions appear on the right and left borders of the canal. The anterior and posterior cushions, project further into the lumen and fuse, resulting in a complete division of the canal into right and left atrioventricular orifices by the end of the fifth week.

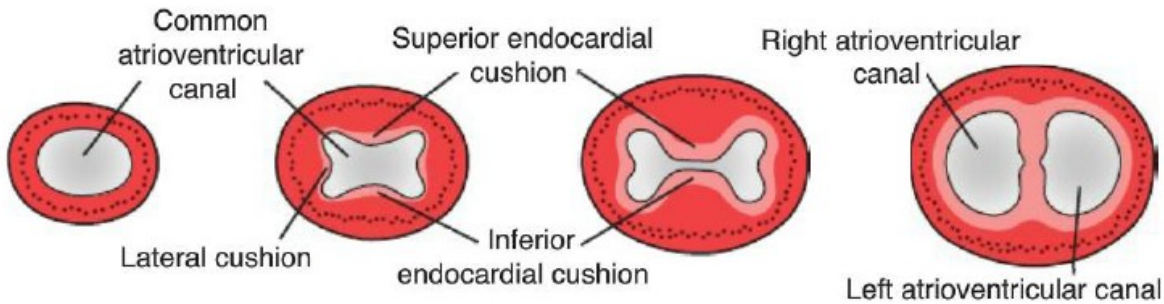

Fig 3.6 Formation of the septum in the atrioventricular canal

Septum Formation in the Truncus Arteriosus and Conus Cordis

During the fifth week, pairs of opposing ridges appear in the truncus, the truncus swellings, or cushions. While growing toward the aortic sac, the swellings twist around each other in a spiral course. After complete fusion, the ridges form the aorticopulmonary septum, dividing the truncus into an aortic and a pulmonary channel.

Similar swellings (cushions) develop along the walls of the conus cordis which grow toward each other and unite with the truncus septum. When the two conus swellings have fused, the septum divides the conus into an anterolateral portion (the outflow tract of the right ventricle) and a posteromedial portion (the outflow tract of the left ventricle).

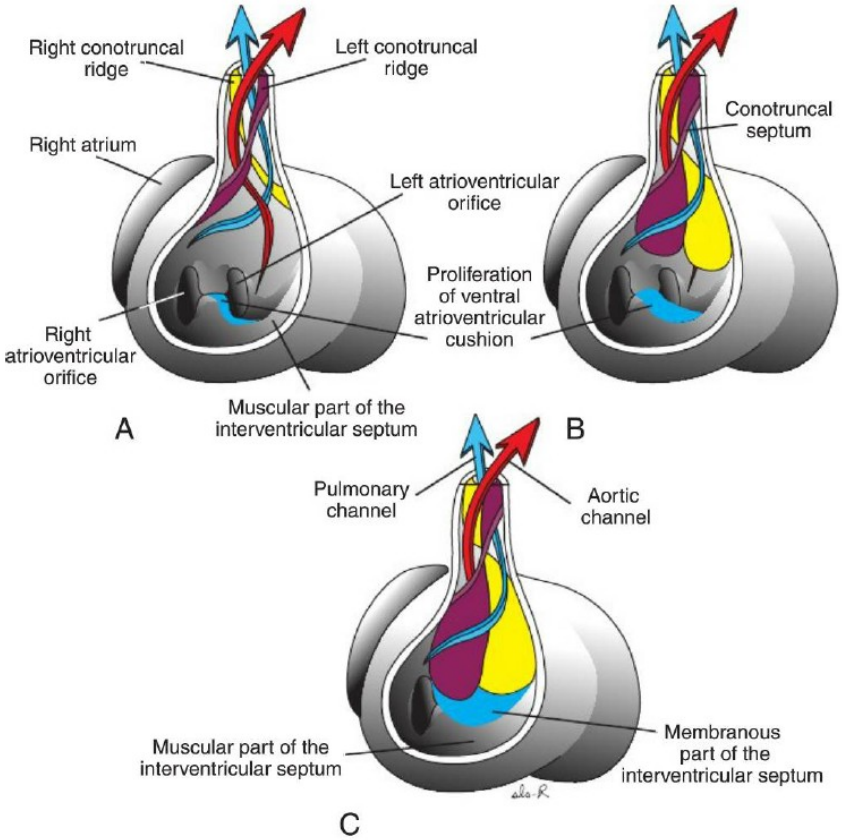

Fig 3.7 Development of the conotruncal ridges (cushions) and closure of the interventricular foramen.

Septum Formation in the Ventricles

By the end of the fourth week, the two primitive ventricles begin to expand. This is accomplished by continuous growth of the myocardium on the outside and continuous diverticulation and trabecula formation on the inside. The medial walls of the expanding ventricles become apposed and gradually merge, forming the muscular interventricular septum. The space between the free rim of the muscular ventricular septum and the fused endocardial cushions permits communication between the two ventricles. It is closed by outgrowth of tissue from the inferior endocardial cushion along the top of the muscular interventricular septum. Complete closure of the interventricular foramen forms the membranous part of the interventricular septum [31].

CARDIAC ANATOMY

The major cardiac structures that can be identified on MRI are:

RIGHT ATRIUM

The morphologic right atrium is derived from the right atrial appendage and sinus venosus [32]. The sinus venosus has a smooth wall and receives the inferior vena cava and superior vena cava–coronary sinus, and the right atrial appendage is triangular-shaped with a wide opening and contains rough trabeculations or pectinate muscles. These two components of the right atrium are separated by the crista terminalis (terminal crest). The crista terminalis is readily visualized on both bright and dark blood sequences and appears isointense to the myocardium. A prominent crista terminalis can mimic a mass. However, the location and signal characteristics on MRI can help confirm that this structure is indeed normal cardiac tissue [33]. The

valves of the coronary sinus (thebesian valve) and inferior vena cava (Eustachian valve) are also readily apparent on MRI.

RIGHT VENTRICLE

The right ventricle receives blood from the right atrium and consists of inlet, outlet, and apical portions [32].The inlet contains the tricuspid valves and associated chordal attachments. Attachment of the chords to the septum is characteristic of the tricuspid valve. The apical portion of the right ventricle is trabeculated, whereas the outlet is smooth and leads to the pulmonary artery. The right ventricle also contains the moderator band, which courses from the apical portion at the anterior papillary muscle insertion to the interventricular septum.

LEFT ATRIUM

The left atrium is the most posterior and superior chamber and receives pulmonary venous return [32]. The left atrium is also attached to the left atrial appendage, which is more elongated and narrower than the right atrial appendage. The left atrium is smaller and contains fewer trabeculations than the right atrium. The interatrial septum separates the right and left atria and features the fossa ovalis, which appears as an area of focal thinning.

LEFT VENTRICLE

The left ventricle comprises inlet, apical, and outlet segments and is separated from the right ventricle by the interventricular septum [32]. The septum normally bulges toward the right ventricle. Consequently, on short-axis views, the left ventricle has a rounded profile. The left ventricle inlet and outlet are continuous with one another and include the mitral and aortic valves, respectively. The apical region of the

left ventricle contains the two papillary muscles, which are larger than those in the right ventricle. In adults, the lateral wall of the normal left ventricle should measureless than 1 cm in thickness [34].

CORONARY ARTERIES

The coronary arteries arise from the aortic sinuses, just distal to the aortic valve. The right coronary artery (RCA) courses along the atrioventricular groove and is dominant in approximately 85% of individuals, giving rise to the posterior descending artery (PDA), which courses along the posterior interventricular sulcus toward the apex. The RCA also supplies the conal branch, right marginal branches, posterolateral ventricular branch, and frequently the sinus node artery. The left main coronary artery is a short trunk that supplies the left anterior descending (LAD) and left circumflex arteries. In up to 30% of individuals an additional ramus intermedius artery arises from the bifurcation of the left main coronary artery [32]. The LAD courses along the anterior interventricular sulcus and give rise to the diagonal and septal branches. The left circumflex artery supplies the obtuse marginal branches and sometimes supplies the sinus node artery and PDA in a left-dominant or codominant system.

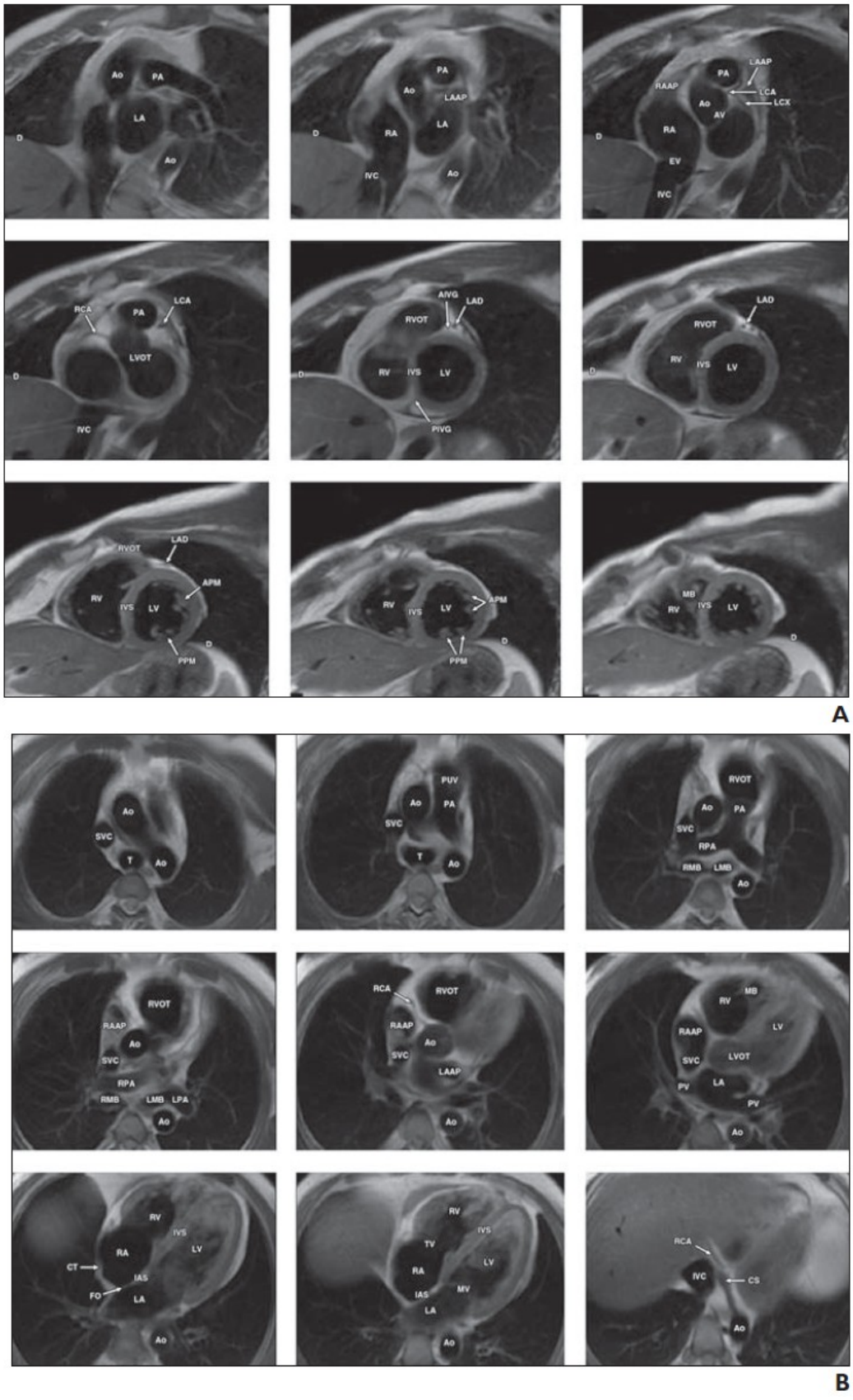

Fig 3.8 Normal cardiac MRI anatomy. Short-axis (A), horizontal long-axis (B)

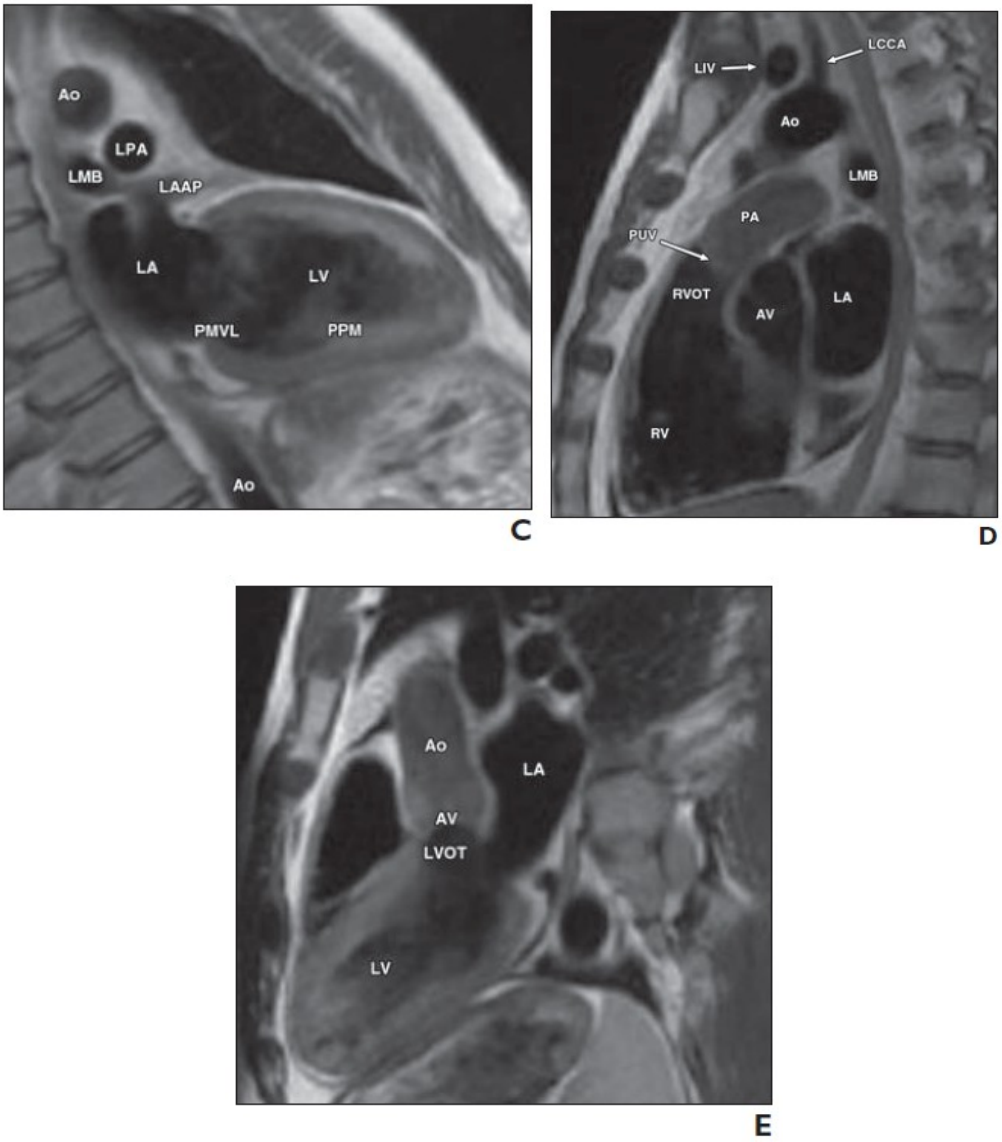

Fig 3.8 Normal cardiac MRI anatomy. Two-chamber (C), right ventricular outflow tract (D), and left ventricular outflow tract (E) views.

Ao = aorta, AIVG = anterior interventricular groove, APM = anterior papillary muscle, AV = aortic valve, CS = coronary sinus, CT = crista terminalis, D = diaphragm, EV = eustachian valve, FO = fossa ovalis, IAS = interatrial septum, IVC = inferior vena cava, IVS = interventricular septum, LA = left atrium, LAAP = left atrial appendage, LAD = left anterior descending artery, LCA = left coronary artery, LCCA = left common carotid artery, LCX = left circumflex artery, LIV = left innominate vein, LMB = left mainstem bronchus, LPA = left pulmonary artery, LV = left ventricle, LVOT = left ventricular outflow tract, MB = moderator band, MV = mitral valve, PA = pulmonary artery, PMVL = posterior mitral valve leaflet, PPM = posterior papillary muscle, PUV = pulmonary valve, RA = right atrium, RAAP = right atrial appendage, RCA = right coronary artery, RMB = right mainstem bronchus, RPA = right pulmonary artery, RV = right ventricle, RVOT = right ventricular outflow tract, SVC = superior vena cava, T = trachea, TV = tricuspid valve, PV = pulmonary vein.

REVIEW OF LITERATURE

MYOCARDIAL DISEASES

Cardiac extracellular matrix (ECM) is a complex mesh-work of fibers comprised of matrix proteins in which cardiac myocytes, fibroblasts, leukocytes, and blood vessels reside. It plays an important role in the maintenance of ventricular shape, size and function. In the normal human heart, it is predominantly made up of collagen types I (80%) and III (11%).

Myocardial fibrosis results from a significant increase in the collagen volume fraction of myocardial tissue (> 25%). The distribution of myocardial fibrosis varies according to the underlying pathology and is always present in end-stage heart failure. According to the cardiomyopathic process three different types of myocardial fibrosis have been described:

1. Reactive interstitial fibrosis

Reactive fibrosis refers to increased ECM deposition due to direct stimulation of fibroblasts without cell injury. It has a progressive onset and a diffuse distribution. This type of fibrosis is present in hypertension and diabetes mellitus, aging heart, idiopathic dilated cardiomyopathy, and in left ventricular pressure- overload and volume-overload states induced by valvular disease.

2. Infiltrative interstitial fibrosis

This subtype of fibrosis is induced by progressive deposit of insoluble proteins (amyloidosis) or glycosphingolipids (Anderson-Fabry disease) in the cardiac interstitium.

3. Replacement fibrosis

Replacement or reparative fibrosis refers to ECM deposition during scar formation as a result of tissue injury or cell death.

It can have a localized distribution (ischaemic cardiomyopathy, myocarditis, hypertrophic cardiomyopathy, and sarcoidosis) or a diffuse distribution (chronic renal insufficiency, toxic cardiomyopathies, inflammatory disease).

Reactive interstitial fibrosis and infiltrative fibrosis ultimately lead to replacement fibrosis in the later stages of disease, where cellular damage and cardiomyocyte necrosis/apoptosis appear [13].

HYPERTROPHIC CARDIOMYOPATHY

Hypertrophic cardiomyopathy (HCM) is the most common inheritable cardiac disorder, which is characterized by abnormal thickening of the left ventricular myocardium. The heart of a patient with archetypal HCM has an asymmetric or a symmetric increase in left ventricular wall thickness with a left ventricular cavity which is reduced in size. There is a broad range of phenotypic expressions with asymmetric involvement of the interventricular septum being the most common pattern. A high proportion of cases are now recognised to be caused by mutations in genes coding for myofibrillary proteins [35]. Most of the clinical manifestations of the disease involve either diastolic or systolic dysfunction, left ventricular outflow tract (LVOT) obstruction, arrhythmias and sudden cardiac death.

DILATED CARDIOMYOPATHY

The term dilated cardiomyopathy (DCM) is applied in the presence of left ventricular or biventricular dilatation and dysfunction following systematic exclusion of all obvious or detectable causes of cardiomyopathy. Common to the whole group is

a poorly contracting dilated left ventricle with a normal or reduced left ventricular wall thickness. The lack of an increase in left ventricular wall thickness tends to mask a significant increase in left ventricular mass. In the terminal stages thrombus may develop in the apices of both ventricles. In up to 50% of cases the etiology remains unknown. Many of the rest can be traced to previous infection, alcohol or drug abuse, or drug toxicity. [36, 37]

RESTRICTIVE CARDIOMYOPATHY

Restrictive cardiomyopathy (RCM), in which the left ventricle is nearly normal in shape but there is a failure of the myocardium to relax in diastole, is one form of cardiomyopathy where cardiac biopsy may help. The most common form is myocardial amyloid. It is usually easy to recognise amyloid on histology by its characteristic green colour under polarised light after staining with Sirius red dye. Other causes of restriction include diffuse perimyocyte fibrosis. This pattern of fibrosis is seen to a degree in many cases of DCM, but when in a uniform distribution it appears to cause predominant restriction. The pathogenesis of this form is unknown. Another form of RCM is familial and associated with myocyte disarray on biopsy, but without other clinical or morphological features of HCM. The gene(s) responsible have not yet been identified [35].

AMYLOIDOSIS

Cardiac amyloidosis is an interstitial deposition of amyloid fibrils that causes concentric thickening of the atrial and ventricular walls, where it leads to secondary restrictive cardiomyopathy. Amyloid is not, however, evenly distributed in the ventricle and false negatives occur. Some cases develop a florid myocardial fibrotic

response masking the amyloid. There are three main types of primary amyloidosis: light chain (AL) amyloidosis, senile systemic amyloidosis and hereditary amyloidosis (mutant form of transthyretin). Cardiac involvement is an important prognostic factor of this disease [13].

MYOCARDITIS

Myocarditis is an acute or chronic inflammatory disease of the myocardium which can be viral, postinfectious immune or primarily organ-specific autoimmune. The diagnosis of myocarditis is a challenging process, because of its diverse presentation, overlapping symptoms and limited sensitivity of endomyocardial biopsies [38]. The clinical picture of acute myocarditis is characterised by the rapid onset of cardiac failure or arrhythmias, or both, with fever, malaise, myalgia, and sometimes pericarditis. It has a morphological counterpart (Dallas criteria)[39] of myocyte necrosis, usually in a multifocal but sometimes regional distribution, with a heavy interstitial infiltrate of T lymphocytes. The reported positivity rate of myocardial biopsy varies is usually no more than 10%. The biopsy negative but clinically positive cases create a diagnostic challenge and are likely to be heterogeneous in origin. Some may be genuine cases of myocarditis, but the biopsy is taken after the T lymphocyte infiltrate has cleared. Other cases may reflect the limitations of cardiac biopsy because with a focal disease the sample taken may come from an area of normal myocardium. Early diagnosis is mandatory to address specific directed therapeutic management that influences patient morbidity and mortality.

The major cause of acute myocarditis is perceived to be viral, involving in particular the coxsackie group of viruses. Viruses other than those from the coxsackie

group like the adeno group. A very wide range of viruses such as those responsible for chicken pox, measles, rubella, and mumps often cause a minor degree myocarditis. A small subgroup of myocarditis may be caused by non-viral organisms, such as the spirochaete Borrelia burgdorferi in Lyme disease, toxoplasma, and leptospira, while in South America Trypanosoma cruzi is by far the most common cause of the acute myocarditis of Chagas' disease. Patients with biopsy positive or negative myocarditis may die in the acute phase or recover. Recovery is usually complete although there are a few reported cases of slow progression into DCM. The Dallas criteria for acute myocarditis on cardiac biopsy defined the need for severe myocyte damage plus a T lymphocyte interstitial inflammatory cell infiltrate [35].

MYOCARDIAL INFARCTION

Myocardial infarction (MI) is defined as myocardial cell death secondary to prolonged ischemia that results in an inadequate supply of oxygenated blood to an area of the myocardium, particularly when ischemia exceeds a critical threshold that overwhelms cellular repair mechanisms. MI is typically caused by luminal thrombosis superimposed on coronary atherosclerosis. Occasionally, it can be caused by coronary spasm, coronary embolism, or thrombosis in nonatherosclerotic vessels. Arteritis, dissection, congenital abnormalities, hypercoagulable states, and cocaine use are uncommon causes.

MI is the leading cause of death and a main cause of morbidity worldwide. In these patients, MI may present as a major catastrophic event, such as sudden cardiac death, or as a minor event in a chronic disease; MI may also remain silent. MI is most

commonly observed in patients aged 40–65 years and are more typically severe or lethal in women [39].

In MI, biochemical and functional abnormalities begin immediately after the onset of ischemia; loss of contractility occurs in 60 seconds and loss of viability occurs in 20–40 minutes. The changes progress from the initial decrease in perfusion, leading to diminished tissue oxygenation, decreased phosphocreatine, repolarization abnormalities, diastolic dysfunction, systolic dysfunction, decreased adenosine triphosphate, edema, and finally tissue necrosis. The infarct progresses like a "wave front" from the endocardium to the epicardium. Complete necrosis takes 2–4 hours or longer, depending on the presence of collateral circulation, persistent or intermittent coronary arterial occlusion, sensitivity of myocytes to ischemia, preconditioning, and individual demand for myocardial oxygen and nutrients.

An infarct is termed microscopic when <10% of the myocardium is involved, moderate when 10%–30% is involved, and large when >30% is involved [40]. Transmural MI affects the full thickness of affected muscle segments, from endocardium through midmyocardium to epicardium; nontransmural MI does not extend through the full thickness of the myocardial segments and is limited to endocardium or to endocardium plus midmyocardium. Clinically, MI can occur as either ST-segment elevation MI (STEMI) or non–ST-segment elevation MI (NSTEMI) [41].

ARRHTMMOGENIC RIGHT VENTRICULAR DYSPLASIA

Arrhythmogenic right ventricular dysplasia (ARVD) is characterised by areas in the right ventricle where there is transmural replacement of the myocytes largely by adipose tissue, but with some fibrosis leading to focal areas of aneurysmal dilatation.

The first cases recognised were first recognised in young subjects with normal exercise tolerance who died suddenly at the extreme end of the spectrum, but family studies and wider clinical studies using magnetic resonance imaging in subjects with unexplained ventricular tachycardia revealed that the areas of abnormality may be small—no more than 1–2 cm across. About a third of cases have concomitant left ventricular involvement with fibrofatty replacement of myocytes, often subpericardial and maximal on the posterior wall. In most but not all cases the myocardial involvement, while acting as a substrate for arrhythmias, does not significantly reduce right or left ventricular contractile function.

In patients with a known family history or with clear ECG and echocardiographic changes suggesting ARVD, cardiac biopsy is a useful confirmatory investigation but is rarely diagnostic in its own right. The focal nature of the disease means false negatives are common, while simple adipose infiltration into the right ventricular myocardium without replacement of myocytes or fibrosis is a common finding in normal subjects, particular women. Biopsy findings of fat in the right ventricular wall can be over interpreted and lead to false positives. The diagnosis of ARVD has to be based on the concordance of clinical and pathological features.

ARVD is genetic and several sites of candidate genes have been identified on different chromosomes. At present what these genes control or produce is unknown. The histological changes are different from those in DCM because although myocytes are being lost in both conditions, in ARVD there is a predominant replacement by adipose tissue. In many cases of ARVD there is an inflammatory cell infiltrate in the abnormal areas of myocardium. This has been interpreted as a myocarditic component but could

be a secondary rather than a primary change. The frequency of ARVD is impossible to establish accurately at present because the less striking cases are underdiagnosed both in life and after death [13, 35].

IMAGING OF MYOCARDIAL DISEASES

ECHOCARDIOGRAPHY

Echocardiography is one among the imaging modalities for diagnostic evaluation, follow-up and analysis of treatment results of myocardial pathologies. It is an accessible, inexpensive and reproducible first-line modality for the assessment of ventricular size and function. The current ultrasound equipments exhibit an impressive improvement of heart image resolution and Doppler effect sensibility. New resources such as tissue Doppler, motivate the development of more studies, whose results are already adding themselves to the current resources on the prognostic and diagnostic evaluation of myocardial diseases. However, echocardiography requires suitable imaging windows and provides limited capability for tissue characterization [43].

Dilated cardiomyopathy

2D echocardiographic findings characteristically show left ventricular (LV) dilatation (with variable involvement of the right ventricle and to a lesser degree the atria), poor systolic myocardial thickening and reduced systolic indices (i.e. LVEF < 50%).Additional features may include mitral or aortic valve incompetence [44].

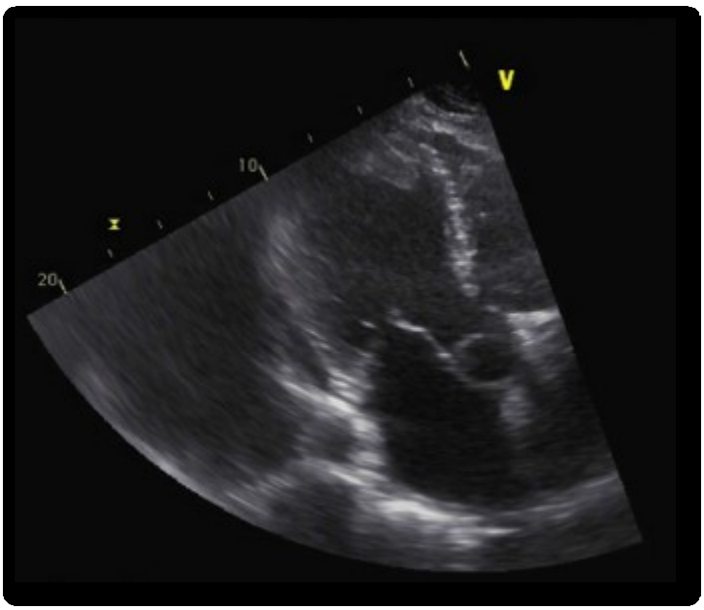

Fig 3.9 Dilated cardiomyopathy - Four chamber echocardiogram showing left ventricular dilatation

Hypertrophic cardiomyopathy

Echocardiography shows LV hypertrophy typically involving the interventricular septum. However, any diffuse or segmental pattern of LV wall thickening is possible. Diagnostic criterion is a maximal LV wall thickness greater than or equal to 15 mm in the end-diastolic phase (normal range ≤12 mm) [45]. Variation of myocardial hypertrophy may include asymmetric or non-contiguous myocardial involvement. Right ventricular (RV) muscular hypertrophy (17%) [46] may also be seen, most commonly involving the mid to apical portion of the right ventricle.

Restrictive cardiomyopathy

Echocardiography usually demonstrates normal LV cavity size and systolic function, biatrial enlargement, with abnormal diastolic function. Furthermore, in restrictive cardiomyopathy, pulmonary venous systolic flow is reduced with a consequent rise in diastolic flow. This can be utilized to exclude constrictive pericarditis. The measurement of transmitral peak flow velocity in early diastole (E)

and during atrial contraction (A), the E/A ratio, is another useful parameter that can be measured via echocardiography [46]. In diastolic dysfunction, due to reduced ventricular compliance, a greater percentage of end diastolic volume results from late rather than early filling because of the stiffness of the ventricle. Therefore E/A ratio is reduced.

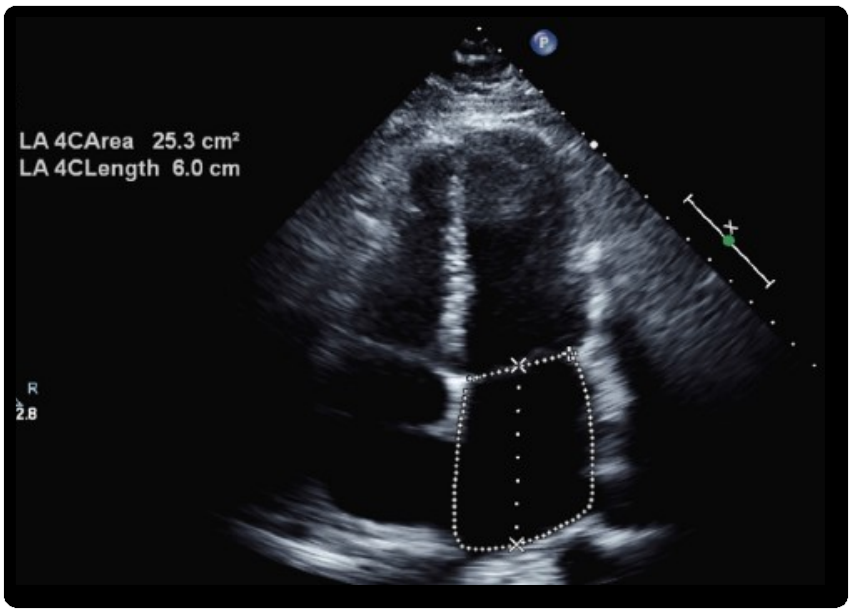

Fig 3.10 Echocardiography four chamber view showing bi-atrial enlargement in restrictive cardiomyopathy

Arrhythmogenic right ventricular dysplasia

Echocardiographic investigation is limited in ARVD because much of the right ventricular free wall lies posterior to the sternum and ribs. Furthermore, it is not useful at demonstrating intramyocardial fat. Echocardiography can demonstrate a hypokinetic and dilated right ventricle. A right ventricular outflow tract (RVOT) dimension >30 mm from the parasternal long-axis view has a sensitivity (89%) and specificity (86%) for the diagnosis of ARVD [47].

COMPUTED TOMOGRAPHY

Computed tomography (CT) achieves excellent tissue characterization, with high spatial resolution in short acquisition times. It excels at cross-sectional, anatomical imaging and has developed as the gold standard for non-invasive angiography. Although less widely utilized for functional analysis, its ability to accurately assess left ventricular (LV) function has been known for many years [48], and it is recommended for such where other methods are unsuitable, and to evaluate right ventricular (RV) morphology and function [49]. Cardiac CT is increasingly relevant to every subspecialty of cardiology. Guidance for revascularization, aetiological diagnosis in heart failure, identification of potentially arrhythmogenic scar, and assessment of complex congenital heart disease are achievable.

While the gold standard modalities for such assessment are cardiac magnetic resonance and echocardiography, these are not universally suitable. Cardiac computed tomography (CT), well-established for the assessment of coronary artery disease (CAD), can be of value in the assessment of myocardial pathology, due to excellent patient compatibility and tolerability, high spatial resolution, and acceptable tissue characterization.

CT is not without limitations and image quality can be impaired by both patient and acquisition factors, including excessive cardiac motion, or respiration[50], although myocardial CT requires less meticulous patient preparation than for coronary analysis, with less restrictive target heart rates. Errors peculiar to CT can occur, such as beam-hardening artefact, due to the disproportionate attenuation of lower energy photons in the X-ray beam by highly dense structures, such as calcium or contrast. This is

particularly problematic where the volume of contrast in the ventricles causes 'shadowing' over the myocardium, limiting evaluation, or mimicking pathology.

The inescapable limitation of CT has been radiation dose, although this has fallen considerably in recent years [51] due to improved methods of acquisition, patient-specific scanning protocols, and novel image reconstruction methods. The latest reconstruction techniques offer potential for even greater dose reductions. Ultra-low-dose techniques can produce some thoracic CT images for as little radiation as a chest radiograph [52].

The assessment of myocardial structure and function is perhaps most comprehensive using retrospective electrocardiographic (ECG) gating, where images are taken throughout a number of cardiac cycles and diagnostic data then retrospectively extracted. This method provides data from entire cycles, permitting visualization of dynamic function but requiring longer, multi-cycle exposure to the X-ray beam and thus a higher radiation dose. This has led to the development of prospective techniques, where the X-ray tube is 'on' for only the portions of the cardiac cycle required for diagnosis; typically for coronary assessment this in mid-diastole or end-systole. Functional information is less readily available with this method.

Contrast timing is also important to consider, particularly when a CT is being used for the assessment of cardiac structure rather than for solely coronary analysis. If both LV and RV analyses are required, the scan must be undertaken using either a larger volume of contrast, or a slower rate (or both) to ensure that the right-sided cardiac chambers remain opacified during left-sided filling. Conversely, if shunts are

suspected then it is important to maintain a contrast differential, so that aberrant blood flow can be clearly demonstrated. When retrospective techniques are still employed, the assessment of myocardial function, including ejection fraction and identification of regional wall motion abnormalities, approaches the accuracy of cardiac magnetic resonance imaging (MRI) [53]. It is concordant with, and potentially superior to, two-dimensional echocardiography, with greater accuracy and reproducibility [54].Such data can be rapidly generated using the semi-automated software to identify the coronary phases, delineate the blood volumes, and calculate chamber sizes and ejection fractions.

As with echo, CT can offer morphological screening, particularly in patients with concomitant cardiomyopathy and coronary artery disease (CAD). Chamber dimensions and wall thickness can be precisely measured, and dilated or hypertrophic cardiomyopathies (HCMs) identified [55]. This must be performed diligently as wall thickness and chamber size require precise measurements, usually in end-diastole.

Other structural pathology is less reliant on accurate timing and with the exception of wall thickness and function, a single-phase examination is usually sufficient. LV non-compaction is readily identifiable on cardiac CT [56], and assessment for LV thrombus can be reliably undertaken. Chamber and conduit identification can also be easily conducted for patients with congenital heart disease, while identifying lesions such as shunts and anomalous coronary arteries (Figure 2C), which may be contributing to myocardial abnormality[57]. In this manner, CT is useful for identifying additional features associated with particular myocardial pathologies.

Ischaemic cardiomyopathy

The assessment of CAD remains the major application for cardiac CT [49]. CT is commonly used to rule out ischaemia as a cause of cardiomyopathy [58]. The co-localization of coronary artery calcification with atheromatous plaque and significant stenosis has led to the use of calcium scoring, where low-dose, non-contrast CT is used to identify coronary calcium deposition and to infer the likelihood of CAD. This has been examined specifically for the assessment of ischaemic cardiomyopathy [59].

Cardiac CT [60] can discriminate between ischaemic and non-ischaemic causes in patients with a dilated phenotype. The gross morphology is non-specific, with ventricular dilatation and dysfunction, myocardial thinning and less commonly, intramyocardial fat.

Delayed enhancement can be identified in a similar manner to late gadolinium enhancement with CMR. The presence of scar adds additional accuracy to the diagnosis of ischaemic cardiomyopathy [61]. The identification of post-infarction scar is facilitated by the tissue differentiation between myocardium and fat. Following infarction, fatty replacement of the myocardium occurs, initially within fibrous scar but eventually leading to significant lipomatous metaplasia. On CT, fat in infarcted myocardium is usually, although not exclusively, subendocardially distributed in a curvilinear pattern, within a coronary artery territory [62]. It is easily visualized, even on non-enhanced images undertaken for calcium scoring, and extremely common.

Dilated cardiomyopathy

The role of cardiac CT (CCT) is in excluding obstructive coronary artery disease. Other characteristic findings of DCM on CCT include increased diastolic LV

internal diameter measurement greater than 5.6 cm (upper limits of normal) [49]. CCT also plays a role in determining DCM prognosis, based on ejection fraction (<35% for symptomatic patients and <30% for asymptomatic patients).

Hypertrophic cardiomyopathy

CCT may demonstrate basal myocardial hypertrophy with a small outflow tract, and an enlarged and elongated mitral valve. The associated haemodynamic obstruction may also demonstrate systolic anterior motion of the mitral valve leaflets and mid-systolic contact with the ventricular septum with either subaortic obstruction or mitral regurgitation. Differentials include hypertensive cardiomyopathy however HCM is usually non-concentric and asymmetric.

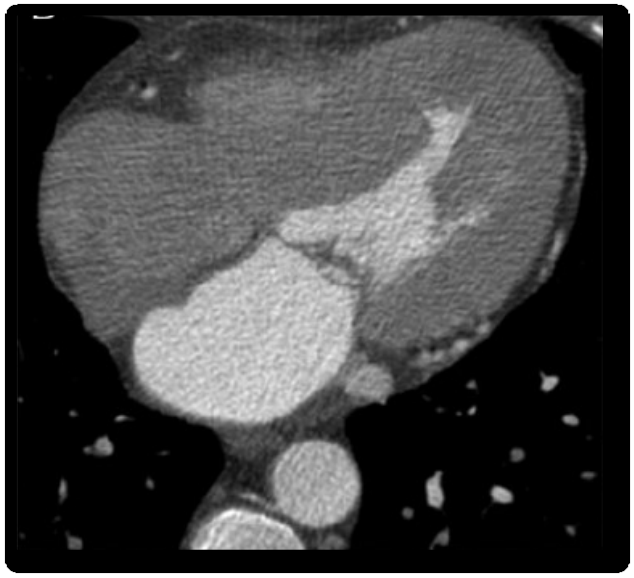

Fig 3.11Cardiac CT - Hypertensive cardiomyopathy with concentric LV hypertrophy

Restrictive cardiomyopathy

CCT can identify similar values attained by echocardiography - LV cavity size and systolic function, biatrial enlargement, with abnormal diastolic function.

Arrhythmogenic right ventricular cardiomyopathy

Cardiac CT is limited compared to CMRI. However, the detection of morphologic and wall motion abnormalities is favourable in patients with implantable defibrillators in situ. Findings that can assist include dilatation of the right ventricle and bulging/scalloped appearance of the RV wall.

Fibrofatty replacement of the myocardium is well recognized as a feature of arrhythmogenic right ventricular cardiomyopathy (ARVC). Involvement of the left heart has been comprehensively described in arrhythmogenic right ventricular cardiomyopathy particularly in advanced disease. Initially, structural and morphological changes are limited to the 'triangle of dysplasia' [63], comprising the RV outflow tract, the inferior RV wall, and the apex.

The diagnostic criteria for ARVC include ECG and clinical parameters, 45 but imaging appearances predominate. While the Task Force Criteria do not consider CT, some of the morphological features are readily apparent and additional indicators have also been proposed. RV dilatation with scalloping of the free wall, and fat deposition in conspicuous trabeculae and the moderator have been described as being suggestive of ARVC on CT.

Furthermore, the right ventricle often appears drastically thinned, due to fibrofatty replacement. LV involvement can also be assessed and has been described most often as wedge-shaped myocardial defects in the free wall.

Myocarditis

10% of severe viral myocarditis cases result in DCM. Echocardiography is useful to exclude causes of DCM and symptomatic heart failure (i.e. ischaemia,

valvular) from myocarditis. Chamber dilation, regional hypertrophy and ventricular remodelling are abnormalities regularly seen in myocarditis [64].

MRI

Cardiac MRI is indicated for evaluating a wide variety of congenital and acquired heart diseases, including cardiac masses, myocardial ischemia or infraction, cardiomyopathies, valvular disease, coronary artery disease, pericardial disease, and complex congenital anomalies [65]. The high soft-tissue contrast, availability of a large FOV, multiplanar acquisition capability, and lack of ionizing radiation are particularly appealing features of cardiac MRI. Cardiac magnetic resonance (CMR) imaging has emerged as the gold standard for the assessment of myocardial pathology. However, the main limitation of cardiac MRI compared with CT is the evaluation of coronary calcifications.

General contraindications for cardiac MRI include iron particles in the globe and intracranial aneurysm clips [65]. Although also traditionally contraindicated for MRI because of concerns of arrhythmia and excess device heating, most patients with modern pacemakers and other types of implanted cardiac devices can safely undergo cardiac MRI examination at 1.5 T provided that appropriate precautions have been implemented [66]. Pregnancy is considered a relative contraindication for cardiac MRI, although there are no known risks to the fetus. Except certain early models, valvular prostheses do not preclude cardiac MRI but their presence can degrade image quality [65].

There are certain technical challenges unique to cardiac MRI. Most notably is the rapid and complex motion of the heart and pulsatility of the great vessels due to

normal contractility. In addition, the effects of respiratory motion and systolic ventricular blood velocities up to 200 cm/s further complicate cardiac imaging. Nevertheless, these issues are generally mitigated by implementation of ECG (cardiac) gating; navigator echo respiratory gating; breath-hold techniques; rapid, high-performance gradients; improved field homogeneity; and advanced pulse sequences. ECG gating can be either prospective or retrospective.

Pulse Sequences

Pulse sequences are software programs that encode the magnitude and timing of the radiofrequency pulses emitted by the MR scanner, switching of the magnetic field gradient, and data acquisition. The components of a pulse sequence are termed "imaging engines" and "modifiers" [67]. Imaging engines are integral features of a pulse sequence, whereas modifiers are optional additions.

Imaging engines include fast spin-echo (FSE), gradient-echo (GRE), steady-state free precession (SSFP), echo-planar imaging (EPI), and single-shot versus segmented modes. Modifiers include fat suppression, inversion prepulse, saturation prepulse, velocity- encoded, and parallel imaging [67].

Dark Blood Imaging

Dark blood imaging refers to the low-signal- intensity appearance of fast-flowing blood and is mainly used to delineate anatomic structures. Traditionally, spin-echo (SE) sequences have been used for dark blood imaging. SE has been supplanted by the newer FSE and turbo spin-echo (TSE) techniques in cardiac imaging.

Bright Blood Imaging

Bright blood imaging describes the high signal intensity of fast-flowing blood and is typically used to evaluate cardiac function. The main pulse sequences used for bright blood imaging include GRE (i.e., spoiled gradient recall [SPGR], turbo FLASH, turbo field echo, and fast-field echo [FFE]) and the technique termed "steady-state free precession" or "SSFP." EPI is another rapid sequence that is often used for functional assessment in cases in which arrhythmia precludes adequate gating.

Modifiers

Inversion recovery (IR) consists of applying additional 180° pulses. Double or triple IR can be used to further null signal from blood for black blood imaging, thereby improving contrast between the cardiac tissues and blood pool. This sequence is particularly useful for tumor imaging, delayed enhancement imaging, and coronary angiography. Fat suppression is accomplished in a similar manner, in which the inversion time of the additional selective 180° pulse is set to match the null time of fat.

Saturation-recover preparatory pulses also improve T1-weighted imaging. It consists of applying a 90° flip angle and is less subject to signal intensity variations than IR techniques. The saturation- recover pulse is often used in combination with GRE and hybrid GRE-EPI pulse sequences for perfusion-weighted imaging and myocardial tagging. Tagging involves labelling the myocardium with a low-signal-intensity grid. This enables quantification of myocardial strain and assessment of pericardial constriction. Tagging is also a more accurate method of assessing infarct-related dysfunction than wall thickness analysis [68].

Phase-contrast imaging with velocity-encoded imaging is a noncontrast technique that is frequently used to estimate pulmonary blood flow (Qp) and systemic blood flow (Qs) to calculate the pulmonary-to-systemic flow ratio (Qp:Qs) to determine shunt fraction. A Qp:Qs > 1.5 usually indicates a significant left to- right shunt that requires surgical or percutaneous correction.

Velocity-encoded imaging can also be used to calculate regurgitant fractions and valve area using the continuity equation. This technique is usually implemented via GRE pulse sequences. The gradient strength must be selected to match the expected velocities. A velocity setting that is too low can cause aliasing, whereas a setting that is too high results in noisy, inaccurate measurements.

Parallel imaging techniques such as sensitivity- encoding (SENSE) and simultaneous acquisition of spatial harmonics (SMASH) enable accelerated imaging acquisition with short breath-hold times [65]. These techniques make use of multiple coil arrays and sample limited portions of k-space over time.

Contrast-Enhanced Techniques and Other Applications of Pulse Sequences

The use of contrast material is an integral part of a myocardial viability study. Evaluation of myocardial viability with MRI is based on the phenomenon of delayed enhancement. This procedure consists of performing IR-GRE approximately 10 minutes after injection of a gadolinium-based contrast medium. Areas of myocardial infarct characteristically display enhancement when imaging is performed at an inversion time at which signal in the myocardium is maximally nulled. Dynamic perfusion imaging is also useful for characterizing myocardial viability and is often carried out via EPI. For tumor imaging, T1-weighted IR-FSE pulse sequences are

typically performed immediately after gadolinium injection. Contrast-enhanced MRI can also be used for evaluating the coronary arteries and great vessels. Maximum intensity projections (MIPs) and 3D vessel surface render renderings are particularly useful adjuncts. Alternatively, ECG-gated balanced SSFP without arterial spin labelling can be applied as an unenhanced angiographic technique for imaging the aorta as well as the coronary arteries. Arterial spin labelling can be further implemented to eliminate signal from venous flow [69].

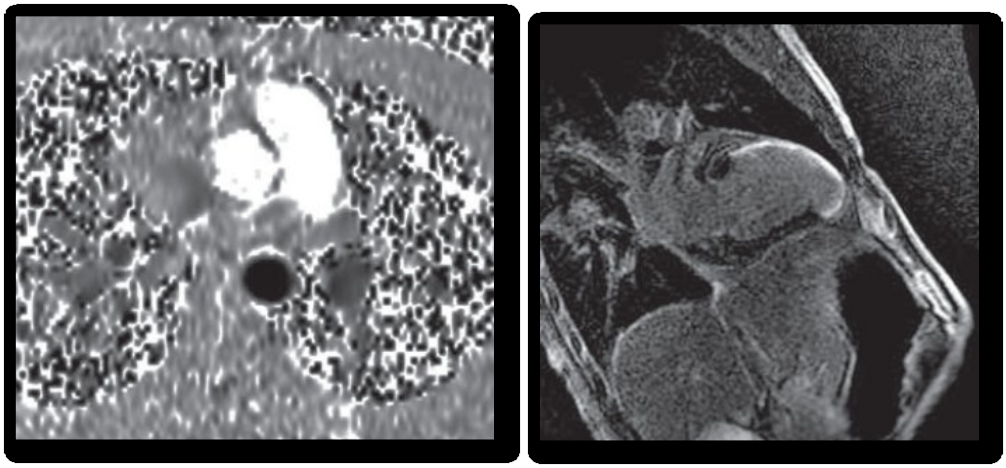

Fig 3.12 Transverse aortic phase-contrast images of a normal subject (Left) Two-chamber delayed enhancement view (Right) shows transmural infarct in the anterior wall, apex, and inferoapex in distribution of LAD

Fig 3.13 Contrast-enhanced cardiac MRI oblique sagittal view of a normal person

Traditional Fibrosis detection by Cardiac MR imaging

Cardiac MR imaging has relied primarily on a qualitative characterization of the myocardium through visual analysis of characteristic enhancement patterns on late gadolinium-enhanced (LGE) MR images. By using a T1-weighted inversion recovery sequence (to null normal myocardium), after gadolinium administration, the signal difference between normal myocardium and focal fibrosis can be identified. Areas of fibrosis demonstrate greater gadolinium accumulation which is represented as a region of high intensity signal with a shorter T1 time than adjacent normal tissue [13].

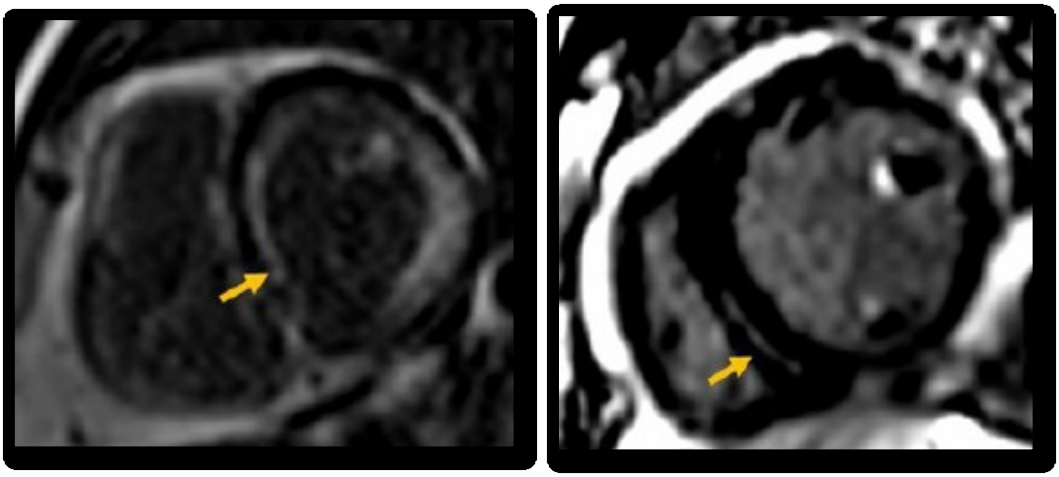

Fig 3.14 Late gadolinium-enhanced (LGE) MR images: Global subendocardial LGE in Amyloidosis (Left), Midwall LGE in Dilated cardiomyopathy (Right)

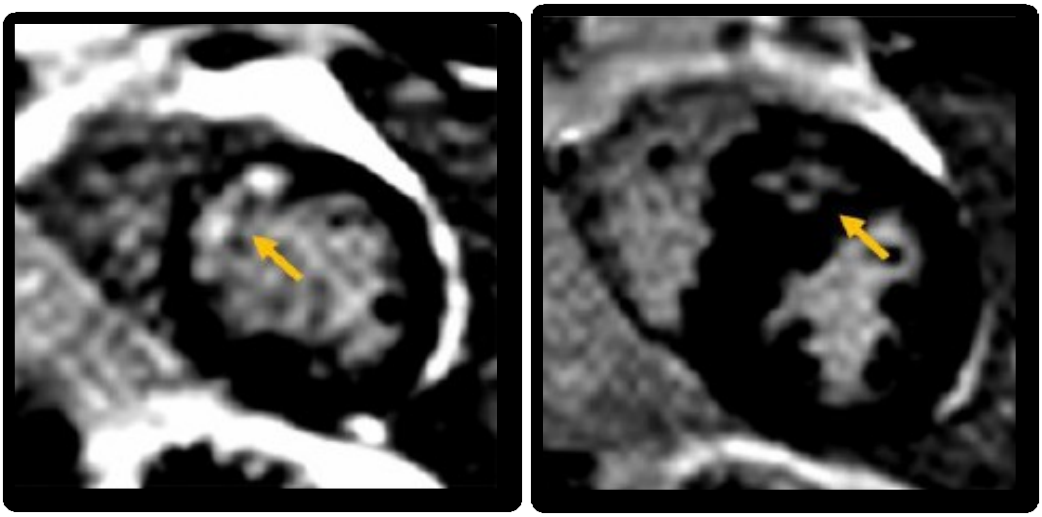

Fig 3.15 Transmural LGE in Ischemic cardiomyopathy (Left), Patchy LGE in Hypertrophic cardiomyopathy

The main limitations of traditional LGE MR images are the identification and characterization of enhancement patterns is subjective, susceptible to inter- and intraobserver variations and that diffuse fibrosis may go undetected, as normal myocardium is needed as a standard of reference to contrast with a pattern of enhancement. To surpass these limitations, new tissue characterization strategies have been proposed, including the so-called T1 and T2 mapping technique.

T1 Mapping technique

T1 mapping refers to parametric maps that are generated from a series of images acquired with different T1 weighting so that each pixel can be assigned a T1 value. T1 maps can be displayed using colour or threshold scales to enable quantitative and visual interpretation. Measured myocardial T1 values are influenced by physiological and technical factors, such as temperature, age, sex, heart rate, field strength and the pulse sequence used.

Multiple CMR T1-based techniques have been employed for quantification of diffuse fibrosis (SASHA, SAPHIRE, etc.). Different T1 mapping sequences possess varying sensitivities to motion artifacts, heart rate, and intrinsic T1 values ranges. Therefore it is important to take it into consideration when comparing results between different studies. The most assessed T1 mapping sequence has been described by Messroghli et al. and is the MOLLI sequence (modified Look Locker inversion recovery). This technique was designed to overcome the limitations of motion and prolonged acquisition time [13].

T1 Mapping - MOLLI: sequence description

T1 mapping is performed using ECG triggered Look-Locker Inversion Recovery (MOLLI).Three sets of Look-Locker (LL) acquisitions are performed successively with increasing inversion times (TI) within one breath hold. Images are acquired with a specific trigger delay (TD) to select end-diastole in consecutive heartbeats.

The groups of images results in a set of 11 source images (traditional MOLLI protocol), which only differ in their inversion time order. By merging these raw images into one data set, T1 values can be computed for every pixel with three-parameter curve fitting; a map of T1 in the imaging section can then be generated from these pixel values.

T1 maps can be obtained any time before or after gadolinium contrast administration. Native T1 distinguishes normal from abnormal myocardium, reflecting myocardial disease involving the myocyte and interstitium [13].

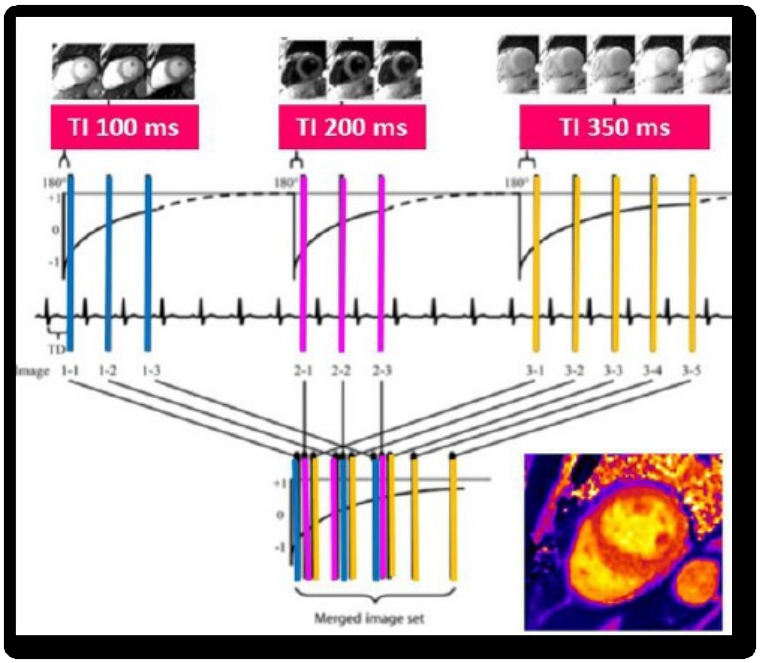

Fig 3.16 Series of images at various inversion times are performed successively, from which a T1 recovery curve is derived. The result is a T1 map that displays the T1 relaxation values pixel by pixel.

NATIVE (noncontrast) T1 MAP

All tissues exhibit a characteristic range of normal T1 relaxation times (longitudinal or spin-lattice) that are based on a composite of their cellular and interstitial components (10). A region of interest (ROI) is placed on the myocardium (4-chamber view or short axis), ensuring that the ROI does not include blood or epicardial fat. The resulting pixel by pixel colour T1 maps are displayed using a customized table (0-2000ms) where normal myocardium is purple and increasing T1 ranges from yellow to orange.

Native myocardial T1 relaxation times vary by magnetic field strength (1.5 vrs.3-T units), equipment manufacturer, and the type of mapping sequence used. Native T1 reflects myocardial disease involving the myocyte and the interstitium. A prolonged native myocardial T1 signal is encountered in various disease states that result in edema or fibrosis, and in amyloid deposition. Shortening of the native T1 relaxation time can be seen with siderosis, Anderson-Fabry disease, and fat deposition. In addition, native T1 does not need to exclude patients with severe renal dysfunction or pregnancy [13].

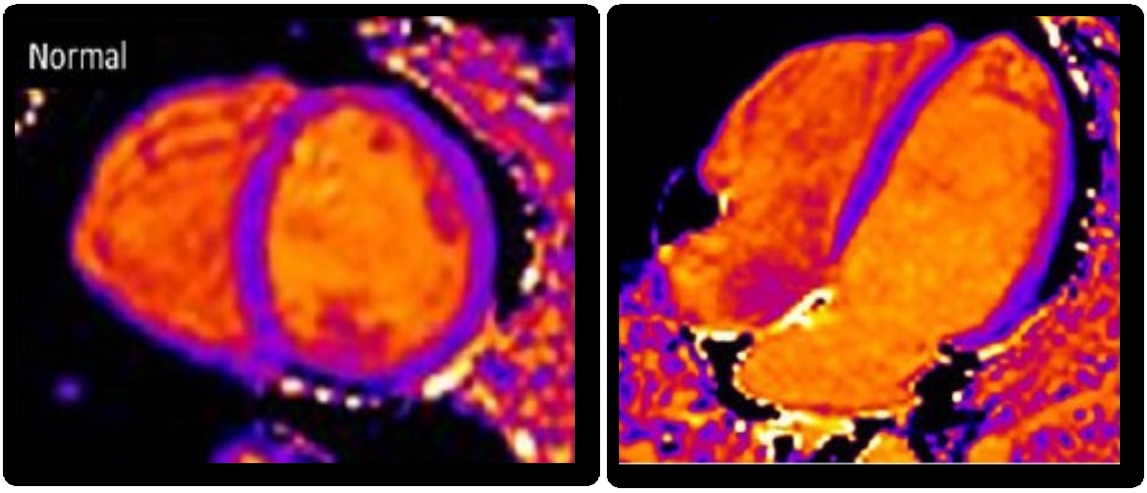

Fig 3.17 Native T1 mapping in a normal person

Contrast-enhanced T1 Mapping

The use of gadolinium-based contrast agents shortens the native T1 relaxation time of myocardium. Areas with a disproportionate accumulation of contrast material (fibrosis) will therefore exhibit shorter T1 relaxation times. However, isolated postcontrast T1 values are influenced by a number of factors, including native T1, the type and dosage of gadolinium contrast used, and the postcontrast acquisition time within the contrast pharmacodynamics redistribution process. The latter depends on numerous systemic variables, such as body fat percentage, hematocrit levels, and glomerular filtration rate [13].

Extracellular Volume (ECV) measurement

Nonenhanced and contrast-enhanced T1 mapping allows evaluation of the proportion of gadolinium-based contrast agent in the blood pool versus in the myocardium. In conjunction with the hematocrit value, mapping enables quantification of the proportion of extracellular (interstitium and extracellular matrix) myocardial volume to cellular (myocyte) volume. An increased ECV is a marker of myocardial remodelling and is most often due to excessive collagen deposition (in the absence of amyloid or edema), which culminates in mechanical, electrical and vasomotor dysfunction. The ECV may be estimated from the concentration of extracellular contrast agent in the myocardium relative to the blood in a dynamic steady state .ECV can be calculated using a specific formula. The reported range of the ECV in healthy subjects is 21%-27% [36].

$$\mathrm{ECV} = \left(1 - \mathrm{hematocrit}\right)\frac{\left(1/\mathrm{T1\,myopost} - \mathrm{T1\,myopre}\right)}{\left(1/\mathrm{T1\,bloodpost} - \mathrm{T1\,bloodpre}\right)}$$

Clinical applications

The presence of fibrosis has been shown to be an independent risk factor for overall mortality and the possible need for cardiac transplantation [6]. Quantifying the degree of fibrosis may guide treatment with regard to revascularization, device implantation, and medical therapy.

Mapping can also noninvasively represent a "sample" of tissue from the entire myocardium and can supplement or potentially replace invasive transvenous myocardial biopsy. Further, it may help identify the most appropriate location for biopsy, if biopsy is deemed clinically necessary [13].

T1 mapping has the potential to be a useful technique for quantification of diffuse myocardial fibrosis in a variety of clinical settings, such as hypertrophic cardiomyopathy, dilated cardiomyopathy, amyloidosis and acute myocardial infarction.

T2 MAPPING

T2W magnetic resonance imaging pulse sequences have been used to detect oedema in patients with acute myocardial infarction, differentiate acute from chronic infarction, and identify acute myocarditis. The T2 mapping technique can accurately and reliably detect areas of myocardial oedema without the limitations of qualitative T2W imaging. T2 mapping sequences are useful for the detection of myocardial oedema due to acute myocardial infarction, myocarditis, stress cardiomyopathy, sarcoidosis, and cardiac allograft rejection [69]. T2 mapping is considered superior compared with standard CMR parameters, global myocardial T1 mapping, and ECV for assessing the activity of myocarditis inpatients with recent-onset heart failure and reduced left ventricular function. Furthermore, T2 mapping was proven to be a novel

non-invasive tool for transplant monitoring, and initial findings support its potential role in rejection detection [69].

However, T2W sequences have various problems including (a) signal intensity variability caused by phased array coils, (b) high signal from slow-moving ventricular blood that can mimic and mask elevated T2 in subendocardium, (c) motion artefacts, and (d) the subjective nature of T2W image interpretation.

Limitations of T1 and T2 Mapping

T1 and T2 mapping offer quantitative assessment of changes in tissue composition. However, one of the major obstacles for their clinical use is the variation in native T1 and T2 values related to imaging equipment and sequence. Further investigation is needed to establish "normal normal" reference ranges for native T1 and T2 relaxation values because there is great variation among manufacturers, magnetic field strengths, and clinical parameters.

These reference values are required to distinguish various disease conditions from normal myocardium, especially in cases of diffuse disease. Knowledge of the properties of specific MR scanners is necessary for the clinical application of these techniques.

Furthermore, the full clinical utility of T1 and T2 mapping is yet unknown because many diseases have not been adequately studied. There are still pending questions about (a) the potential replacement of LGE by native T1 mapping in the assessment of fibrosis, (b) whether native T1 mapping is more useful than T2 mapping in the evaluation of myocardial infarction, or whether they are complementary, and (c) how ECV can influence the clinical management of patients with heart disease [69].

HYPERTROPHIC CARDIOMYOPATHY

Traditional cardiac MR imaging plays a valuable role in the analysis of ventricular morphology and function, with contrast-enhanced studies revealing patchy delayed enhancement in areas of hypertrophy. However, carriers of the mutation may have increased diffuse myocardial fibrosis without showing any other phenotypic trait of the disease. In this population, T1-mapping techniques may be extremely helpful. In addition to its use in primary diagnosis, myocardial mapping may also be useful on the prognosis and stratification of risk for adverse events by providing a longitudinal quantitative follow up of the degree of fibrosis.

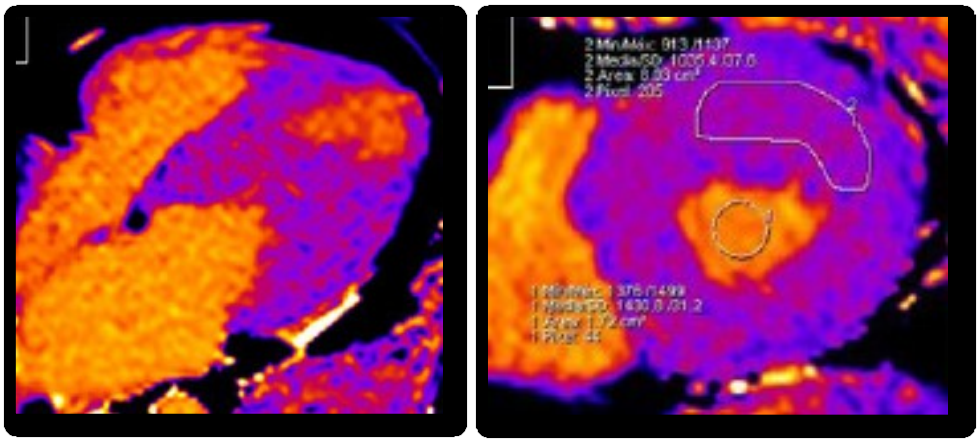

Fig 3.18 T1 mapping in hypertrophic cardiomyopathy. Four chamber view (Left) Short-axis nonenhanced MOLLI T1 map demonstrates prolonged T1 values in the area of myocardial hypertrophy (Right)

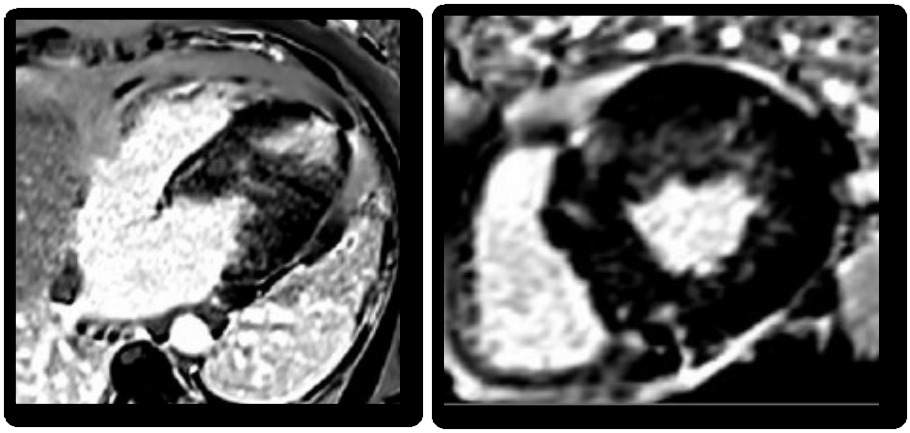

Fig 3.19 LGE MR image four-chamber and two-chamber view through the same plane shows patchy wall enhancement characteristic of hypertrophic cardiomyopathy

DILATED CARDIOMYOPATHY

By detecting the pattern of fibrosis, LGE contributes significantly to ruling out ischemic etiology (excluding subendocardial enhancement) in cases of dilated cardiomyopathy. Cardiac mapping can quantify the degree of myocardial T1 abnormality and thus the degree of underlying fibrosis, which may have diagnostic and prognostic value [13].

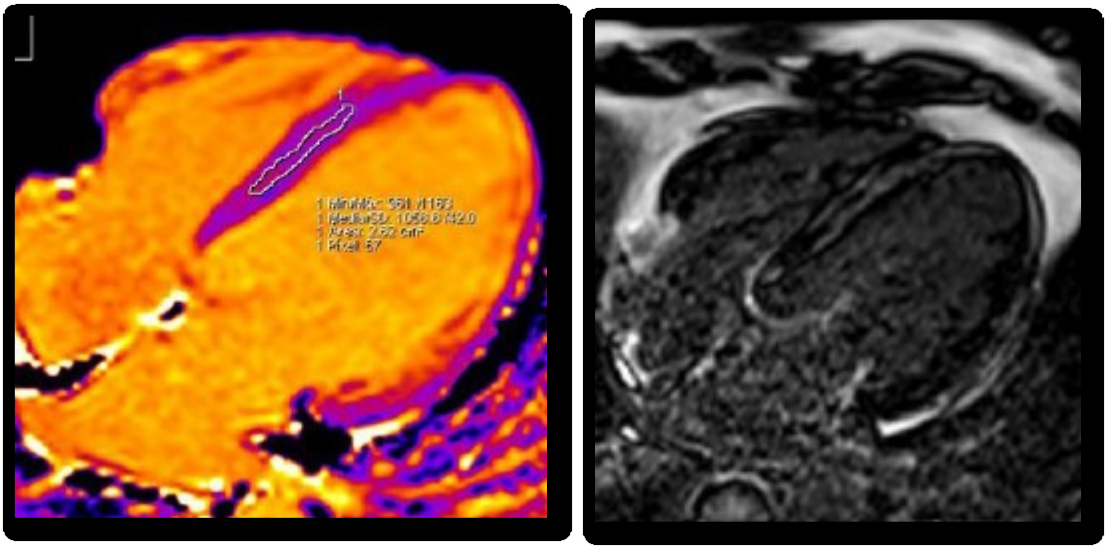

Fig 3.20 T1 mapping in nonischemic dilated cardiomyopathy. Four-chamber nonenhanced T1 map shows elevated diffuse T1 values (Left). Four-chamber LGE MR images show mesocardial enhancement.

RESTRICTIVE CARDIOMYOPATHY - AMYLOIDOSIS

The classic pattern on LGE T1-weighted MR images is global left ventricular subendocardial enhancement. Added features include left ventricular hypertrophy and abnormal diastolic function. In cases of diffuse myocardial involvement, the lack of a normal region of myocardium for comparison can make traditional cardiac MR images difficult to interpret.

Noncontrast T1 mapping and myocardial ECV fraction are effective methods to noninvasively quantify cardiac amyloid burden and provide diagnostic information in

patients with suspected cardiac amyloidosis. An elevated myocardial T1 value reflects the severity of cardiac involvement and correlates well with markers of systolic and diastolic dysfunction [16].

T1 mapping has also demonstrated to be effective in distinguishing subtypes of amyloidosis, as that T1 times in hereditary amyloidosis may not be as high as in the AL subtype. This differentiation is clinically relevant because treatment and prognosis vary by subtype [13].

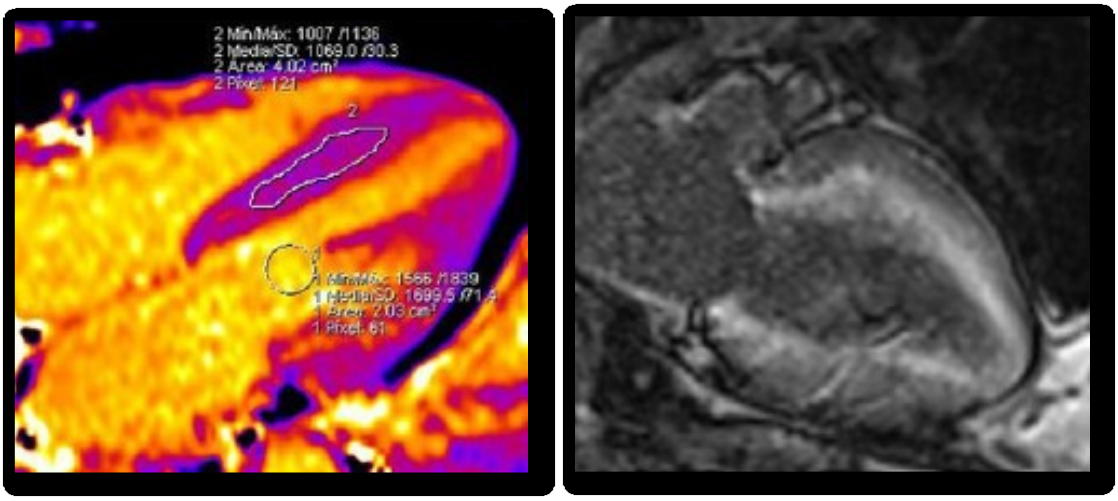

Fig 3.21 T1 mapping in amyloidosis. Nonenhanced four chamber MOLLI T1 map shows diffusely increased T1 values (Left). Two chamber LGE MR image shows subendocardial enhancement (Right).

MYOCARDITIS

Cardiac MR imaging is the imaging tool of choice in diagnosing acute myocarditis. Subepicardial patchy or nodular LGE in conjunction with an underlying wall-motion abnormality is a classic finding during the first week; however, the enhancement pattern usually becomes diffuse within 7 days after infection.

T1 mapping has shown higher sensitivity compared with T2-weighted and LGE MR imaging techniques alone, in the detection of acute myocarditis [13].

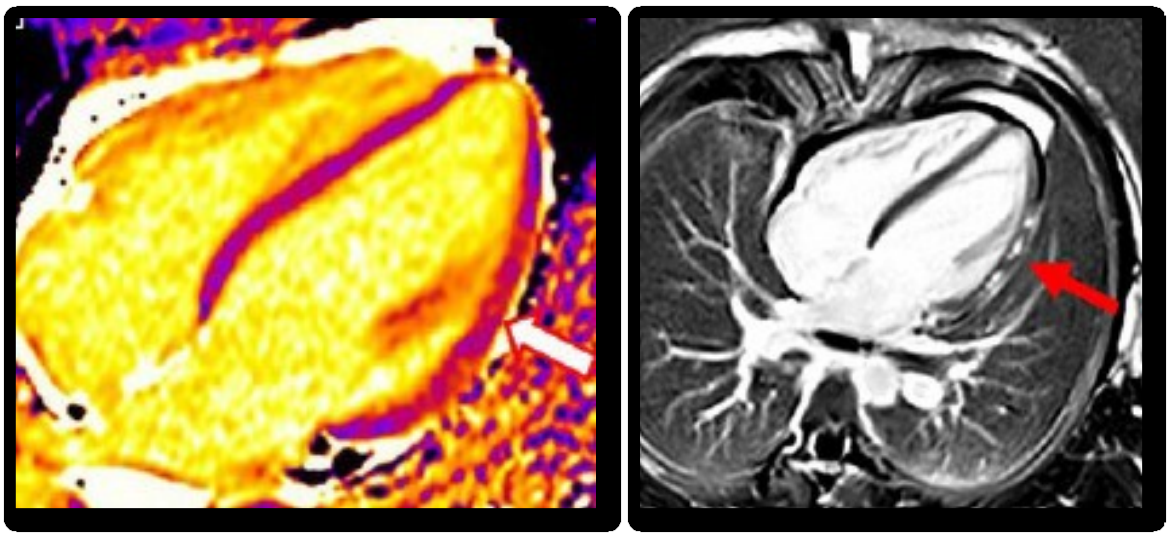

Fig 3.22 T1 mapping in myocarditis. Four-chamber nonenhanced MOLLI T1 map shows prolonged focal areas of T1 relaxation times in the lateral wall (Left), corresponding to the epipericardial enhancement on four chamber LGE (Right).

MYOCARDIAL INFARCTION

Magnetic resonance (MR) imaging plays an important role in evaluating the various stages of MI. MR imaging is valuable in establishing a diagnosis of chronic MI and distinguishing this condition from nonischemic cardiomyopathies, mainly through use of delayed-enhancement patterns. MR imaging also provides clinicians with several prognostic indicators that enable risk stratification, such as scar burden, microvascular obstruction, hemorrhage, and peri-infarct ischemia. The extent and transmurality of scar burden have been shown to have independent and incremental prognostic power over a range of left ventricular function. The extent of scarring at MR imaging is an important predictor of successful outcome after revascularization procedures, and extensive scarring in the lateral wall indicates poor outcome after cardiac resynchronization therapy. Scar size at MR imaging is also a useful surrogate end point in clinical trials. Finally, MR imaging can be used to detect complications of

MI, such as aneurysms, pericarditis, ventricular septal defect, thrombus, and mitral regurgitation.

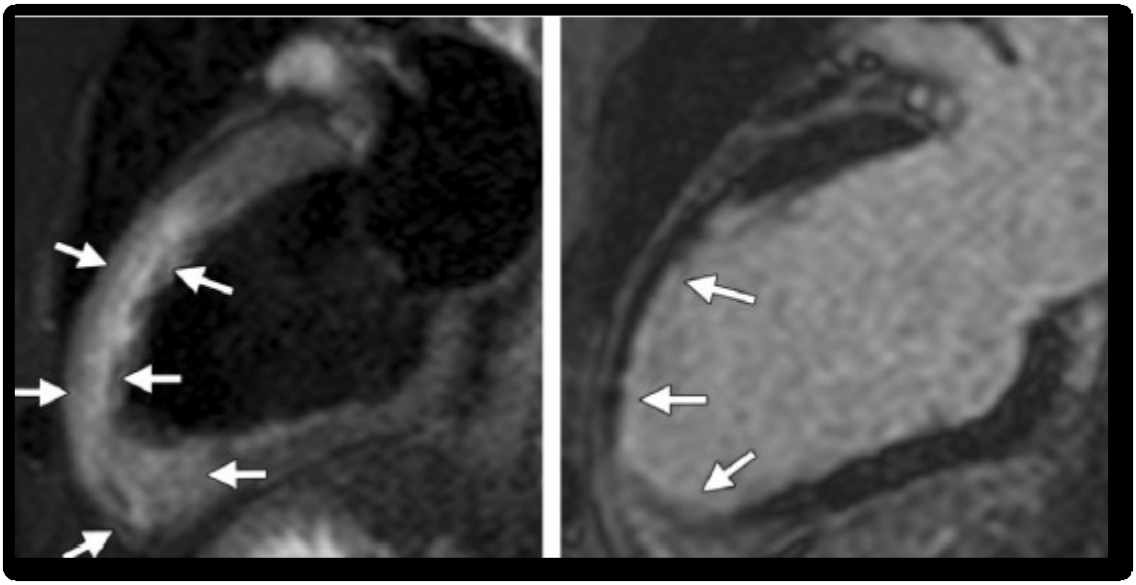

Fig 3.23 MR imaging findings in acute MI. Two-chamber T2-weighted STIR image shows high-signal-intensity myocardial edema in the mid and apical anterior wall (Left). Two-chamber delayed-enhancement image shows subendocardial scarring in the mid to apical anterior wall (Right)

ARRHYTHMOGENIC RIGHT VENTRICULAR DYSPLASIA

CMRI black blood spin echo (SE) images will show fibrofatty replacement of the RV free walls (fat saturation will enhance this accuracy). However, recently black blood imaging is thought to be less sensitive in diagnosis of ARVC compared to demonstration of RV systolic and diastolic dysfunction. Thus, cine imaging with a quantitative measure of increased RV volumes (end-diastolic volume >150 mL, end-systolic volume >70 mL indexed to body surface area) is also diagnostic.

Apart from the above volume and functional abnormalities, other morphologic irregularities in tissue characterization that may occur in ARVC include focal wall thinning (<2 mm), wall hypertrophy (>6 mm), moderator band hypertrophy, and trabeculae thickening.

LGE can demonstrate scarring of the RV wall. However, it should be noted that infiltration of the RV free wall also occurs in elderly and obese patients as well as long-term steroid users. In addition, LGE of the RV myocardium is also present in cardiac sarcoidosis and chronic right-sided myocarditis. Thus, it is imperative that diagnosis of ARVC should not be based solely on CMRI findings [44].

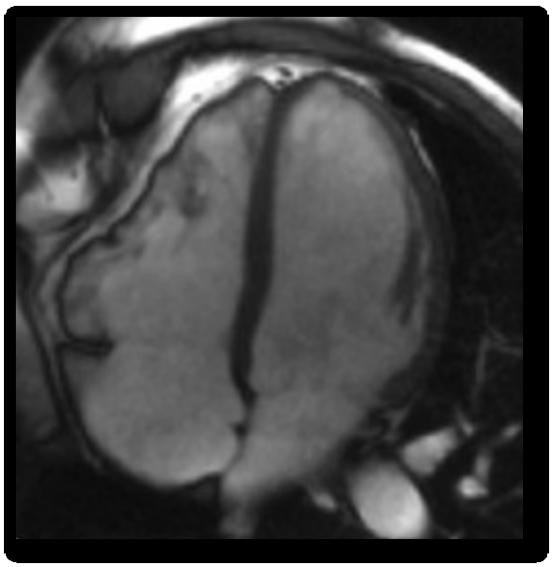

Fig 3.24 Arrhythmogenic right ventricular cardiomyopathy Long-axis four-chamber steady state free precession cine MRI image demonstrating the characteristic irregular contour of the right ventricular free wall

PREVIOUS STUDIES ON MYOCARDIAL T1 AND T2 MAPPING:

A review of the literature revealed some articles which studied myocardial T1 and T2 mapping in evaluation of myocardial diseases.

Dabir et al[70]**,**who used a 3 T scanner (Ingenia, Philips Healthcare, Best, The Netherlands) and Modified Look- Locker inversion recovery for T1 mapping reported mean native T1 value of 1052 ± 23ms in healthy controls.

Dass et al[71], who used a Siemens 3T Trio MR system (Siemens Healthcare Erlangen, Germany) and shortened MOLLI for T1 mapping reported a mean native T1 value of 1178±13 ms in normal control patients. The study also reported that mean T1

relaxation time was increased in HCM and DCM (HCM 1209±28 ms, DCM 1225±42 ms, normal 1178±13 ms, P<0.05) and T1 values correlated with disease severity.

Puntmann et al.[72], who used MOLLI sequence for T1 mapping in a 3-T scanner (Achieva TX, Philips Healthcare, Best, the Netherlands) reported a mean native T1 value of 1,070±55ms for subjects with healthy hearts. They also reported that native T1 value was significantly longer in patients with cardiomyopathy (HCM 1,254±43ms, NIDCM 1,239±57ms) compared with control subjects (1,070±55ms) ($p < 0.01$) and that native T1 could differentiate between healthy and diseased myocardium with high diagnostic accuracy.

Lurz et al.[73], who also performed T1 mapping with a modified Look-Locker inversion recovery sequence in a 3-T scanner (Verio, Siemens Healthcare, Erlangen, Germany) reported mean native T1 value of 1,159±62ms for subjects with healthy hearts and that values for native T1 were significantly higher in patients with acute myocarditis (1,203±71ms) than in patients with no myocarditis.

Leutkens et al[74] reported mean native T1 value of 1089.1±44.9ms in control subjects using 3-T MR imaging system (Ingenia 3T; Philips Healthcare, Best, the Netherlands) andMOLLI for T1 mapping. They observed that native T1 relaxation times were significantly longer in patients with acute myocarditis than in control subjects (1185.3±49.3 vs 1089.1±44.9, respectively; $P < .001$).

Hinojar et al[75] reported a mean native T1 value of 1,045±23ms in subjects with healthy hearts using a 3.0-T scanner (Achieva, Philips Healthcare, Best, the Netherlands). This study reported mean native T1 value of 1,189±52ms in acute myocarditis and that native T1 was superior to T2-weighted imaging and late

gadolinium enhancement with high diagnostic accuracy and positive and negative predictive values to distinguish health and disease.

Toussaint et al.[76]**,** who used a 3 Tesla scanner (Magnetom Trio Tim; Siemens AG Healthcare Sector, Erlangen, Germany) and MOLLI sequence for myocardial T1 was determined reported mean native T1 value of 1155.3±63.9ms in subjects with healthy hearts and a mean T1 relaxation time of 1179.2±48.3ms in myocarditis cases.

Boomen et al.[77], in their systematic review and meta-analysis of native T1 reference values for nonischemic cardiomyopathies reported a weighted mean T1 value of 1081±45 msec in controls at 3T. Their systematic review and meta-analysis concluded that native T1 mapping can potentially assess myocardial changes in HCM, DCM, MC compared to controls. They reported a mean T1 value of 1166±55 msec in HCM patients and 1193±60 msec for DCM patients. The mean T1 value in acute MC patients was 1193±60 msec. The metaanalysis showed a significant increase of the myocardial T1 values for HCM, DCM patients and acute MC patients compared with controls.

Dall'Armellina E et al[78] reported a mean T1 value of 1257±97 ms in infarcted myocardium normal (n=10) 1166±60ms

von Knobelsdorff-Brenkenhoff F et al[79] reported normal myocardial T2 value of 45.1 ms at 3T [77] .

Spieker et al[80] reported that T2 values were significantly increased in acute myocarditis (68.1 ± 5.8ms) compared to controls (60.0 ± 4.2ms) and decreased over time. Patients with clinical recovery revealed significantly decreased T2 relaxation times at follow-up examinations; however, T2 values were still elevated compared to healthy controls.

4. AIM OF THE STUDY

OBJECTIVES

1. To identify normal baseline T1 and T2 values of myocardium in 3T MRI using Myomaps

2. To assess the value of native T1 and T2 relaxation times in various diffuse myocardial diseases

5 MATERIALS AND METHODS

5.1 Study Area : Barnard Institute of Radiology, Madras Medical College, Chennai.

5.2 Study Period : 12 months (June 2017 – May 2018)

5.3 Sample Size : 52

5.4 Study Design : Prospective study

5.5 Inclusion criteria:

CASES: Subjects with established myocardial disease and cardiac magnetic resonance finding suggestive of the same

CONTROLS: Healthy volunteers who were nonsmokers, had no history of cardiac disease, comorbidities, had a normal ECG and ECHO were taken as controls after obtaining informed consent

5.6 Exclusion criteria:

Patients with orthopnea, claustrophobia, MRI non-compatible devices

5.7 METHODOLOGY

This prospective study was performed after obtaining clearance from our Institutional Ethics Committee and institutional informed consent guidelines were observed.

5.7.1 Study Population:

Between June 2017 and July 2018, 38 unselected consecutive subjects (19 female, 19 male) referred for CMR were primarily included in this study. The patients were screened using the drawn inclusion/ exclusion criteria. Assignment to the above mentioned diagnoses was performed by experienced cardiologists in consensus using

all available clinical information (medical history, ECG, laboratory tests and echocardiography). Diagnosis of myocarditis, DCM, HCM, and RCM was made in accordance to established diagnostic criteria.

12 healthy volunteers who were nonsmokers, had no history of cardiac disease, hypertension, family history of cardiomyopathy or sudden death, had a normal 12-lead ECG and ECHO and no other comorbidities were taken as controls after obtaining informed consent. All patients were required to provide written informed consent before study participation.

5.7.2 MRI Examination:

All MRI studies were done on a 3-Tesla MRI system (MAGNETOM Skyra, Siemens Healthineers, Erlangen, Germany).Coil used was phased array 18 channel body coil.

MRI PROTOCOL

A standardized cardiac MR protocol was used which included the following sequences:

1. T2 HASTE axial
2. True FISP CINE images – four chamber view, two chamber view and short axis views
3. T2 STIR axial in selected cases
4. Native T1 and T2 mapping
5. PSIR post contrast images in selected cases

Retrospective ECG gating was used for Cine True FISP images and prospective ECG gating for other sequences.

For cine imaging steady-state free precession (SSFP) images were acquired in standard long and short axis views (TR 39ms, TE 1.4ms, matrix 139 x 208, field of view 420 x 380 mm2, flip angle 57°, bandwidth 962 Hz/pixel, slice thickness 6 mm).

Native T1 and T2 mapping was performed using Siemens Myomap protocol in short axis slices through the apex, mid-body and base. The average native myocardial T1and T2 values were obtained from region of interest (ROI) drawn in the anterior, septal, inferior and posterolateral walls in each of these slices.

The parameters for native T1 are as follows:

1. For RR interval >700ms, TR 280ms, TE 1.12 ms, matrix 256 x 144, field of view 360 x 306 mm^2, flip angle 35°, bandwidth 1085 Hz/pixel, slice thickness 8 mm;
2. For RR interval <700ms, TR 272ms, TE 1.2ms, matrix 195 x 132, field of view 360 x 307 mm2, flip angle 35°, bandwidth 1085 Hz/pixel, slice thickness 5 mm)

The parameters for native T2 are TR 207ms, TE 1.32ms, matrix 192 x 116, field of view 360 x 288 mm^2, flip angle 12°, bandwidth 1184 Hz/pixel, slice thickness 8 mm;

MYOCARDIAL MAPPING FORMAT

HR, beats/min :

BP, mm Hg :

	BASE				MID-BODY				APEX			
	SEPTUM	ANTERIOR WALL	LATERAL WALL	INFERIOR WALL	SEPTUM	ANTERIOR WALL	LATERAL WALL	INFERIOR WALL	SEPTUM	ANTERIOR WALL	LATERAL WALL	INFERIOR WALL
NATIVE T1 (ms)												
NATIVE T2 (ms)												

CASE 1 – NORMAL CONTROL

History: Normal control

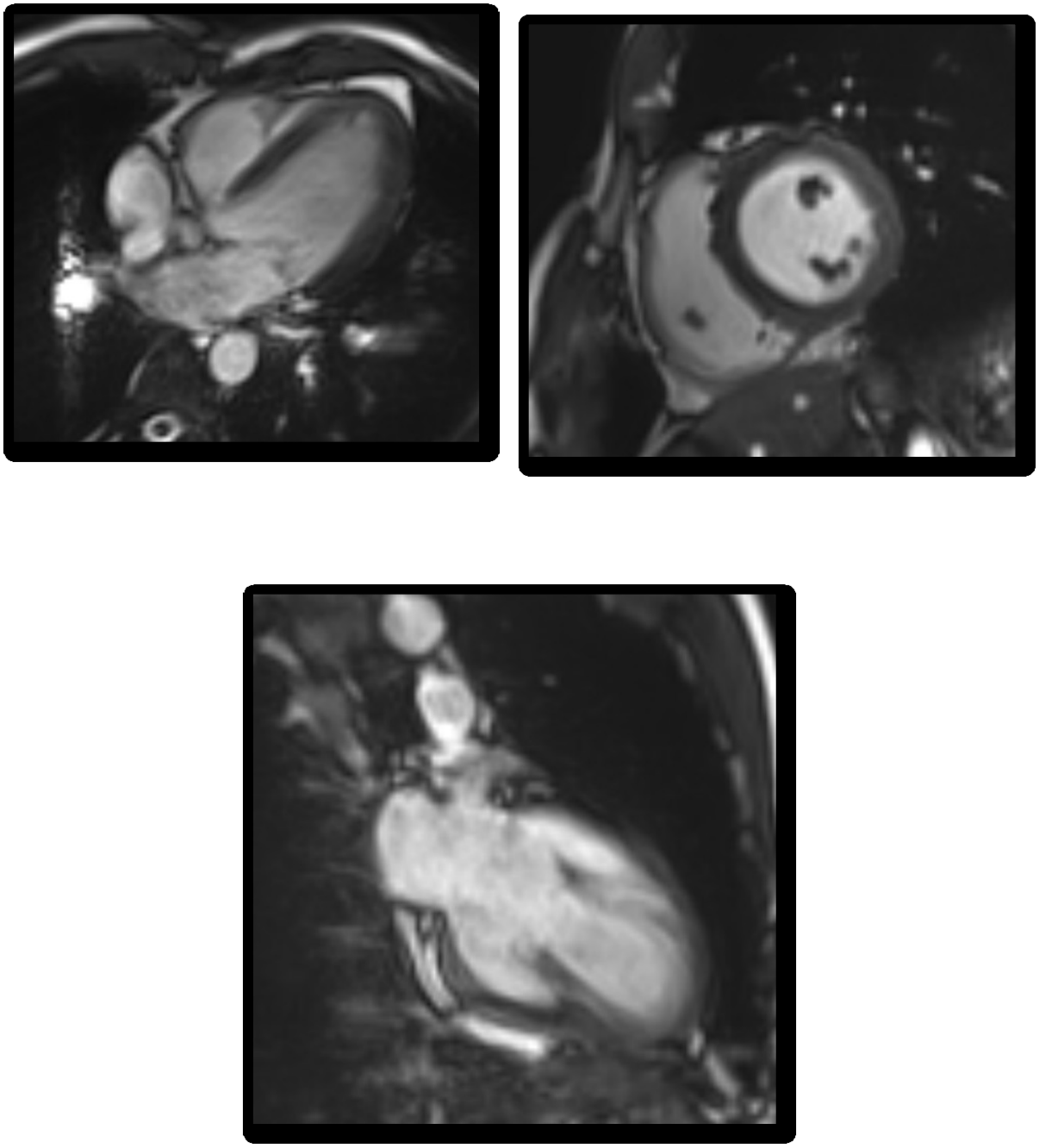

FIG 5.14 True FISP four chamber (top left), short axis midbody (top right) and two chamber (bottom)

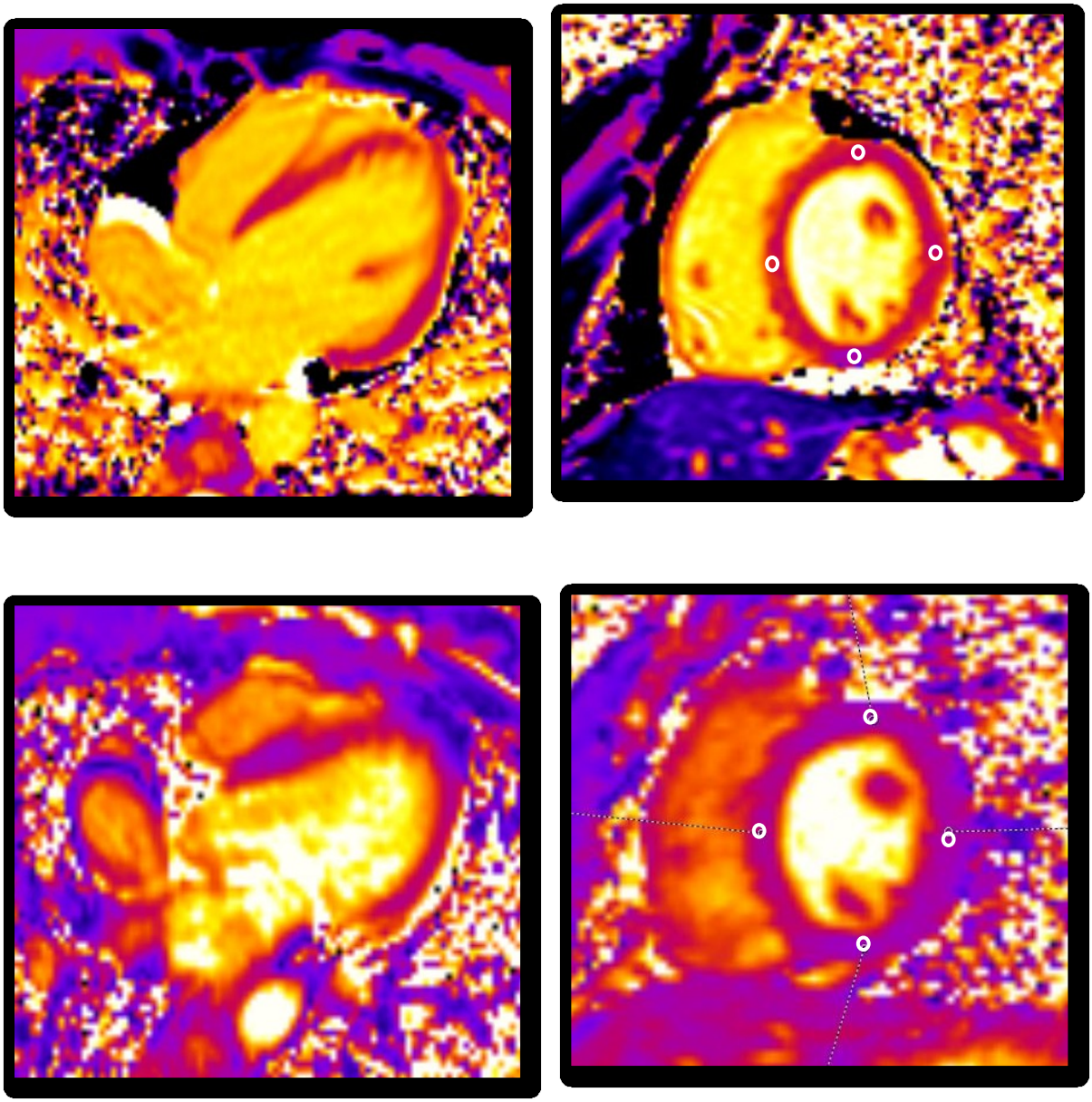

FIG 5.11 Native T1 map four chamber view (top left), short axis mid body (top right) native T2 map four chamber view (bottom left) and short axis mid body (bottom right)

	LV WALL			
	ANTERIOR	**SEPTUM**	**INFERIOR**	**LATERAL**
T1(ms)	1150	1191	1041	1133
T2(ms)	34.7	41	33.8	37.3

Normal mean native T1 and T2 values

CASE 2 - ASYMMETRIC SEPTAL HYPERTROPHIC TYPE OF CARDIOMYOPATHY

History: 16 year old male patient presented with worsening dyspnoea on exertion.

ECHO showed LV hypertrophy involving the interventricular septum.

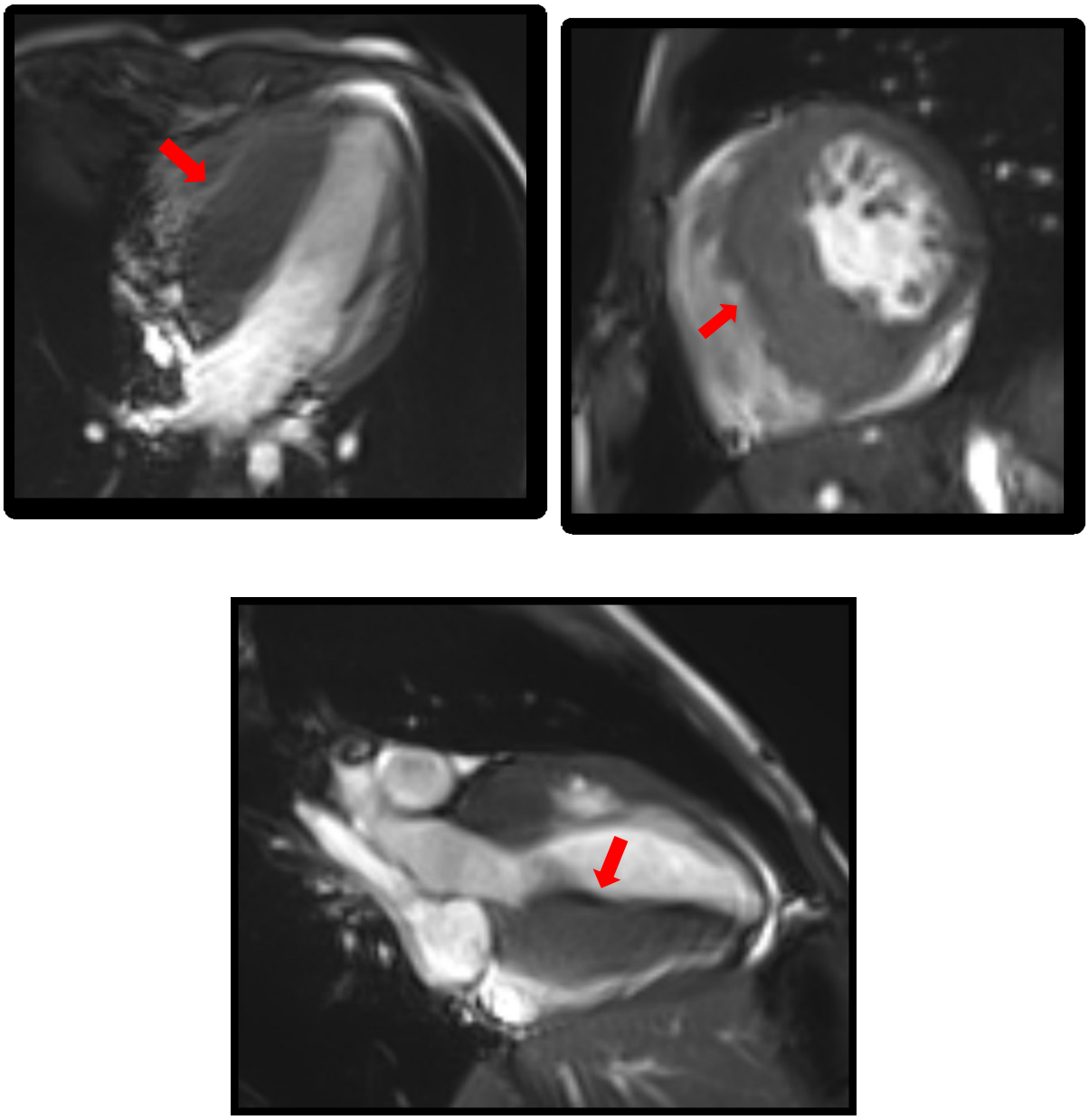

FIG 5.1 White blood imaging four chamber (top left), short axis midbody (top right) and two chamber (bottom) shows asymmetrical hypertrophy of interventricular septum

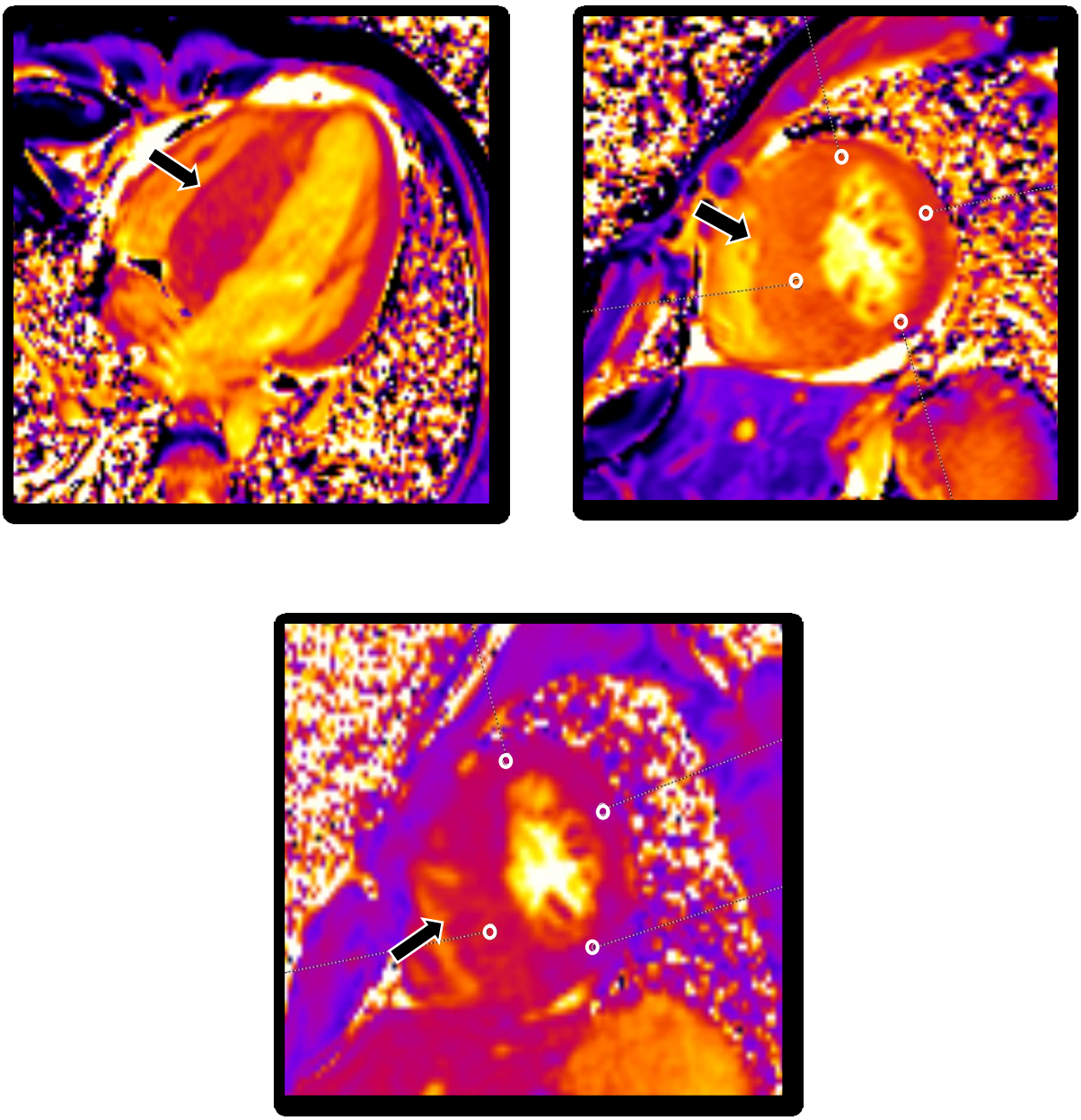

FIG 5.2 Native T1 map four chamber view (top left), short axis mid body (top right) and native T2 map short axis midbody (bottom)

	LV WALL			
	ANTERIOR	**SEPTUM**	**INFERIOR**	**LATERAL**
T1(ms)	1319.8	1389	1265	1275.7
T2(ms)	39	48.8	37.8	36.5

There is increased native T1 values in LV wall especially in the septal wall and increased native T2 value in septal wall

CASE 3 - HYPERTROPHIC CARDIOMYOPATHY CONCENTRIC TYPE

History: 9 year old female patient presented with moderate dyspnoea on exertion.

ECHO showed hypertrophy of LV walls.

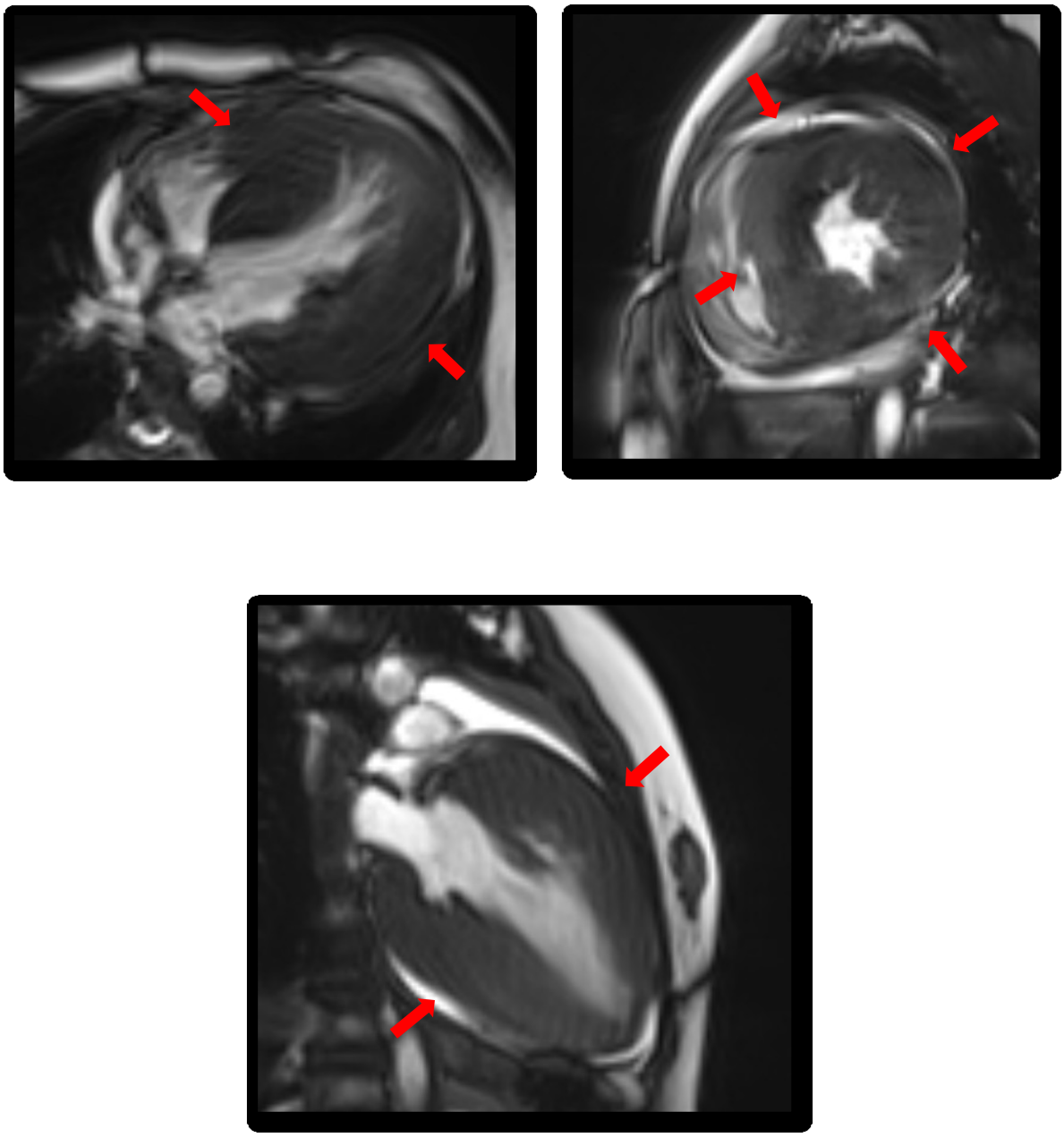

FIG 5.3 White blood imaging four chamber (top left), short axis midbody (top right) and two chamber (bottom) shows concentric hypertrophy of left ventricle

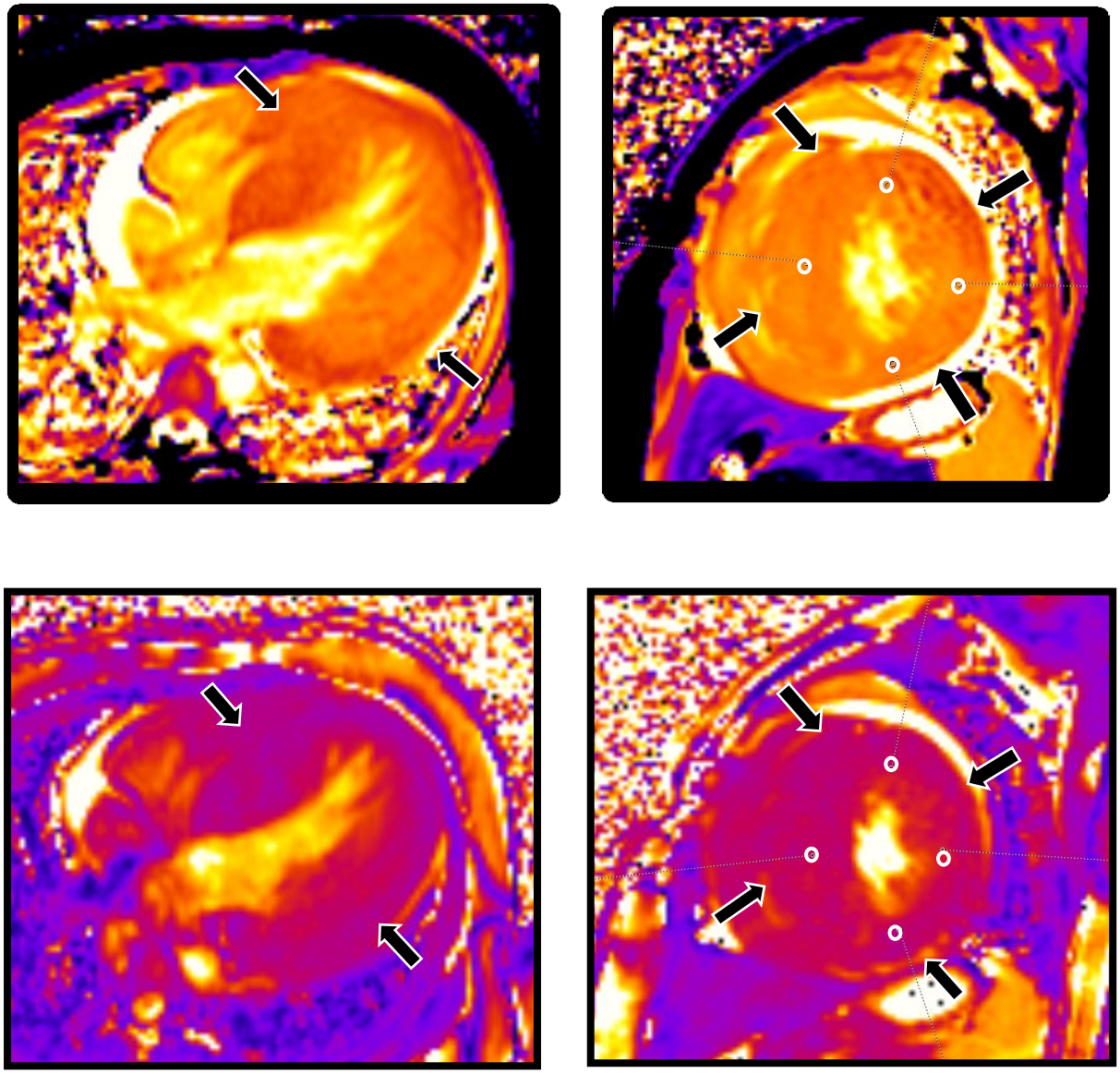

FIG 5.4 Native T1 map four chamber view (top left), short axis mid body (top right) native T2 map four chamber view (bottom left) and short axis mid body (bottom right).

	LV WALL			
	ANTERIOR	**SEPTUM**	**INFERIOR**	**LATERAL**
T1(ms)	1448	1437	1412	1492
T2(ms)	49.6	47.2	44.2	53.2

There is significantly increased native T1 and T2 values in anterior, septal, inferior and lateral LV walls

CASE 4 - DILATED CARDIOMYOPATHY

History: 19 year old male patient presented with breathlessness and pedal edema since childhood. ECHO showed dilated left atrium and left ventricle.

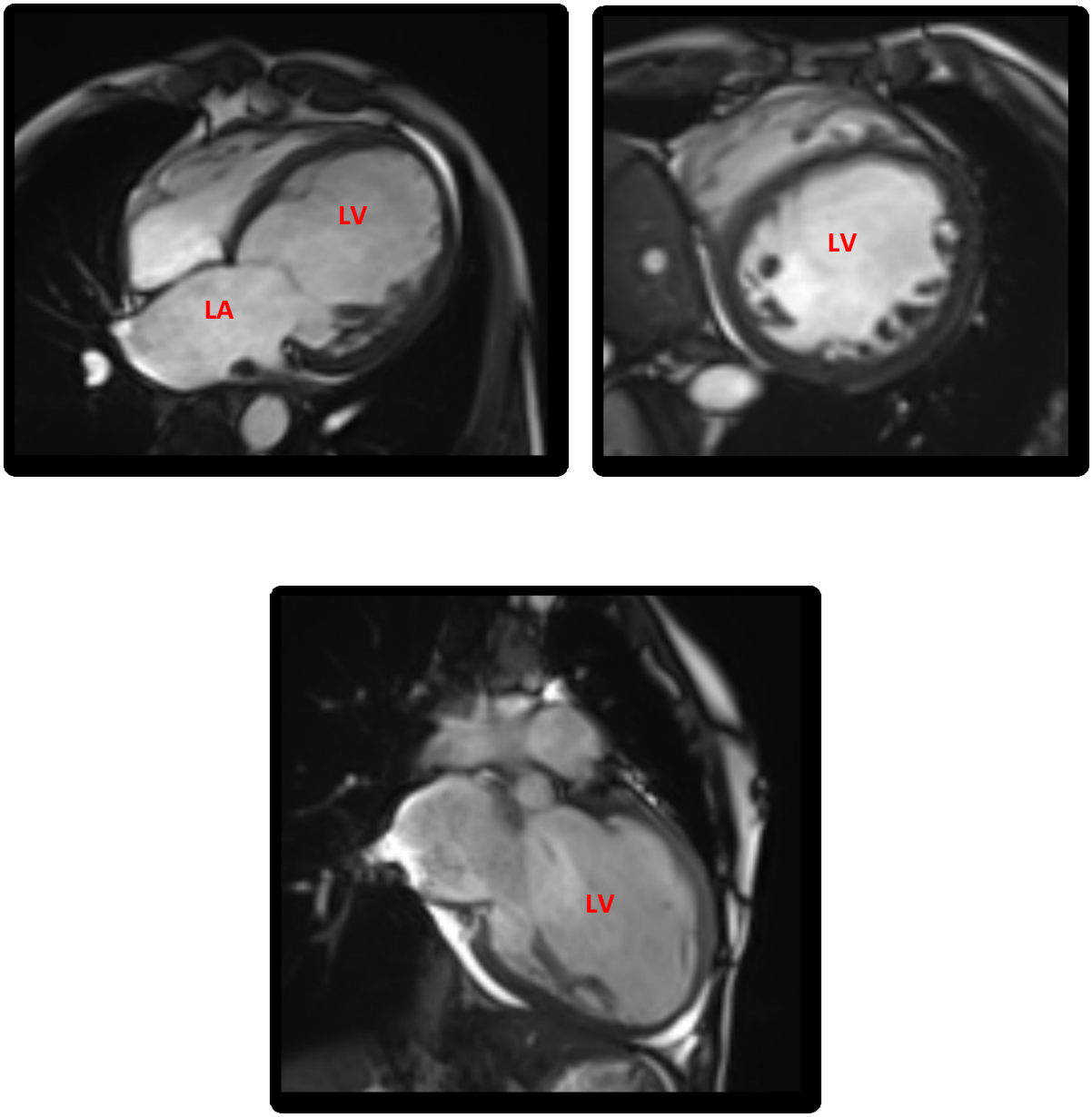

FIG 5.5 White blood imaging four chamber (top left), short axis midbody (top right) and two chamber (bottom) shows mildly dilated left atrium and significantly dilated left ventricle

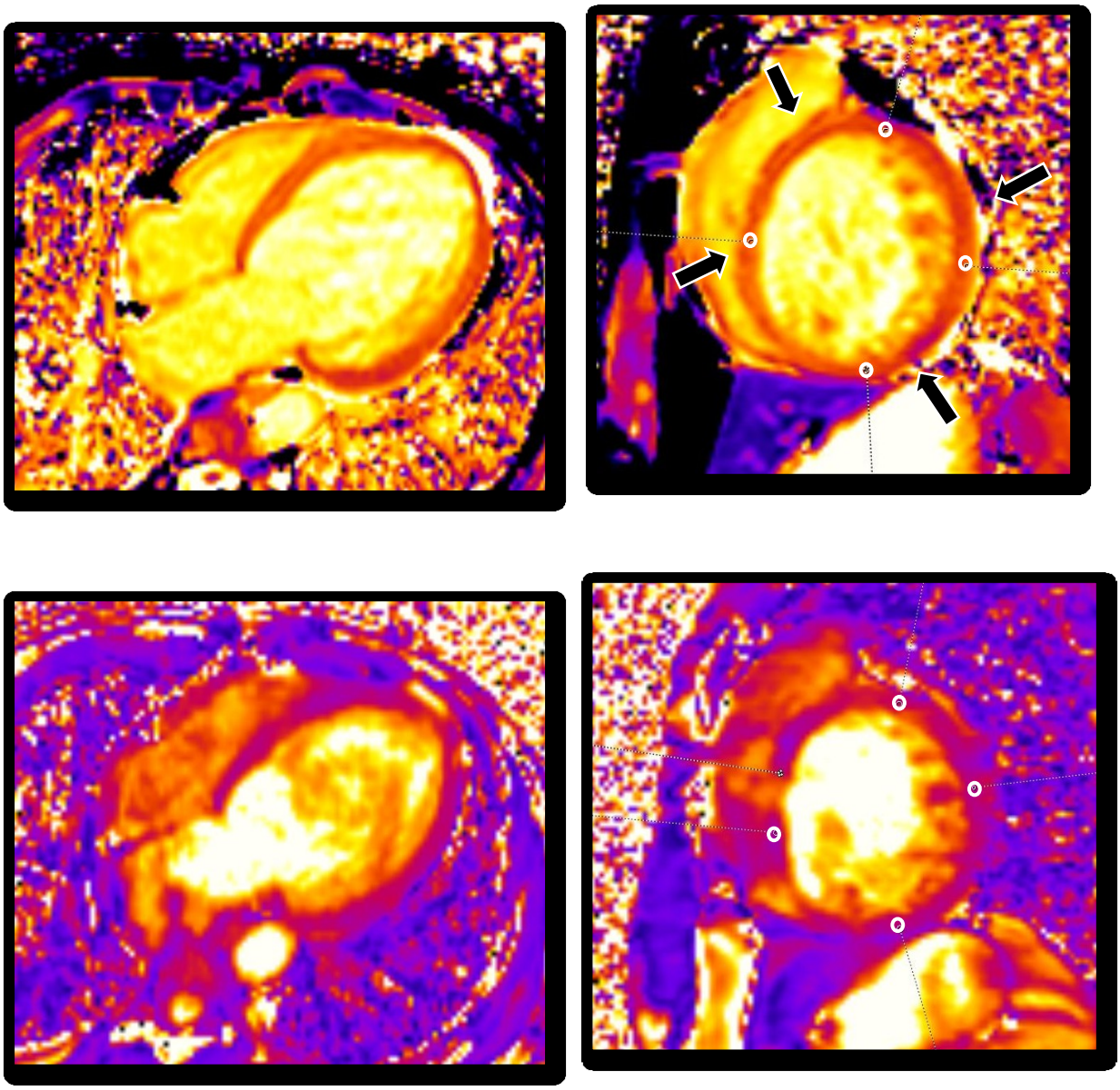

FIG 5.6 Native T1 map four chamber view (top left), short axis mid body (top right) native T2 map four chamber view (bottom left) and short axis mid body (bottom right)

	LV WALL			
	ANTERIOR	**SEPTUM**	**INFERIOR**	**LATERAL**
T1(ms)	1339	1367	1344	1377
T2(ms)	40.7	40.5	41.55	39.9

There is increased native T1 values in anterior, septal, inferior and lateral LV walls. No significantly increased native T2 values.

CASE 5 – RESTRICTIVE CARDIOMYOPATHY (AMYLOIDOSIS)

History: 55 year old male patient presented with shortness of breath. Fatigue and palpitations for past 4 months.

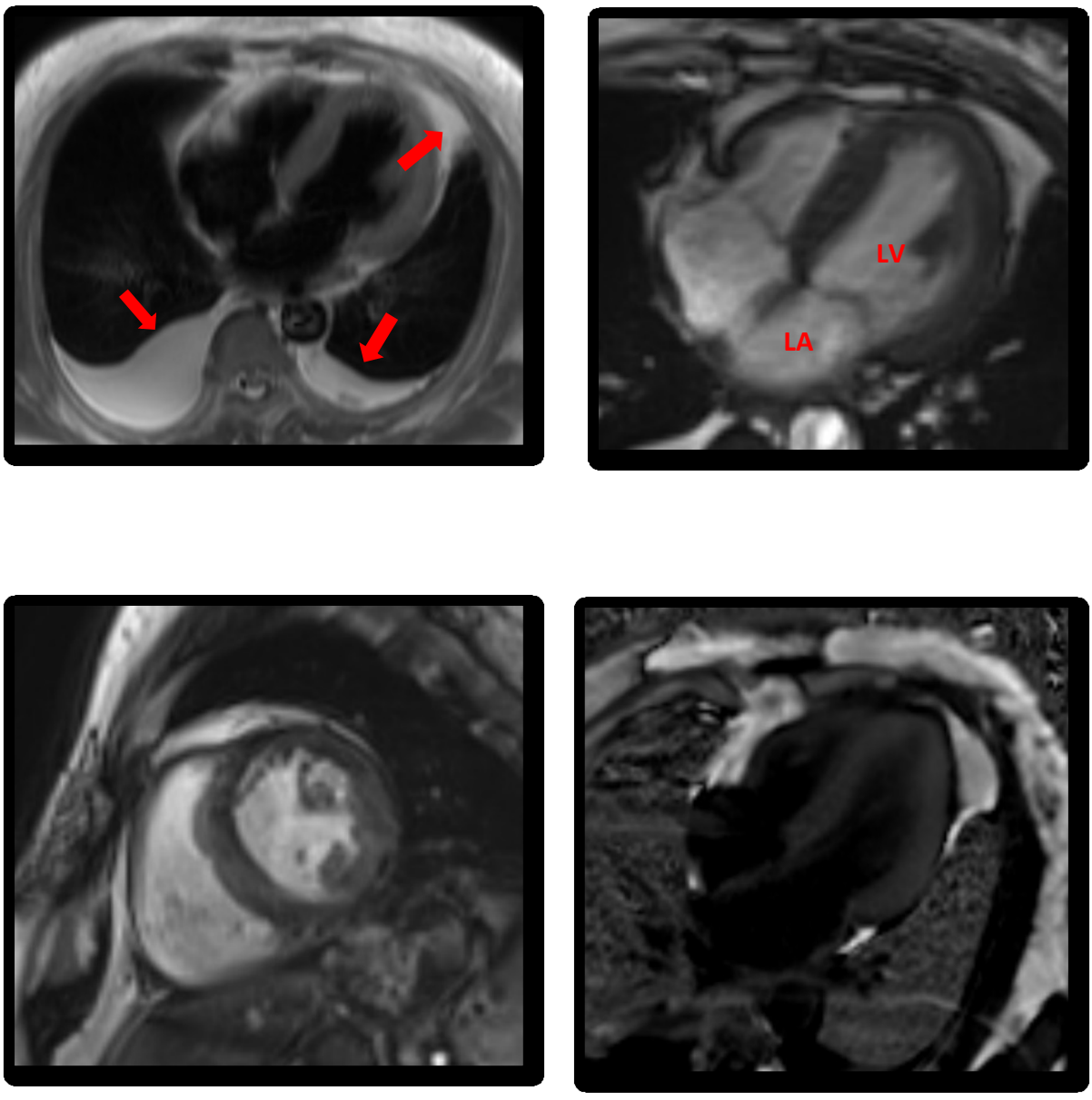

FIG 5.5 T2 HASTE axial (top left), True FISP four chamber (top right) and short axis midbody (bottom) shows mildly dilated left atrium, significantly dilated left ventricle, bilateral pleural effusions, minimal pericardial effusion and diffuse mild patchy delayed upper enhancement.

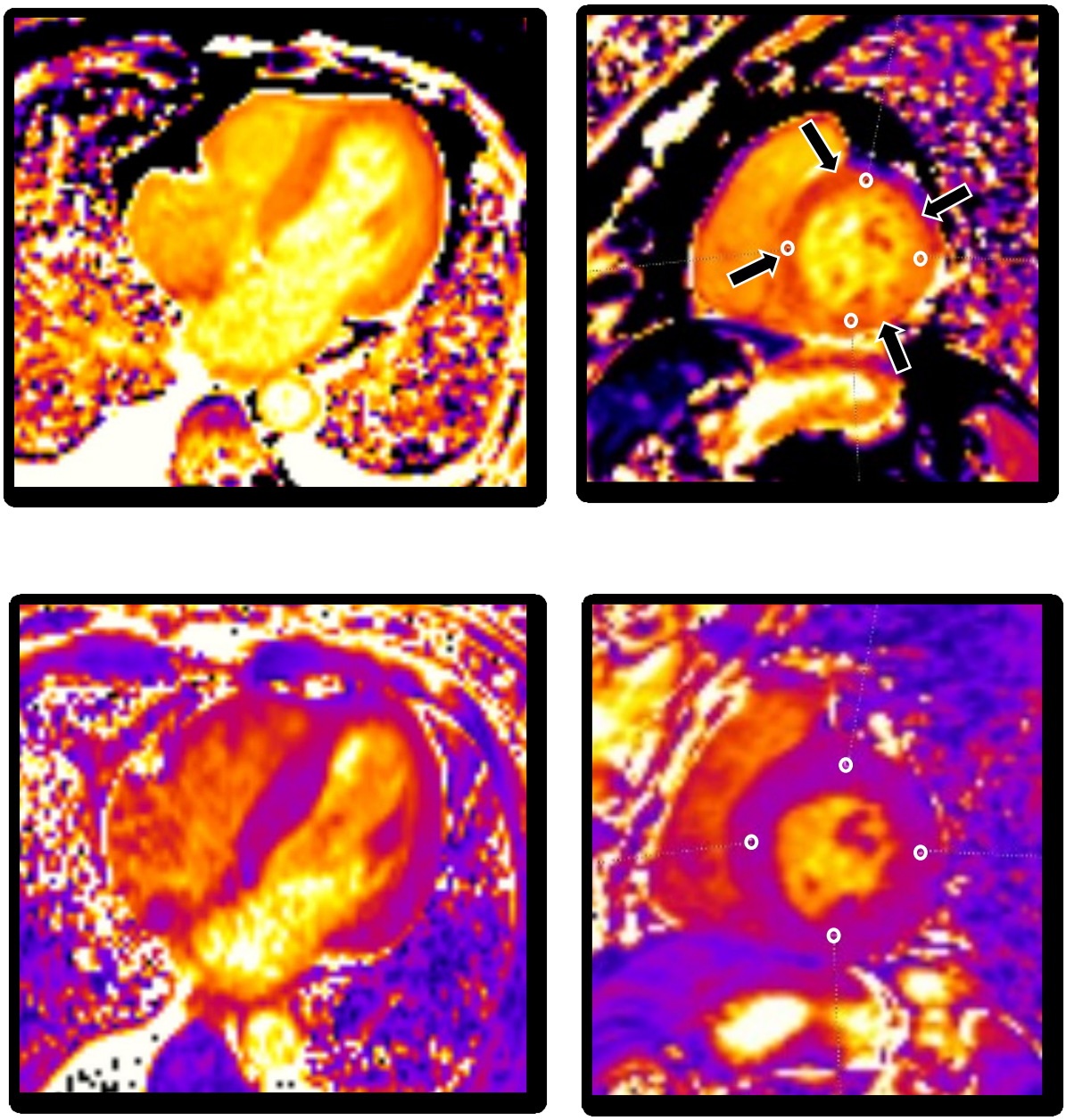

FIG 5.8 Native T1 map four chamber view (top left), short axis mid body (top right) native T2 map four chamber view (bottom left) and short axis mid body (bottom right)

	LV WALL			
	ANTERIOR	**SEPTUM**	**INFERIOR**	**LATERAL**
T1(ms)	1351	1362	1354	1448
T2(ms)	35.3	40.6	40.4	39.5

There is significantly increased native T1 values in anterior, septal, inferior and lateral LV walls. No significantly increased native T2 values.

CASE 6 - RESTRICTIVE CARDIOMYOPATHY (ENDOMYOCARDIAL FIBROSIS)

History: 55 year old male patient presented with dyspnoea and pedal edema.

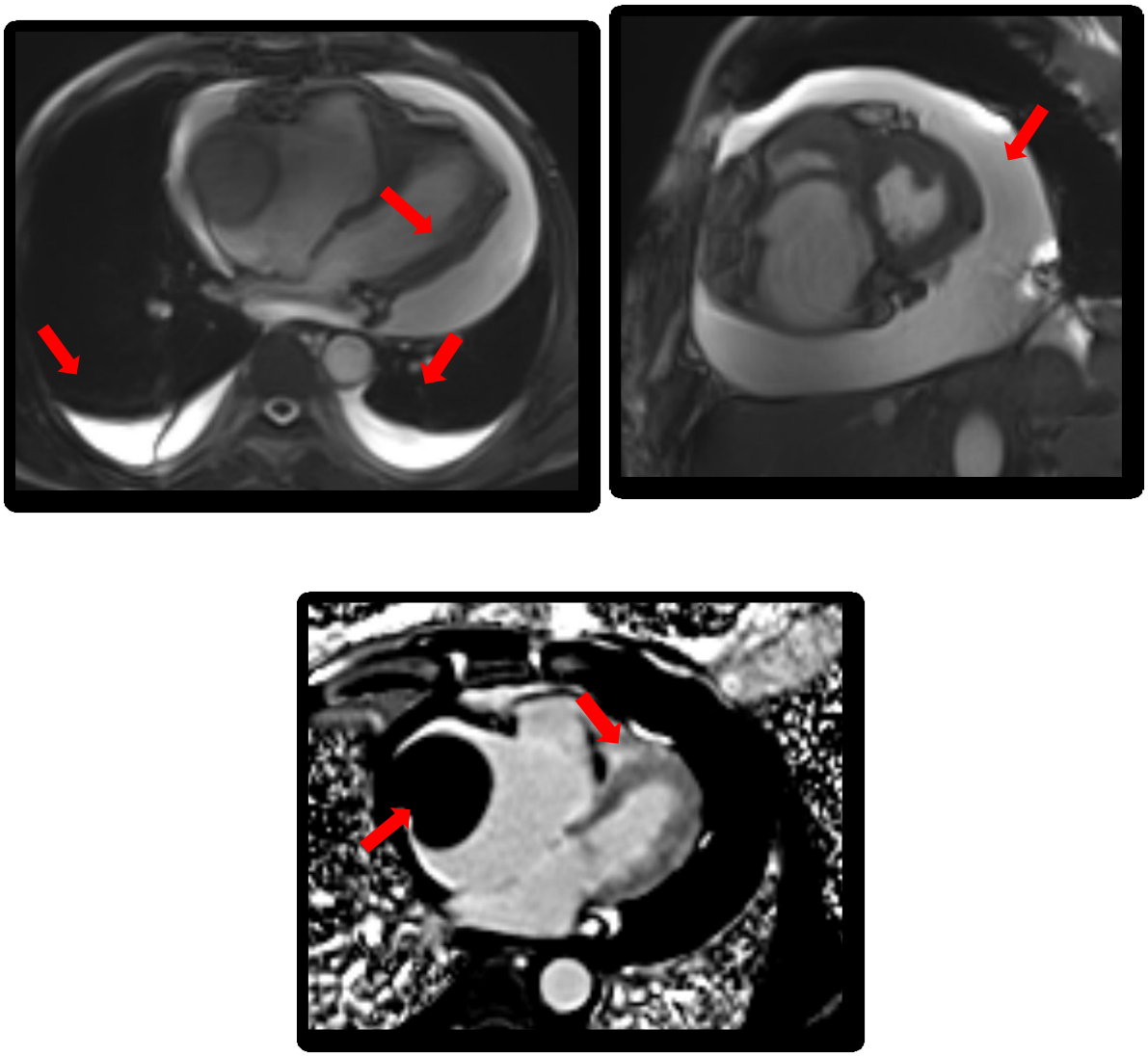

FIG 5.9 True FISP four chamber (top left), post contrast late gadolinium enhancement images (top right) and short axis midbody (bottom) shows apical soft tissue thickening in right ventricle apex with subendocardial delayed hyperenhancement, non enhancing thrombus attached to right atrial free wall, dilated right atrium and right ventricle, bilateral pleural effusions and moderate pericardial effusion

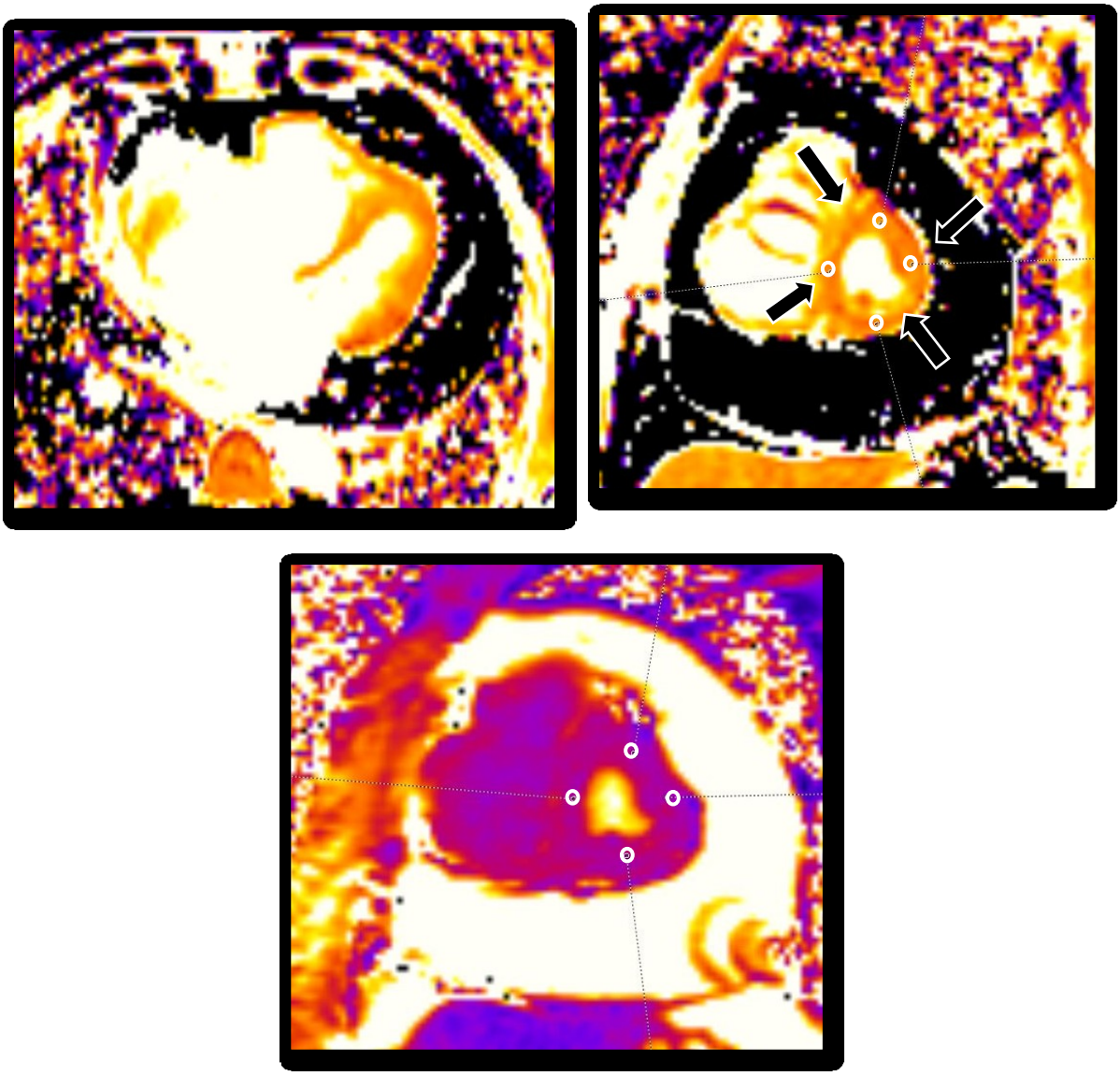

FIG 5.10 Native T1 map four chamber view (top left), short axis mid body (top right) native T2 map short axis mid body (bottom)

	LV WALL			
	ANTERIOR	**SEPTUM**	**INFERIOR**	**LATERAL**
T1(ms)	1553	1467	1379	1483
T2(ms)	36.6	39.8	42.2	38.2

There is significantly increased native T1 values in anterior, septal, inferior and lateral LV walls. No significantly increased native T2 values.

CASE 7 – MYOCARDIAL INFARCTION

History: 52 year old male patient known case of coronary artery disease, planned for coronary bypass surgery came for myocardial viability assessment

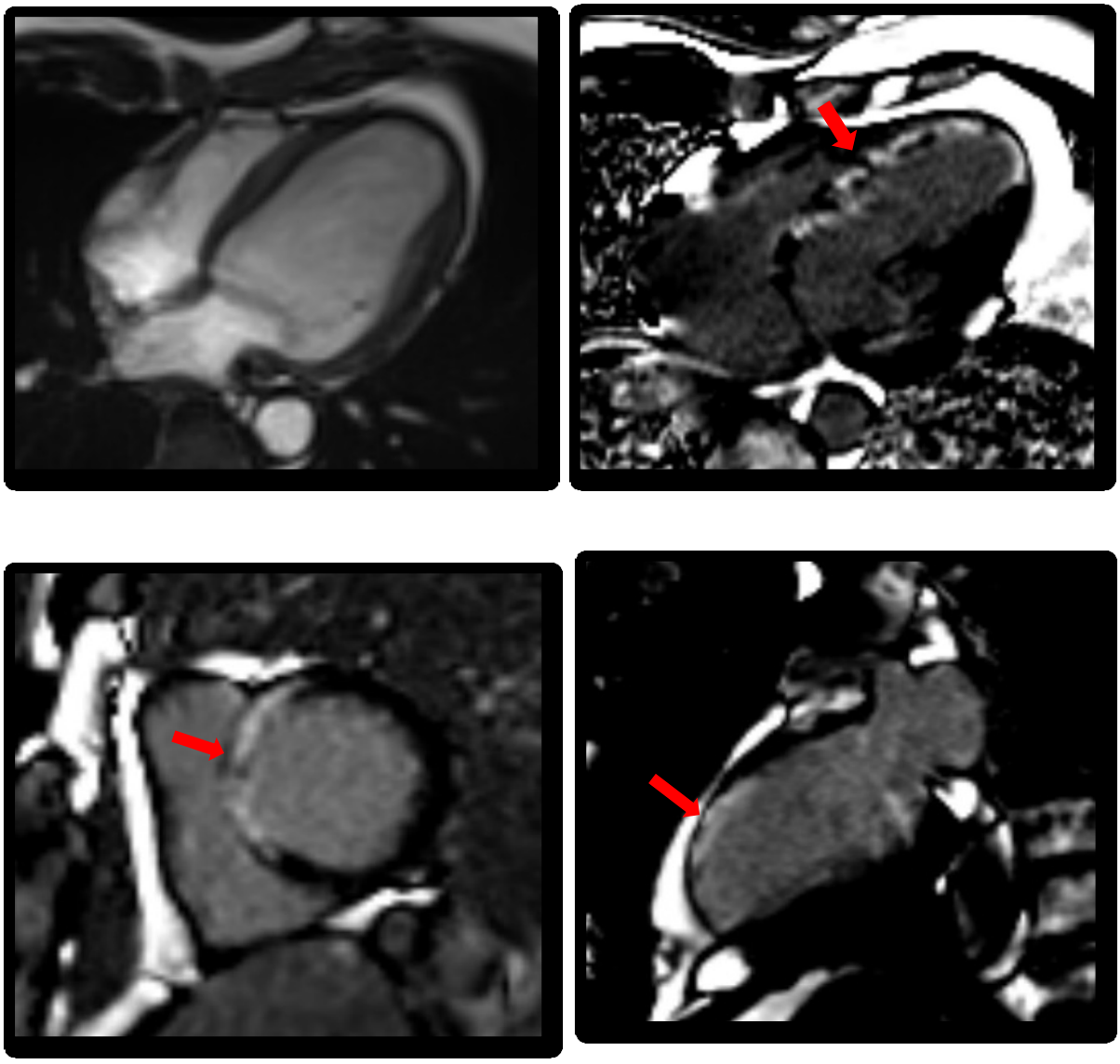

FIG 5.10 True FISP four chamber (top left), post contrast late gadolinium enhancement four chamber view (top right), short axis midbody (bottom left) and two chamber (bottom right) shows delayed myocardial hyperenhancement in the anterior ,anteroseptal and inferoseptal walls of left ventricle

.

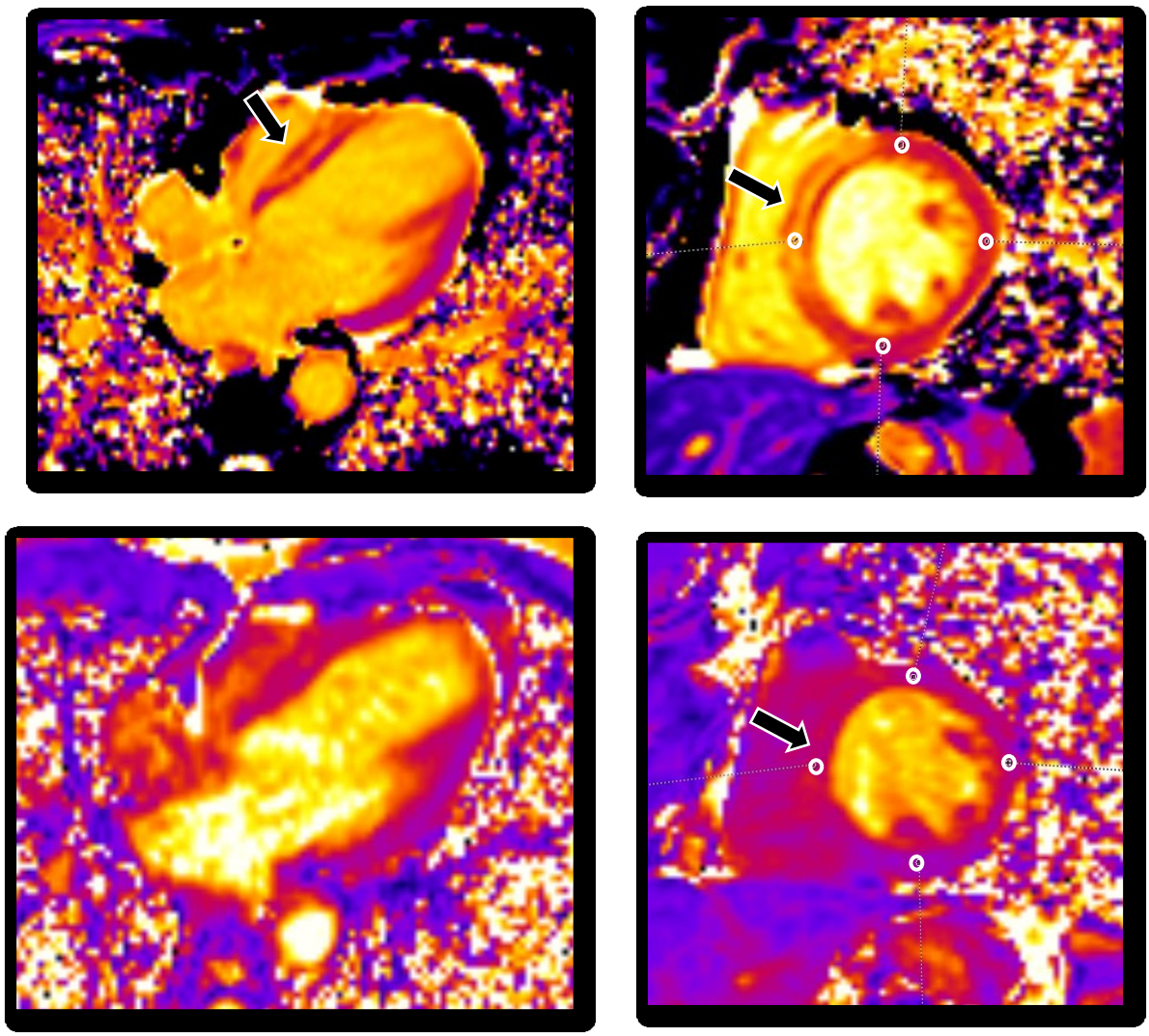

FIG 5.11 Native T1 map four chamber view (top left), short axis mid body (top right) native T2 map four chamber view (bottom left) and short axis mid body (bottom right)

	LV WALL			
	ANTERIOR	**SEPTUM**	**INFERIOR**	**LATERAL**
T1(ms)	1212	1566.5	1176	1190
T2(ms)	38.7	47	36.9	43.3

Native T1 and T2 values are significantly increased in the septum.

CASE 8 - MYOCARDITIS

History: 40 year old female patient presented with fever, arrhythmia (recurrent ventricular tachycardia)

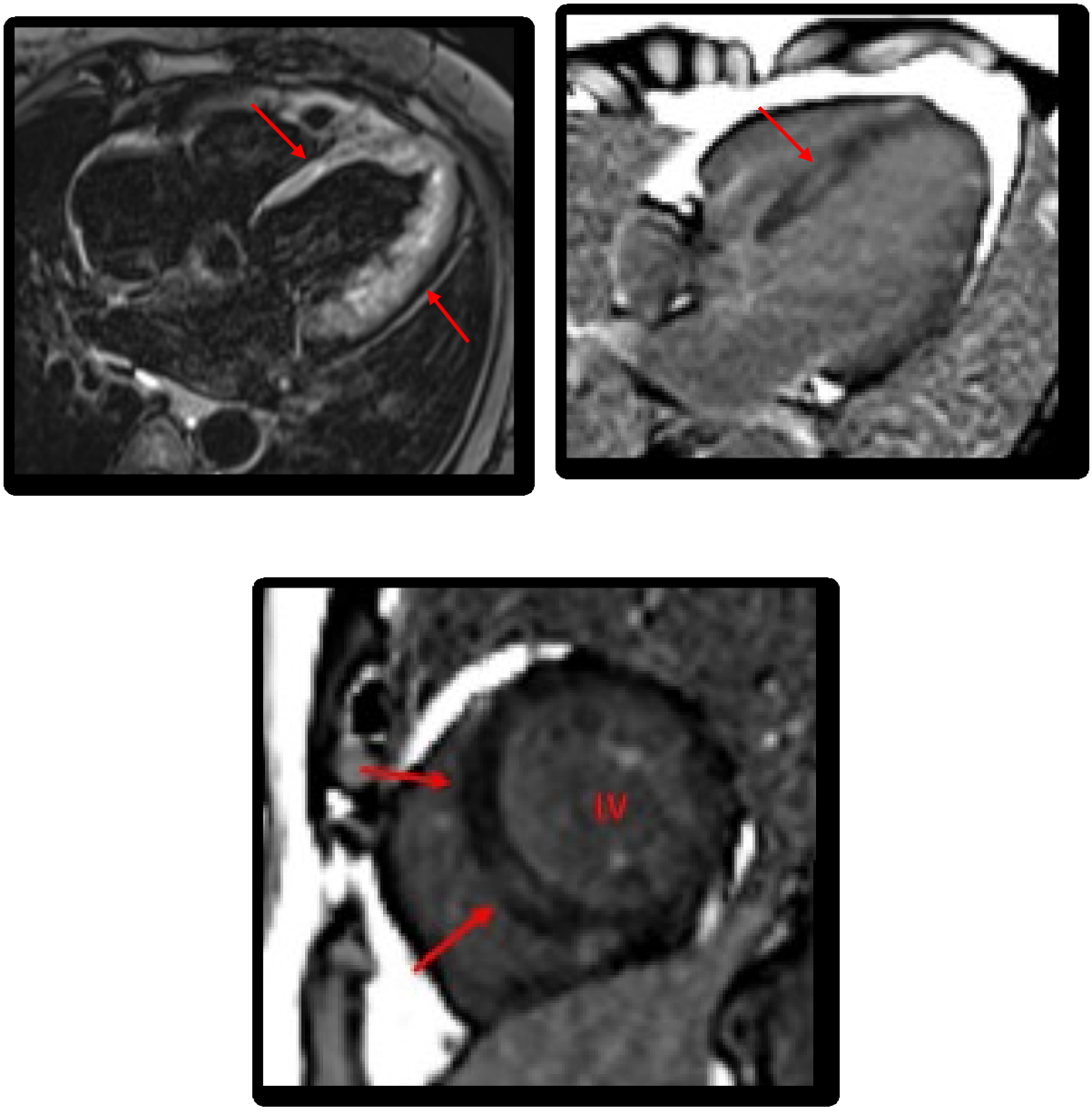

FIG 5.12 STIR axial (top left), PSIR post contrast images four chamber view (top right) and short axis midbody (bottom) shows patchy STIR hyperintensity in LV wall and patchy mid myocardial enhancement in the anteroseptal and inferoseptal walls of left ventricle

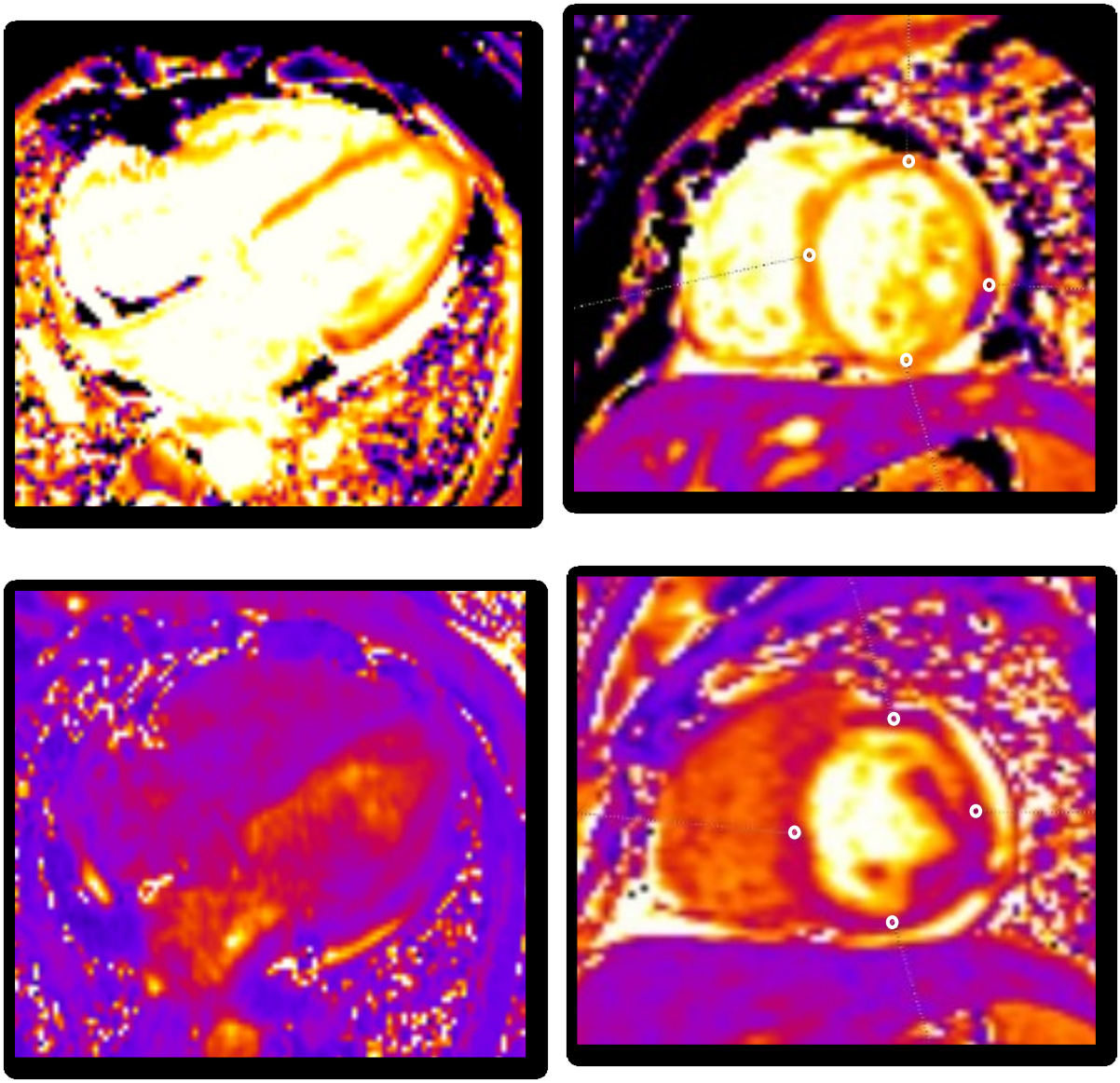

FIG 5.11 Native T1 map four chamber view (top left), short axis mid body (top right) native T2 map four chamber view (bottom left) and short axis mid body (bottom right)

	LV WALL			
	ANTERIOR	**SEPTUM**	**INFERIOR**	**LATERAL**
T1(ms)	1372	1424	1398	1336
T2(ms)	45.9	45.1	43.4	45.3

There is significantly increased native T1 and T2 values in anterior, septal, inferior and lateral LV walls

6. STATISTICAL ANALYSIS

PLANNING OF STATISTICAL ANALYSIS

The collected data were analysed with IBM.SPSS statistics software 23.0Version.

To describe about the data descriptive statistics frequency analysis, percentage analysis were used for categorical variables and the mean & S.D were used for continuous variables.

To find the significant difference in the multivariate analysis the one way ANOVA with Tukey's Post-Hoc test was used.

To find the significance in categorical data Chi-Square test was used.

In all the above statistical tools the probability value .05 is considered as significant level.

7. OBSERVATION & RESULTS

7.1 AGE RANGE DISTRIBUTION

Table 7.1 TABLE SHOWING AGE WISE DISTRIBUTION OF CONTROLS

AGE GROUP	FREQUENCY	PERCENT
UPTO 25 YRS	3	25
26-35 YRS	2	16.6
36-45 YRS	2	16.6
46-55 YRS	5	41.6
TOTAL	12	100

FIG 7.1.1 BAR CHART SHOWING AGE DISTRIBUTION OF CONTROLS

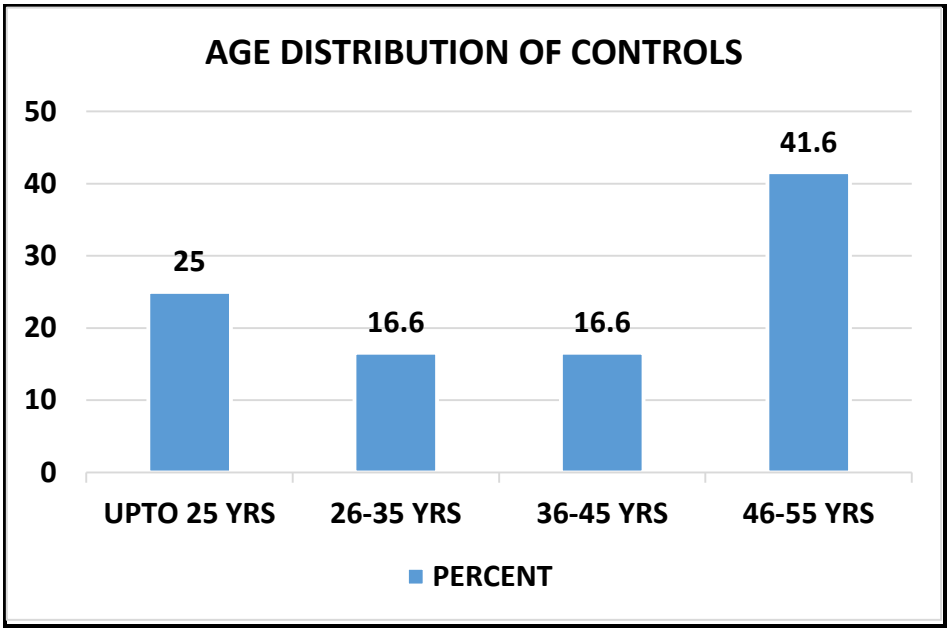

Table 7.1.2 TABLE SHOWING AGE WISE DISTRIBUTION OF CASES

AGE GROUP	FREQUENCY	PERCENT
UPTO 25 YRS	4	10
26-35 YRS	6	15
36-45 YRS	14	35
46-55 YRS	13	32.5
56-65 YRS	3	7.5
TOTAL	40	100

FIG 7.1.2 BAR CHART SHOWING AGE DISTRIBUTION OF CASES

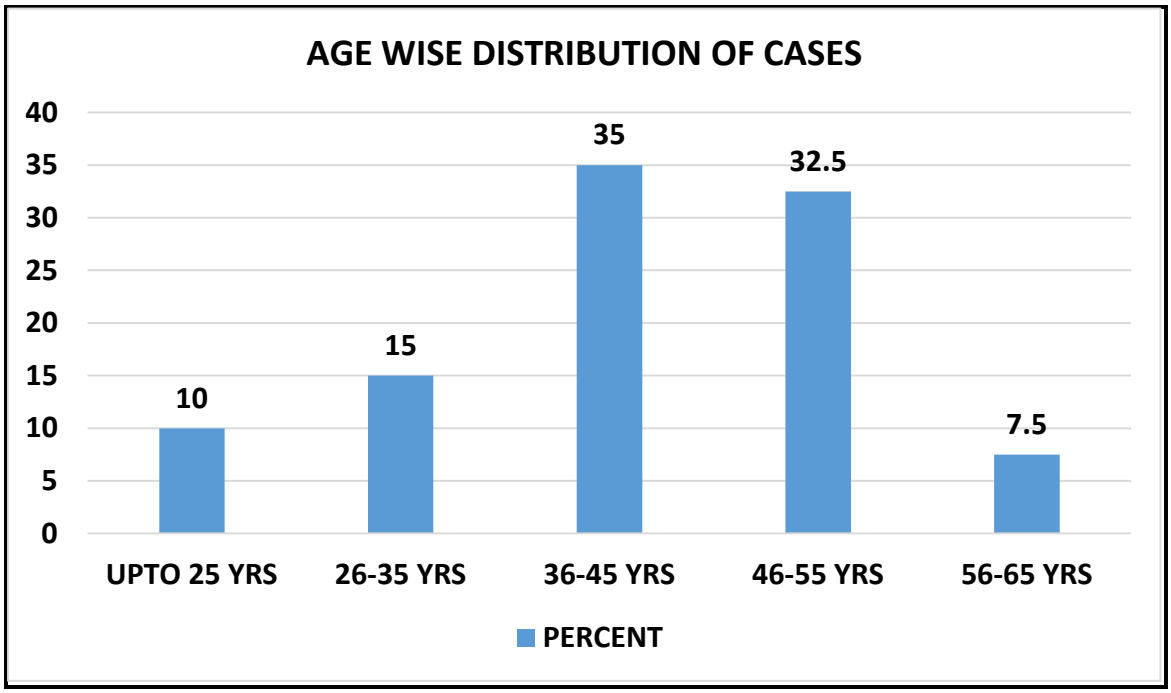

7.2 GENDER DISTRIBUTION

Table 7.2 TABLE SHOWING GENDER DISTRIBUTION AMONG STUDY GROUP

	FEMALES	MALES
CONTROLS	4	8
CASES	19	21
TOTAL	23	29

FIG 7.2 BAR CHART SHOWING GENDER DISTRIBUTION AMONG STUDY GROUP

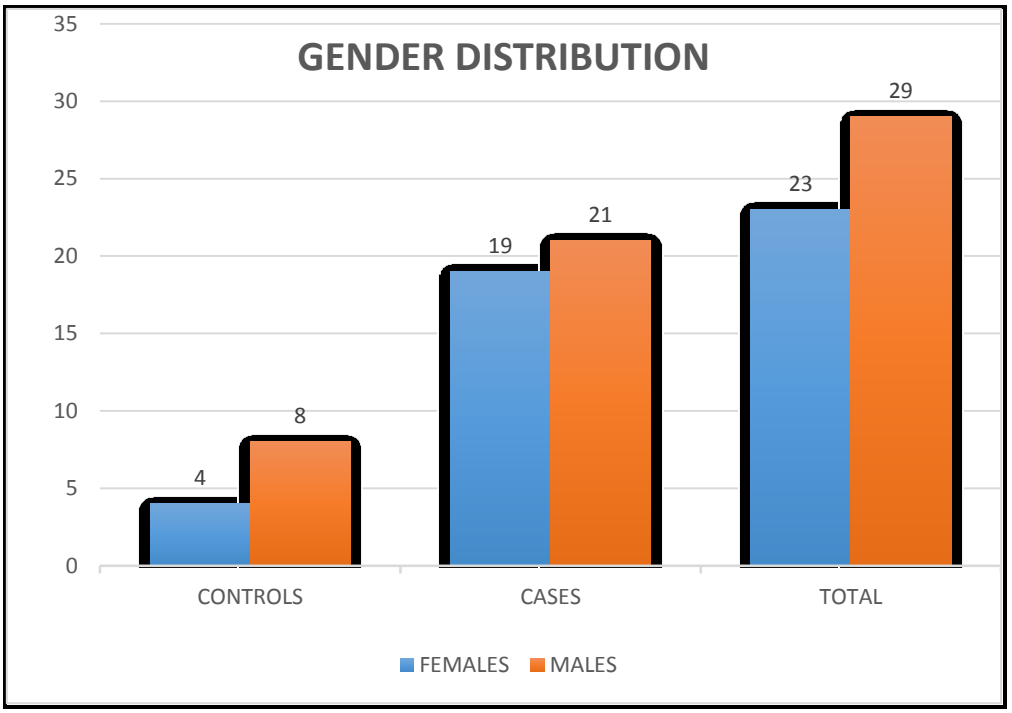

7.3 FREQUENCY DISTRIBUTION AMONG CASES

Table 7.3 TABLE SHOWING FREQUENCY DISTRIBUTION AMONG CASES

GROUPS	FEMALES	MALES	TOTAL	PERCENT
Hypertrophic cardiomyopathy	5	3	8	20
Dilated cardiomyopathy	4	3	7	17.5
Restrictive cardiomyopathy	2	4	6	15
ARV	2	4	6	15
Myocarditis	4	1	5	12.5
Myocardial infraction	2	6	8	20
Total	19	21	40	100

FIG 7.3 BAR CHART SHOWING FREQUENCY DISTRIBUTION AMONG CASES

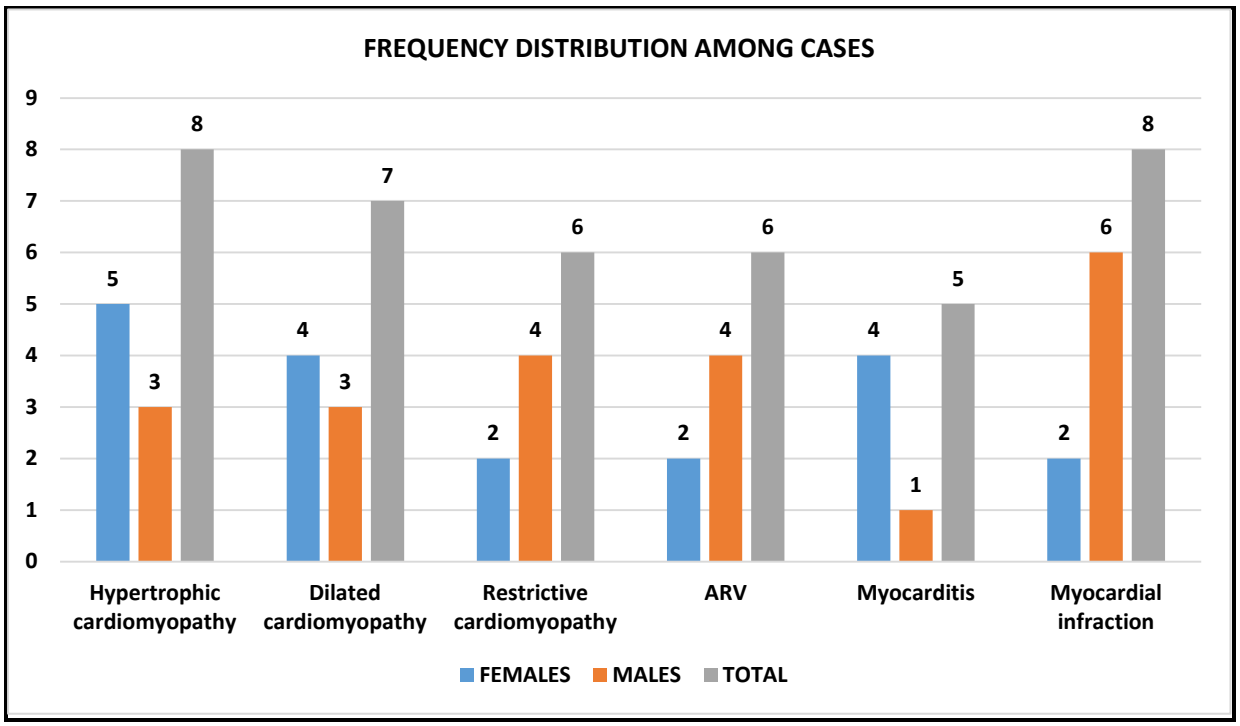

7.4 NATIVE T1 VALUES AMONG STUDY GROUP

Table 7.3 TABLE SHOWING NATIVE T1 VALUES AMONG STUDY GROUP

Groups	N	Mean	Std. Deviation	95% Confidence Interval for Mean		Minimum	Maximum
				Lower Bound	Upper Bound		
Hypertrophic cardiomyopathy	8	1355.86	44.67	1318.52	1393.20	1308.42	1415.17
Dilated cardiomyopathy	7	1341.31	41.48	1302.94	1379.67	1266.25	1388.75
Restrictive cardiomyopathy	6	1370.37	97.75	1267.79	1472.95	1276.47	1472.25
ARVD	6	1289.48	49.68	1237.34	1341.61	1223.52	1348.67
Myocarditis	5	1418.68	8.62	1407.98	1429.39	1404.58	1428.17
Myocardial infraction	8	1316.26	48.20	1275.96	1356.56	1256.00	1398.17
Normal	12	1186.47	45.67	1157.45	1215.49	1108.83	1261.92
Total	52	1308.77	90.14	1283.68	1333.87	1108.83	1472.25

FIG 7.3 BAR CHART SHOWING NATIVE T1 VALUES AMONG STUDY GROUP

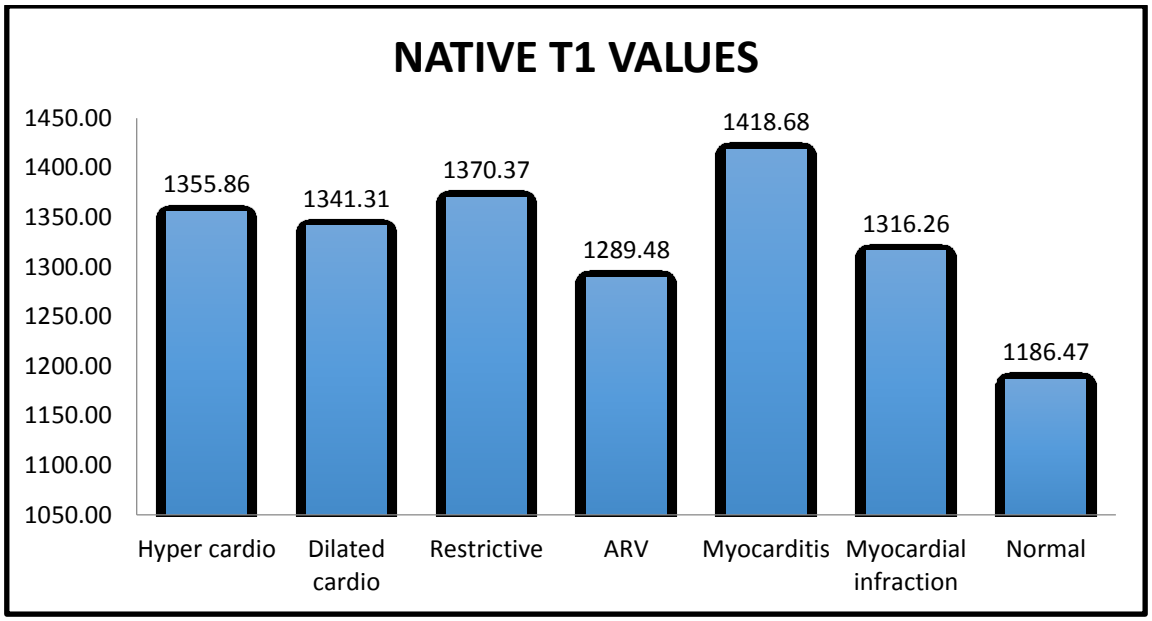

7.4 NATIVE T2 VALUES AMONG STUDY GROUP

Table 7.4 TABLE SHOWING NATIVE T2 VALUES AMONG STUDY GROUP

Groups	N	Mean	Std. Deviation	95% Confidence Interval for Mean		Minimum	Maximum
				Lower Bound	Upper Bound		
Hypertrophic cardiomyopathy	8	42.11	2.38	40.13	44.10	39.17	44.75
Dilated cardiomyopathy	7	40.64	1.62	39.14	42.14	37.83	43.25
Restrictive cardiomyopathy	6	41.46	3.06	38.24	44.67	35.58	43.75
ARVD	6	41.43	3.45	37.81	45.05	38.25	47.25
Myocarditis	5	44.37	0.63	43.58	45.15	43.58	45.08
Myocardial infraction	8	40.16	2.52	38.05	42.26	36.75	44.83
Normal	12	38.25	1.49	37.30	39.20	35.08	40.17
Total	52	40.79	2.79	40.01	41.56	35.08	47.25

FIG 7.4 BAR CHART SHOWING NATIVE T2 VALUES AMONG STUDY GROUP

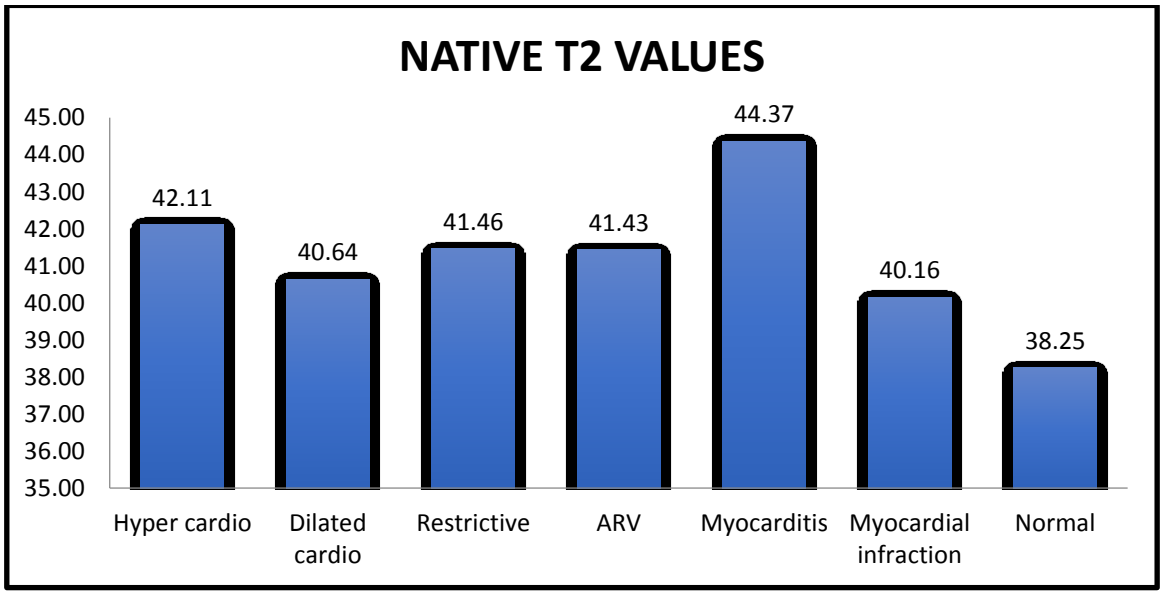

7.4 COMPARISON OF NATIVE T1 VALUES BETWEEN CONTROLS AND CASES

Table 7.4TABLE SHOWING COMPARISON OF NATIVE T1 VALUES BETWEEN CONTROLS AND CASES

Dependent Variable		Mean Difference (I-J)	Std. Error	Sig.	95% Confidence Interval	
					Lower Bound	Upper Bound
Normal	Hypertrophic cardiomyopathy	-169.38715*	23.95166	.000	-243.2897	-95.4846
	Dilated cardiomyopathy	-154.83373*	24.95706	.000	-231.8384	-77.8290
	Restrictive cardiomyopathy	-183.89722*	26.23773	.000	-264.8534	-102.9410
	ARVD	-103.00278*	26.23773	.005	-183.9590	-22.0466
	Myocarditis	-232.21111*	27.93220	.000	-318.3956	-146.0267
	Myocardial infraction	-129.78819*	23.95166	.000	-203.6907	-55.8856

7.5 COMPARISON OF NATIVE T2 VALUES BETWEEN CONTROLS AND CASES

Table 7.4TABLE SHOWING COMPARISON OF NATIVE T2 VALUES BETWEEN CONTROLS AND CASES

Dependent Variable		Mean Difference (I-J)	Std. Error	Sig.	95% Confidence Interval	
					Lower Bound	Upper Bound
Normal	Hypertrophic cardiomyopathy	-3.86458*	1.03693	.009	-7.0640	-.6652
	Dilated cardiomyopathy	-2.39286	1.08046	.308	-5.7266	.9409
	Restrictive cardiomyopathy	-3.20833	1.13590	.093	-6.7131	.2965
	ARVD	-3.18056	1.13590	.098	-6.6854	.3242
	Myocarditis	-6.11667*	1.20926	.000	-9.8478	-2.3855
	Myocardial infraction	-1.90625	1.03693	.530	-5.1057	1.2932

RESULTS

Among 52 subjects studied, 29 were males and 23 were females, i.e., 55.8% were males and 44.2% were females.

The study group consisted of 8 cases (15.4%) of Hypertrophic cardiomyopathy, 7 cases (13.5%) of Dilated cardiomyopathy, 6 cases (11.5%) of Restrictive cardiomyopathy, 6 cases (11.5%) of arrhythmogenic right ventricular dysplasia, 5 cases (9.6%) of myocarditis, 8 cases (15.4%) of myocardial infarction and 12 controls (23.1%).

Mean native T1 and T2 values for controls, hypertrophic cardiomyopathy, dilated cardiomyopathy, restrictive cardiomyopathy, arrhythmogenic right ventricular dysplasia, myocarditis and myocardial infarction are summarized in the tables and bar charts above. The comparison among mean native T1 and T2 values of normal controls and cases with myocardial disease showed the following results:

1. The native T1 values for the healthy control group on our 3T MRI system was 1186.47±45.67ms.

2. The average native myocardial T1 value ranged in the group of subjects with healthy hearts between 1108.83 and 1261.91 ms

3. The average native T1 value ranged in the joint analysis of all patients with diffuse diseased myocardium between 1266.25 and 1428.16 ms.

4. The mean T1 value of the groups HCM was 1355.86±44.67ms, DCM was 1341.31±41.48ms, RCM was 1370.37±90.14ms, ARVD was 1289.48±49.68ms, acute myocarditis was 1418.68±8.62ms and myocardial infarction was 1316.26±48.20ms.

5. The highest T1 values were observed in the myocarditis group (1418.68±8.62ms) and the lowest T1 values were observed in the ARVD group (1289.48±49.68ms).

6. The mean T1 values of the groups HCM (1355.86±44.67ms, $p<0.05$), DCM (1341.31±41.48ms, $p<0.05$), RCM (1370.37±90.14ms. $p<0.05$), ARVD (1289.48±49.68ms, $p<0.05$), acute myocarditis (1418.68±8.62ms, $p<0.05$) and myocardial infarction (1316.26±48.20ms, $p<0.05$) were significantly higher than that of the healthy control group.

7. Thus the average native T1 value in cardiac MR imaging can be useful in differentiating between healthy and diffuse myocardial disease groups.

8. The native T2 values for the healthy control group on our 3T MRI system was 38.25±1.49ms.

9. The average native myocardial T2 value ranged in the group of subjects with healthy hearts between 35.08 and 40.17ms

10. The average native T2 value ranged in the joint analysis of all patients with diffuse diseased myocardium between 35.58 and 47.25ms.

11. The mean T2 value of the groups HCM was 42.11±2.38ms, DCM was 40.64±1.62ms, RCM was 41.46±3.06ms, ARVD was 41.43±3.45ms, acute myocarditis was 44.37±0.63ms and myocardial infarction was 40.16±2.52ms.

12. The highest T2 values were observed in the myocarditis group (44.37±0.63ms)and the lowest T2 values were observed in the myocardial infarction group (40.16±2.52ms).

13. The mean T2 values of the groups HCM (42.11±2.38ms, $p<0.05$) and acute myocarditis (44.37±0.63ms, $p<0.05$) were significantly higher than that of the healthy control group.

14. There was no statistically significant difference in mean T2 values between the groups DCM (40.64±1.62ms, $p=0.3$), RCM (41.46±3.06ms, $p=0.09$), ARVD (41.43ms, $p=0.09$), myocardial infarction (40.16±0.63ms, $p=0.53$) and healthy control group.

15. Thus the average native T2 value in cardiac MR imaging can be useful in differentiating between healthy and groups with HCM and myocarditis.

8. DISCUSSION

Myocardial fibrosis is a fundamental process in the development of myocardial dysfunction in majority of myocardial pathologies, leading to poor outcomes. It is an independent risk factor for overall mortality. Early identification of this underlying process is important for diagnosis and essential for further management.

Endomyocardial biopsy was the only available method for assessment of myocardial fibrosis. But due to risk of serious complications and sampling error associated with this technique, it was hence seldom performed.

With advancements in cardiac magnetic resonance imaging (CMR), several novel techniques for the detection and characterization of myocardial pathologies were developed. Cardiac MR has become a standard investigation for the evaluation of several cardiac pathologies. Cardiac MR imaging primarily relied on qualitative characterization of the myocardium and detecting focal myocardial fibrosis through visual analysis of characteristic enhancement patterns on late gadolinium-enhanced (LGE) MR images. However, myocardial signal intensity in diffuse myocardial fibrosis may be nearly isointense and thus be “nulled” appearing like normal tissue. Moreover as LGE involves intravenous administration of gadolinium-based contrast agents, it is contraindicated in those with renal failure. Novel techniques, including native T1 and T2 mapping which directly quantifies signal from the myocardium, have been developed to surpass these limitations in the detection of diffuse myocardial diseases. Thus mapping techniques may supplement or potentially replace invasive myocardial biopsy. Moreover, as gadolinium is not used in this technique, it can be used in patients with renal dysfunction.

In addition to myocardial fibrosis, native T1 measurement can also detect excess of water as in oedema [14, 15], protein deposition [16, 17], and lipid [13, 14] or iron (haemorrhage, siderosis) [20]. The changes of myocardial native T1 mapping reflect cardiac diseases, such as acute coronary syndromes, infarction, myocarditis, and diffuse fibrosis (that present with high T1) [21], and systemic diseases, such as cardiac amyloid (high T1) [21] Anderson-Fabry disease (low T1) [22], and siderosis (low T1).
The T2 mapping technique can accurately and reliably detect areas of myocardial oedema in conditions like acute myocardial infarction [23], myocarditis [24, 25], and cardiac allograft rejection.

In our study, out of 52 subjects, 29 (55.8%) were males and 23 (44.2%) were females. The study group consisted of 8 cases (15.4%) of Hypertrophic cardiomyopathy, 7 cases (13.5%) of Dilated cardiomyopathy, 6 cases (11.5%) of Restrictive cardiomyopathy, 6 cases (11.5%) of arrhythmogenic right ventricular dysplasia, 5 cases (9.6%) of myocarditis, 8 cases (15.4%) of myocardial infarction and 12 controls (23.1%).The age and gender distribution of myocardial diseases and their frequency distribution were almost similar to previous studies in literature.

Our study aimed to identify normal baseline T1 and T2 values of myocardium in 3T MR and to assess the value of native T1 and T2 relaxation in the differentiation between healthy and diseased myocardium. In our study, native T1 and T2 mapping was performed using Siemens Myomap protocol in short axis slices through the apex, mid-body and base. The average native myocardial T1 and T2 values for controls, hypertrophic cardiomyopathy, dilated cardiomyopathy, restrictive cardiomyopathy, arrhythmogenic right ventricular dysplasia, myocarditis and myocardial infarction

were obtained from region of interest (ROI) drawn in the anterior, septal, inferior and posterolateral walls in each of these slices.

Native T1 and T2 relaxation times are genuine tissue parameters at a given field strength. However they are affected by the type of sequence used, sequence parameters and by the MR system.

NATIVE T1 MAPPING

A mean native T1 value of 1052 ± 23ms in healthy controls was reported **Dabir et al**[70]**,**who used a 3T scanner (Ingenia, Philips Healthcare, Best, The Netherlands) and Modified Look- Locker inversion recovery for T1 mapping.

Dass et al[71], who used a Siemens 3T Trio MR system (Siemens Healthcare Erlangen, Germany) and shortened MOLLI for T1 mapping reported a mean native T1 value of 1178±13 ms in normal control patients. The study also reported that mean T1 relaxation time was increased in HCM and DCM (HCM 1209±28 ms, DCM 1225±42 ms, normal 1178±13 ms, $P<0.05$) and T1 values correlated with disease severity.

Puntmann et al [72], who used MOLLI sequence for T1 mapping in a 3-T scanner (Achieva TX, Philips Healthcare, Best, the Netherlands) reported a mean native T1 value of 1,070±55ms for subjects with healthy hearts. They also reported that native T1 value was significantly longer in patients with cardiomyopathy (HCM 1,254±43ms, NIDCM 1,239±57ms) compared with control subjects (1,070±55ms) ($p < 0.01$) and that native T1 could differentiate between healthy and diseased myocardium with high diagnostic accuracy.

Lurz et al.[73], who also performed T1 mapping with a modified Look-Locker inversion recovery sequence in a 3-T scanner (Verio, Siemens Healthcare, Erlangen,

Germany) reported mean native T1 value of 1,159±62ms for subjects with healthy hearts and that values for native T1 were significantly higher in patients with acute myocarditis (1,203±71ms) than in patients with no myocarditis.

Leutkens et al[74] reported mean native T1 value of 1089.1±44.9ms in control subjects using 3-T MR imaging system (Ingenia 3T; Philips Healthcare, Best, the Netherlands) and MOLLI for T1 mapping. They observed that native T1 relaxation times were significantly longer in patients with acute myocarditis than in control subjects (1185.3±49.3 vs 1089.1±44.9, respectively; $P < .001$).

Hinojar et al[75] reported a mean native T1 value of 1,045±23ms in subjects with healthy hearts using a 3.0-T scanner (Achieva, Philips Healthcare, Best, the Netherlands). This study reported mean native T1 value of 1,189±52ms in acute myocarditis and that native T1 was superior to T2-weighted imaging and late gadolinium enhancement with high diagnostic accuracy and positive and negative predictive values to distinguish health and disease.

Toussaint et al.[76]**,** who used a 3 Tesla scanner (Magnetom Trio Tim; Siemens AG Healthcare Sector, Erlangen, Germany) and MOLLI sequence for myocardial T1 was determined reported mean native T1 value of 1155.3±63.9ms in subjects with healthy hearts and a mean T1 relaxation time of 1179.2±48.3ms in myocarditis cases.

Boomen et al.[77], in their systematic review and meta-analysis of native T1 reference values for nonischemic cardiomyopathies reported a weighted mean T1 value of 1081±45 msec in controls at 3T. Their systematic review and meta-analysis concluded that native T1 mapping can potentially assess myocardial changes in HCM, DCM, MC compared to controls. They reported a mean T1 value of 1166±55 msec in

HCM patients and 1193±60 msec for DCM patients. The mean T1 value in acute MC patients was 1193±60 msec. The metaanalysis showed a significant increase of the myocardial T1 values for HCM, DCM patients and acute MC patients compared with controls.

Dall'Armellina E et al[78] reported a mean T1 value of 1257±97 ms in infarcted myocardium normal (n=10) 1166±60ms

The mean native T1 values for the healthy control group on our 3T MRI system was 1186.47±45.67ms. This was comparable to the mean native T1 values reported by **Dass et al**[71] **(**1178±13 ms) and **Lurz et al**[73] (1,159±62ms). The average native myocardial T1 value ranged in the group of subjects with healthy hearts between 1108.83 and 1261.91 ms. The average native T1 value ranged in the joint analysis of all patients with diffuse diseased myocardium between 1266.25 and 1428.16 ms.

The mean T1 value of the groups HCM was 1355.86±44.67ms, DCM was 1341.31±41.48ms, RCM was 1370.37±90.14ms, ARVD was 1289.48±49.68ms, acute myocarditis was 1418.68±8.62ms and myocardial infarction was 1316.26±48.20ms. These values were slightly higher than mean T1 values reported by above mentioned studies. This might reflect the differences in the type of sequence used, sequence parameters and by the MR system. The highest T1 values were observed in the myocarditis group.

The mean T1 values of the groups HCM (1355.86±44.67ms, $p<0.05$), DCM (1341.31±41.48ms, $p<0.05$), RCM (1370.37±90.14ms. $p<0.05$), ARVD (1289.48±49.68ms, $p<0.05$), acute myocarditis (1418.68±8.62ms, $p<0.05$) and myocardial infarction (1316.26±48.20ms, $p<0.05$) were significantly higher than that

of the healthy control group. Thus the average native T1 value in cardiac MR imaging can be useful in differentiating between healthy and diffuse myocardial disease groups.

NATIVE T2 MAPPING

von Knobelsdorff-Brenkenhoff F et al[79] reported normal myocardial T2 value of 45.1 ms at 3T [77] .

Spieker et al[80] reported that T2 values were significantly increased in acute myocarditis compared to controls and decreased over time. Patients with clinical recovery revealed significantly decreased T2 relaxation times at follow-up examinations; however, T2 values were still elevated compared to healthy controls.

The native T2 values for the healthy control group on our 3T MRI system was 38.25±1.49ms. This was slightly lower than reported by previous studies. The average native myocardial T2 value ranged in the group of subjects with healthy hearts between 35.08 and 40.17ms. The average native T2 value ranged in the joint analysis of all patients with diffuse diseased myocardium between 35.58 and 47.25ms.

The mean T2 value of the groups HCM was 42.11±2.38ms, DCM was 40.64±1.62ms, RCM was 41.46±3.06ms, ARVD was 41.43±3.45ms, acute myocarditis was 44.37±0.63ms and myocardial infarction was 40.16±2.52ms. The highest T2 values were observed in the myocarditis group. Our mean T2 values in acute myocarditis were comparable with previous studies. Only a limited degree of comparison of our data with previous studies is possible with regards to T2 values in groups HCM, DCM, RCM and ARVD as sufficient studies on 3T MR system have not been published in literature in these disease groups.

The mean T2 values of the groups HCM (42.11±2.38ms, $p<0.05$) and acute myocarditis (44.37±0.63ms, $p<0.05$) were significantly higher than that of the healthy control group. There was no statistically significant difference in mean T2 values between the groups DCM (40.64±1.62ms, $p=0.3$), RCM (41.46±3.06ms, $p=0.09$), ARVD (41.43ms, $p=0.09$), myocardial infarction (40.16±0.63ms, $p=0.53$) and healthy control group. Thus the average native T2 value in cardiac MR imaging can be useful in differentiating between healthy and groups with HCM and myocarditis.

9. LIMITATION OF THE STUDY

The number of patients in some subgroups of myocardial pathologies is rather small. Hence further studies on larger cohorts are required.

10. CONCLUSION

Cardiac MR is a non-invasive, quantifiable, and feasible technique which allows the evaluation of myocardial diseases.

This study, despite some limitations, showed the feasibility of native T1 and T2 mapping in discriminating between healthy and diseased myocardium, which can aid in further management. Significant differences in native T1 and T2 values between normal controls and various groups of cases with myocardial pathologies were apparent in this study. This data may justify the more routine use of this technique in the characterisation, assessment and follow-up of myocardial diseases.

Other potential benefits include the ability of this technique in identifying diffuse or early myocardial pathologies which may be missed on traditional CMR method ssuch as late gadolinium enhancement (LGE) imaging. Moreover as native myocardial mapping does not involve intravenous administration of gadolinium-based contrast agents, it can be used in those with renal failure as opposed to late gadolinium enhancement (LGE) imaging which is contraindicated in this group of people.

Myocardial mapping technique may also possibly help in avoiding unnecessary myocardial biopsies in certain cases of myocardial diseases. Further, it may help identify the most appropriate location for biopsy, if it is deemed clinically necessary.

CMR with the LGE imaging method is the gold standard for non-invasive myocardial tissue characterization and scar imaging/quantification. T1 and T2 mapping takes this forward to the measurement of diffuse processes in a quantitative pixel-by-pixel approach. It is one of the most rapidly developing and evolving fields

in CMR. Recent advances in acquisition sequences have made it possible for short acquisition times, improved accuracy and precision, and robust reproducibility without the need for contrast material. Its clinical applications extend from rare diseases such as Fabry disease to more frequent ones like cardiac amyloidosis to conditions encountered in everyday clinical practice like myocardial infarction.

Quantitative T1maps enhance the ability of CMR to characterize the myocardium by allowing depiction of diffuse myocardial fibrosis. Consequently, native T1 mapping might supply a CMR biomarker for myocardial fibrosis, justifying their use in clinical practice. However, more research and multicenter studies are required before a large-scale application in clinical decision-making. More effort towards setting reference ranges for the different pathologies that alter T1and T2 values, standardization of the acquisition techniques and creating differentiating algorithms for their overlapping values are required.

To conclude, native T1 and T2 mapping techniques can be readily incorporated into the existing cardiac MR protocols, and their combined use may provide important knowledge into fundamental disease processes affecting the myocardium that can otherwise be difficult to detect. This will further our understanding of pathological mechanisms in the myocardium and lead to early detection, better diagnostic path-ways, improved prognostication, and improved monitoring of therapy.

Our study has assessed native T1 and T2 values in 3T SIEMENS SKYRA system, which yielded comparable results to other SIEMENS systems. Native T1 and T2 mapping can be a potential biomarker in the prognostication and follow up of various diffuse myocardial diseases like myocarditis and cardiomyopathies.

REFERENCES

1. Mewton N, Liu CY, Croisille P, Bluemke D, Lima JA (2011) Assessment of myocardial fibrosis with cardiovascular magnetic resonance. J Am Coll Cardiol 57: 891-903.
2. Hill JA, Olson EN. Cardiac plasticity. N Engl J Med 2008;358:1370–80.
3. Van den Borne SW, Diez J, Blankesteijn WM, Verjans J, Hofstra L, Narula J. Myocardial remodeling after infarction: the role of myofibroblasts. Nat Rev Cardiol 2010;7:30 –7.
4. Barallobre-Barreiro J, Didangelos A, Schoendube FA, et al. Proteomics analysis of cardiac extracellular matrix remodeling in a porcine model of ischemia-reperfusion injury. Circulation 2012;125:789–802.
5. Ho CY, Lopez B, Coelho-Filho OR, et al. Myocardial fibrosis as an early manifestation of hypertrophic cardiomyopathy. N Engl J Med 2010;363: 552–63.
6. Bruder O, Wagner A, Jensen CJ, et al. Myocardial scar visualized by cardiovascular magnetic resonance imaging predicts major adverse events in patients with hypertrophic cardiomyopathy. J Am Coll Cardiol 2010;56:875–87.
7. Picano E, Pelosi G, Marzilli M, et al. In vivo quantitative ultrasonic evaluation of myocardial fibrosis in humans. Circulation 1990;81:58-64.
8. Knaapen P, Boellaard R, Götte MJ, et al. Perfusable tissue index as a potential marker of fibrosis in patients with idiopathic dilated cardiomyopathy. J Nucl Med 2004;45:1299-304.

9. Díez J, Panizo A, Gil MJ, et al. Serum markers of collagen type I metabolism in spontaneously hypertensive rats: relation to myocardial fibrosis. Circulation 1996;93:1026-32.

10. Van den Borne SW, Diez J, Blankesteijn WM, et al. Myocardial remodeling after infarction: the role of myofibroblasts. Nat Rev Cardiol 2010;7:30-7.

11. Pennell DJ, Sechtem UP, Higgins CB, Manning WJ, Pohost GM, et al. (2004) Clinical indications for cardiovascular magnetic resonance (CMR): Consensus Panel report. J Cardiovasc Magn Reson 6: 727-765.

12. Sibley CT, Noureldin RA, Gai N, et al. T1 mapping in cardiomyopathy at cardiac MR: comparison with endomyocardial biopsy. Radiology 2012;265(3):724-732.

13. Exhibit E, Caballeros FM, Madrid JM, Garcia A, Pueyo JC, Bastarrika G. T1 mapping of the myocardium : what a resident needs to know. 2016;1–17.

14. Ugander M, Bagi PS, Oki AJ, Chen B, Hsu LY: Myocardial edema as detected by pre-contrast T1 and T2 CMR delineates area at risk associated with acute myocardial infarction. JACC Cardiovasc Imaging 2012; 5: 596−603.

15. Ferreira VM, Piechnik SK, Dall' Armellina E, Karamitsos TD, Francis JM: Non-contrast T1-mapping detects acute myocardial edema with high diagnostic accuracy. J Cardiovasc Magn Reson 2012; 14: 42.

16. Karamitsos TD, Piechnik SK, Banypersad SM, Fontana M, Ntusi NB, Ferreira VM: Noncontrast T1 mapping for the diagnosis of cardiac amyloidosis. JACC Cardiovasc Imaging 2013;6: 488−497.

17. Bull S, White SK, Piechnik SK, Flett AS, Ferreira VM, Loudon M, Francis JM: Human non-contrast T1 values and correlation with histology in diffuse fibrosis. Heart 2013; 99: 932−937.

18. Sado DM, White SK, Piechnik SK, Banypersad SM, Treibel T, Captur G, Fontana: Identification and assessment of Anderson-Fabry disease by noncontrast myocardial T1 mapping. Circ Cardiovasc Imaging 2013; 6: 392−398.

19. Scholz TD, Fleagle SR, Parrish FC, Breon T, Skorton DJ: Effect of tissue fat and water content on nuclear magnetic resonance relaxation times of cardiac and skeletal muscle. Magn Reson Imaging 1990; 8: 605−611.

20. Pedersen SF, Thrysoe SA, Robich MP, Paaske WP, Ringgaard S: Assessment of intramyocardial hemorrhage by T1-weighted cardiovascular magnetic resonance in reperfused acute myocardial infarction. J Cardiovasc Magn Reson 2012; 14: 59.

21. Puntmann VO, D’ Cruz D, Smith Z, Pastor A, Choong P, Voigt T: Native myocardial T1 mapping by cardiovascular magnetic resonance imaging in subclinical cardiomyopathy in patients with systemic lupus erythematosus. Circ Cardiovasc Imaging 2013; 6: 295− 301.

22. Sado DM, White SK, Piechnik SK, Banypersad SM, Treibel T, Captur G: The identification and assessment of Anderson-Fabry disease by non-contrast myocardial T1 mapping. Circ Cardiovasc Imaging 2013; 6: 392−398.

23. Verhaert D, Thavendiranathan P, Giri S, Mihai G, Rajagopalan S, Simonetti OP, et al: Direct T2 quantification of myocardial edema in acute ischemic injury. JACC Cardiovasc Imaging 2011; 4: 269−278.

24. Thavendiranathan P, Walls M, Giri S, Verhaert D, Rajagopalan S, Moore S, et al: Improved detection of myocardial involvement in acute inflammatory cardiomyopathies using T2 mapping. Circ Cardiovasc Imaging 2012; 5: 102−110.

25. Roller FC, Harth S, Schneider C, Krombach GA: T1, T2 mapping and extracellular volume fraction (ECV): application, value and further perspectives in myocardial inflammation and cardiomyopathies. Rofo 2015; 187: 760−770.

26. Sibley CT, Noureldin RA, Gai N, Nacif MS,Liu S, Turkbey EB, Mudd JO, van der Geest RJ: T1 mapping in cardiomyopathy at cardiac MR: comparison with endomyocardial biopsy. Radiology 2012; 265: 724−732.

27. Crouser ED, Ono C, Tran T, He X, Raman SV: Improved detection of cardiac sarcoidosis using magnetic resonance with myocardial T2 mapping. Am J Respir Crit Care Med 2014;189: 109−112.

28. Usman AA, Taimen K, Wasielewski M, Mc-Donald J, Shah S, Giri S, et al: Cardiac magnetic resonance T2 mapping in the monitoring and follow-up of acute cardiac transplant rejection: a pilot study. Circ Cardiovasc Imaging 2012; 5: 782−790.

29 Bohnen S, Radunski UK, Lund GK, Kandolf R, Stehning C: Performance of t1 and t2 mapping cardiovascular magnetic resonance to detect active myocarditis

in patients with recent-onset heart failure. Circ Cardiovasc Imaging 2015; 8:e003073

30 Usman AA, Taimen K, Wasielewski M, Mc- Donald J, Shah S, Giri S: Cardiac magnetic resonance T2 mapping in the monitoring and follow-up of acute cardiac transplant rejection: a pilot study. Circ Cardiovasc Imaging 2012; 5: 782−790.

31. Sadler TW. Langman's Essential Medical Embryology. Langmans Essential Medical Embryology. 2014.

32. Bogaert J, Dymarkowski S, Taylor AM, eds. Clinical cardiac MRI. New York, NY: Springer-Verlag, 2005

33. Mirowitz SA, Gutierrez FR. Fibromuscular elements of the right atrium: pseudomass at MR imaging. Radiology 1992; 182:231–233

34. Boxt LM. Cardiac MR imaging: a guide for the beginner. RadioGraphics 1999; 19:1009–1025; discussion, 1026–1028

35. Davies MJ. The cardiomyopathies: an overview. 2000;469–74.

36. Scot, A., Travis, S. et al. Mapping the Future of Cardiac MR Imaging: Casebased Review of T1 and T2 Mapping Techniques. RadioGraphics 2014; 34:1594-1611

37. Parsai, C. et al. Diagnostic and prognostic value of cardiovascular magnetic resonance in non-ischaemic cardiomyopathies. Journal of Cardiovascular Magnetic Resonance 2012, 14:54

38. Olimulder, M, et al. The importance of cardiac MRI as a diagnostic tool in viral myocarditis-induced cardiomyopathy. Neth Heart J. 2009 Dec; 17(12): 481-486.

39. Mason J. Endomyocardial biopsy—the balance of success and failure. Circulation 1985;71:185–8.

40. Ryan TJ, Antman EM, Brooks NH, et al. 1999 update: ACC/AHA guidelines for the management of patients with acute myocardial infarction: a report of the American College of Cardiology/American Heart Association Task Force on Practice Guidelines (Committee on Management of Acute Myocardial Infarction). J Am Coll Cardiol 1999;34(3):890–911.

41. Thygesen K, Alpert JS, White HD; Joint ESC/AC CF/AHA/WHF Task Force for the Redefinition of Myocardial Infarction. Universal definition of myocardial infarction. J Am Coll Cardiol 2007;50 (22):2173–2195.

42. Raijah P, Desay M, Kwon D, Flamm S. MR Imaging of Myocardial. Radiographics. 2013;33(5):1383–412.

43. Valente JM. The Current Role of Echocardiography in the Evaluation of Primary Cardiomyopathies. 1995;i.

44. Gunaratnam K, Wong LH, Nasis A, Ellims A, Nandurkar D, Soo G, et al. Review of cardiomyopathy imaging. Eur J Radiol [Internet]. Elsevier Ireland Ltd; 2013;82(10):176375.Available from:http://dx.doi.org/10.1016/j.ejrad.2013.05.041

45. Williams LK, Frenneaux MP, Steeds RP. Echocardiography in hypertrophic cardiomyopathy diagnosis, prognosis, and role in management. European

Journal of Echocardiography: The Journal of the Working Group on Echocardiography of the European Society of Cardiology 2009;10:iii9–14.

46. O'Donnell DH, Abbara S, Chaithiraphan V, et al. Cardiac MR imaging of nonischemic cardiomyopathies: imaging protocols and spectra of appearances. Radiology 2012;262:403–22.

47. Yoerger DM, Marcus F, Sherrill D, et al. Echocardiographic findings in patients meeting task force criteria for arrhythmogenic right ventricular dysplasia: new insights from the multidisciplinary study of right ventricular dysplasia. Journal of the American College of Cardiology 2005;45:860–5.

48. YamamuroM, Tadamura E, Kubo S, Toyoda H, Nishina T, OhbaMet al. Cardiac functional analysis with multi-detector rowCT and segmental reconstruction algorithm: comparison with echocardiography, SPECT, and MR imaging. Radiology 2005;234:381–90.

49. Taylor AJ, Cerqueira M, Hodgson JM, Mark D, Min J, O'Gara P et al. ACCF/SCCT/ ACR/AHA/ASE/ASNC/NASCI/SCAI/SCMR 2010 Appropriate Use Criteria for Cardiac Computed Tomography. Circulation 2010;122:e525–55.

50. Raney AR, Saremi F, Kenchaiah S, Gurudevan SV, Narula J, Narula N et al. Multidetector computed tomography shows intramyocardial fat deposition. J Cardiovasc Comput Tomogr 2008;2:152–63.

51. Gosling O, Morgan-Hughes G, Iyengar S, StrainW, Loader R, Shore A et al. Computed tomography to diagnose coronary artery disease: a reduction in radiation dose increases applicability. Clin Radiol 2013;68:340–5.

52. Neroladaki A, Botsikas D, Boudabbous S, Becker CD, Montet X. Computed tomography of the chest with model-based iterative reconstruction using a radiation exposure similar to chest X-ray examination: preliminary observations. Eur Radiol 2013;23:360–6.

53. YamamuroM, Tadamura E, Kubo S, Toyoda H, Nishina T, OhbaMet al. Cardiac functional analysis with multi-detector rowCT and segmental reconstruction algorithm: comparison with echocardiography, SPECT, and MR imaging. Radiology 2005;234: 381–90.

54. Burianova L, Riedlbauchova L, Lefflerova K, Marek T, Lupinek P, KautznerovaDet al. Assessment of left ventricular function in non-dilated and dilated hearts: comparison of contrast-enhanced 2-dimensional echocardiography with multi-detector rowCT angiography. Acta Cardiol 2009;64:787–94.

55. Williams TJ, Manghat NE, McKay-Ferguson A, Ring NJ, Morgan-Hughes GJ, Roobottom CA. Cardiomyopathy: appearances on ECG-gated 64-detector row computed tomography. Clin Radiol 2008;63:464–74.

56. Zenooz NA, Zahka KG, Siwik ES, Gilkeson RC. Noncompaction syndrome of the myocardium: pathophysiology and imaging pearls. J Thorac Imaging 2010;25:326–32.

57. Nicol ED, Gatzoulis M, Padley SPG, Rubens M. Assessment of adult congenital heart disease with multi-detector computed tomography—beyond coronary lumenography. Clin Radiol 2007;62:518–27.

58. Manghat NE, Morgan-Hughes GJ, Shaw SR, Broadley AJ, Gogola L, Marshall AJ et al. Multi-detector row CT coronary angiography in patients with cardiomyopathy—initial single-centre experience. Clin Radiol 2007;62:632–8.

59. Budoff MJ, Shavelle DM, Lamont DH, Kim HT, Akinwale P, Kennedy JM et al. Usefulness of electron beam computed tomography scanning for distinguishing ischemic from nonischemic cardiomyopathy. J Am Coll Cardiol 1998;32:1173–8.

60. Andreini D, Pontone G, Pepi M, Ballerini G, Bartorelli AL, Magini A et al. Diagnostic accuracy of multidetector computed tomography coronary angiography in patients with dilated cardiomyopathy. J Am Coll Cardiol 2007;49:2044–50.

61. Ghostine S, Caussin C, Habis M, Habib Y, Cle´ment C, Sigal-Cinqualbre A et al. Noninvasive diagnosis of ischaemic heart failure using 64-slice computed tomography. Eur Heart J 2008;29:2133–40.

62. Ghostine S, Caussin C, Habis M, Habib Y, Cle´ment C, Sigal-Cinqualbre A et al. Noninvasive diagnosis of ischaemic heart failure using 64-slice computed tomography. Eur Heart J 2008;29:2133–40.

63. Marcus FI, FontaineGH, Guiraudon G, Frank R, Laurenceau JL, MalergueCet al. Right ventricular dysplasia: a report of 24 adult cases. Circulation 1982;65:384–98.

64. Clayton B, Roobottom C, Morgan-Hughes G. Assessment of the myocardium with cardiac computed tomography. Eur Heart J Cardiovasc Imaging. 2014;15(6):603–9.

65. Boxt LM. Cardiac MR imaging: a guide for the beginner. RadioGraphics 1999; 19:1009–1025; discussion, 1026–1028

66. Martin ET, Coman JA, Shellock FG, Pulling CC, Fair R, Jenkins K. Magnetic resonance imaging and cardiac pacemaker safety at 1.5-Tesla. J Am Coll Cardiol 2004 7; 43:1315–1324

67. Kim HW, Klem I, Kim RJ. Detection of myocardial ischemia by stress perfusion cardiovascular magnetic resonance. Cardiol Clin 2007; 25:57–70, vi

68. Detsky JS, Graham JJ, Vijayaraghavan R, et al. Free-breathing, nongated real-time delayed enhancement MRI of myocardial infarcts: a comparison with conventional delayed enhancement. J Magn Reson Imaging 2008; 28:621–625

69. Ginat DT, Fong MW, Tuttle DJ, Hobbs SK, Vyas RC. Cardiac imaging: Part 1, MR pulse sequences, imaging planes, and basic anatomy. Am J Roentgenol. 2011;197(4):808–15.

70. Dabir D, Child N, Kalra A, Rogers T, Gebker R, Jabbour A, et al. Reference values for healthy human myocardium using a T1 mapping methodology: results from the International T1 Multicenter cardiovascular magnetic resonance study. J Cardiovasc Magn Reson. 2014;16(1):69.

71. Dass S, Suttie JJ, Piechnik SK, Ferreira VM, Holloway CJ, Banerjee R, et al. Myocardial tissue characterization using magnetic resonance noncontrast T1 mapping in hypertrophic and dilated cardiomyopathy. Circ Cardiovasc Imaging. 2012;5(6):726–33.

73. Puntmann VO, Voigt T, Chen Z, Mayr M, Karim R, Rhode K, et al. Native T1 mapping in differentiation of normal myocardium from diffuse disease in

hypertrophic and dilated cardiomyopathy. JACC Cardiovasc Imaging [Internet]. Elsevier Inc.; 2013;6(4):475–84. Available from: http://dx.doi.org/10.1016/j.jcmg.2012.08.019

74. Lurz P, Luecke C, Eitel I, Föhrenbach F, Frank C, Grothoff M, et al. Comprehensive Cardiac Magnetic Resonance Imaging in Patients with Suspected Myocarditis the MyoRacer-Trial. J Am Coll Cardiol. 2016;67(15):1800–11.

75. Luetkens JA, Doerner J, Thomas DK, Dabir D, Gieseke J, Sprinkart AM, et al. Acute Myocarditis: Multiparametric Cardiac MR Imaging. Radiology [Internet]. 2014;273(2):383–92. Available from:http://pubs.rsna.org/doi/10.1148/radiol.3540

76. Toussaint M, Gilles RJ, Azzabou N, Marty B, Vignaud A, Greiser A, et al. Characterization of benign myocarditis using quantitative delayed-enhancement imaging based on MOLLI T1 mapping. Med (United States). 2015;94(43):1–5.

77. van den Boomen M, Slart RHJA, Hulleman E V., Dierckx RAJO, Velthuis BK, van der Harst P, et al. Native T 1 reference values for nonischemic cardiomyopathies and populations with increased cardiovascular risk: A systematic review and meta-analysis. J Magn Reson Imaging [Internet]. 2017; Available from: http://doi.wiley.com/10.1002/jmri.25885

78. Dall'Armellina E, Ferreira VM, Kharbanda RK, Prendergast B, Piechnik SK, Robson MD, et al. Diagnostic value of pre-contrast T1 mapping in acute and chronic myocardial infarction. JACC Cardiovasc Imaging. 2013;6(6):739–42.

79. Von Knobelsdorff-Brenkenhoff F, Prothmann M, Dieringer MA, Wassmuth R, Greiser A, Schwenke C, et al. Myocardial T1 and T2 mapping at 3 T: Reference values, influencing factors and implications. J Cardiovasc Magn Reson. 2013;

80. Spieker M, Haberkorn S, Gastl M, Behm P, Katsianos S, Horn P, et al. Abnormal T2 mapping cardiovascular magnetic resonance correlates with adverse clinical outcome in patients with suspected acute myocarditis. J Cardiovasc Magn Reson. Journal of Cardiovascular Magnetic Resonance; 2017;19(1):1–9.

ABBREVIATIONS

ECM	-	Extracellular Matrix
CMR/CMRI	-	Cardiac magnetic resonance imaging
LGE	-	Late gadolinium enhancement
MRI	-	Magnetic resonance imaging
RCA	-	Right coronary artery
PDA	-	Posterior descending artery
LAD	-	Left anterior descending
HCM	-	Hypertrophic cardiomyopathy
LVOT	-	Left ventricular outflow tract
DCM	-	Dilated cardiomyopathy
RCM	-	Restrictive cardiomyopathy
MI	-	Myocardial infarction
NSTEMI	-	Non–ST-segment elevation myocardial infarction
ARVD	-	Arrhythmogenic right ventricular dysplasia
LV	-	Left ventricle
RV	-	Right ventricle
RVOT	-	Right ventricular outflow tract

CT	-	Computed tomography
CAD	-	Coronary artery disease
CCT	-	Cardiac Computed tomography
ARVC	-	Arrhythmogenic right ventricular cardiomyopathy
FSE	-	Fast spin-echo
GRE	-	Gradient-echo
SSFP	-	Steady-state free precession
EPI	-	Echo-planar imaging
SE	-	Spin-echo
TSE	-	Turbo spin-echo
SPGR	-	Spoiled gradient recall
FFE	-	Fast-field echo
IR	-	Inversion recovery
SENSE	-	Sensitivity- encoding
SMASH	-	Simultaneous acquisition of spatial harmonics
MIP	-	Maximum intensity projections
MOLLI	-	Modified Look Locker inversion recovery
TD	-	Trigger delay

ECV	-	Extracellular Volume
ROI	-	Region of interest
HASTE	-	Half Fourier single shot turbo spin echo
FISP	-	Fast imaging with steady state free precession
STIR	-	Short tau inversion recovery
PSIR	-	Phase sensitive inversion recovery

PATIENT PROFORMA

STUDY TITLE:

"MYOCARDIAL MAPPING IN EVALUATION OF MYOCARDIAL DISEASES AND ASSESSING NORMATIVE VALUES IN CONTROLS"

Sl. No:

Name:

Age/Sex:

Occupation:

Address:

Presenting Complaints and History:

ECG Findings:

ECHO Findings:

DATA COLLECTION PROFORMA:

HR, beats/min :

BP, mm Hg :

	BASE				MID-BODY						APEX			
	SEPTUM	ANTERIOR WALL	LATERAL WALL	INFERIOR WALL	SEPTUM	ANTERIOR WALL	LATERAL WALL	INFERIOR WALL	SEPTUM	ANTERIOR WALL	LATERAL WALL	INFERIOR WALL
NATIVE T1 (ms)												
NATIVE T2 (ms)												

PATIENT INFORMATION SHEET

"MYOCARDIAL MAPPING IN EVALUATION OF MYOCARDIAL DISEASES AND ASSESSING NORMATIVE VALUES IN CONTROLS''

- Your cooperation would be valuable to us for the same
- The privacy of patients in the research will be maintained throughout the study. In the event of any publication or presentation resulting from the research, no personally identifiable information will be shared.
- Taking part of the study is voluntary. You are free to decide whether to participate in this study or to withdraw at any time. Your decision will not result in any loss of benefits to which you are otherwise entitled.
- The result of the special study may be intimated to you at the end of the study period or during the study if anything is found abnormal which may aid in the management or treatment.

Signature of the investigator Signature of participant

Dr. VIMAL CHACKO MONDY

Date:

PATIENT CONSENT FORM

STUDY TITLE:

"MYOCARDIAL MAPPING IN EVALUATION OF MYOCARDIAL DISEASES AND ASSESSING NORMATIVE VALUES IN CONTROLS''

PARTICIPANT'S NAME:

AGE: SEX: IP.NO. :

I confirm that I have understood the purpose of procedure for the above study. I have the opportunity to ask the questions and all my questions and doubts have been answered to my satisfaction.

I have been explained about the pitfall in the procedure. I have been explained about the safety, advantage and disadvantage of the technique.

I understand that my participation in the study is voluntary and that I'm free to withdraw at any time without giving any reason.

I understand that investigator, regulatory authorities and the ethics committee will not need my permission to look at my health records both in respect to current study and any further research that may be conducted in relation to it, even if I withdraw from the study.

I understand that my identity will not be revealed in any information released to third parties or published, unless as required under the law. I agree not to restrict the use of any data or results that arise from the study.

I HEREBY CONSENT TO UNDERGO COMPLETE PHYSICAL EXAMINATION, BIOCHEMICAL AND RADIOLOGICAL INVESTIGATION PERTAINING TO THE STUDY.

Signature/Thumb Impression of Participant

ஆராய்ச்சிதகவல்தாள்

ஆராய்ச்சி தலைப்பு

காந்த அதிர்வு அலை வரைவின் (எம்.ஆர்.ஐ) பல்வேறு வரிசைகளைப் பயன்படுத்தி பெறப்படும் இருதய தசை நோய்களின் தன்மையை, பொது நிலை அளவு முடிவுகளுடன் ஒப்பிட்டு ஆய்வு செயதல்

தங்களுடைய பங்களிப்பும் ஒத்துழைப்பும் ஆராய்ச்சி நன்முறையில் வெற்றி பெற பெரிதும் உதவியாக அமையும்.

நீங்களும் இந்த ஆராய்ச்சியில் பங்கேற்க நாங்கள் விரும்புகிறோம்.
இந்த ஆராய்ச்சியில் உங்களுக்கு பரிசோதனைகள் செய்து அதன் தகவல்களை ஆராய்வோம் அதனால் தங்களது நோயின் ஆய்வறிக்கையோ அல்லது சிகிச்சையோ பாதிப்பு ஏற்படாது என்பதையும் தெரிவித்து கொள்கிறோம்.

முடிவுகளை அல்லது கருத்துகளை வெளியிடும்போதோ அல்லது ஆராய்ச்சியின் போதோ தங்களது பெயரையோ அல்லது அடையாளங்களையோ வெளியிட மாட்டோம் என்பதையும் தெரிவித்து கொள்கிறோம்.

இந்த ஆராய்ச்சியில் பங்கேற்பது தங்களுடைய விருப்பத்தின் பேரில் தான் இருக்கிறது. மேலும் நீங்கள் எந்நேரமும் இந்த ஆராய்ச்சியிலிருந்து பின்வாங்கலாம் என்பதையும் தெரிவித்து கொள்கிறோம்.

இந்த சிறப்பு பரிசோதனையின் முடிவுகளை ஆராய்ச்சியின்போது அல்லது ஆராய்ச்சியின் முடிவின் போது தங்களுக்கு அறிவிக்கப்படும் என்பதையும் தெரிவித்து கொள்கிறோம்.

ஆராய்ச்சியாளர் கையொப்பம் பங்கேற்பாளர் கையொப்பம்

நாள்:

இடம்:

ஆராய்ச்சி ஒப்புதல் கடிதம்

ஆராய்ச்சி தலைப்பு

காந்த அதிர்வு அலை வரைவின் (எம்.ஆர்.ஐ) பல்வேறு வரிசைகளைப் பயன்படுத்தி பெறப்படும் இருதய தசை நோய்களின் தன்மையை, பொது நிலை அளவு முடிவுகளுடன் ஒப்பிட்டு ஆய்வு செயதல்

பெயர்	:	தேதி	:
வயது	:	உள் நோயாளி எண்	:
பால்	:	ஆராய்ச்சி சேர்க்கை எண்	:

இந்த ஆராய்ச்சியின் விவரங்களும் அதன் நோக்கங்களும் முழுமையாக எனக்கு தெளிவாக விளக்கப்பட்டது.

எனக்கு விளக்கப்பட்ட விஷயங்களை நான் புரிந்துகொண்டு எனது சம்மதத்தை தெரிவிக்கிறேன்.

இந்த ஆராய்ச்சியில் பிறரின் நிர்பந்தமின்றி என் சொந்த விருப்பத்தின்பேரில் பங்கு பெறுகின்றேன். இந்த ஆராய்ச்சியில் இருந்து நான் எந்நேரமும் பின்வாங்கலாம் என்பதையும் அதனால் எந்த பாதிப்பும் ஏற்படாது என்பதையும் நான் புரிந்துகொண்டேன்.

நான் இந்த ஆராய்ச்சியின் விபரங்களைக் கொண்ட ஆராய்ச்சித் தகவல் தாளைப் பெற்றுக் கொண்டேன்.

இதன் மூலம் எந்த பின்விளைவும் ஏற்படாது என்று மருத்துவர் மூலம் தெரிந்து கொண்டு, நான் என்னுடைய சுய நினைவுடனும் மற்றும் முழு சுதந்திரத்துடனும் இந்த மருத்துவ ஆராய்ச்சியில் என்னை சேர்த்துக்கொள்ள சம்மதம் தெரிவிக்கிறேன்.

தேதி: **பங்கேற்பாளர் கையொப்பம்**

MASTER CHART

S. NO	NAME	AGE	SEX	DIAGNOSIS	T1				T2			
					ANTERIOR	SEPTUM	INFERIOR	LATERAL	ANTERIOR	SEPTUM	INFERIOR	LATERAL
1	DHAKSHANAMOORTHY	16	M	HCM	1319.8	1389	1265	1275.7	39	48.8	37.8	36.5
2	ANANDHI	34	F	Myocarditis	1423	1485	1416	1372	43.1	46.9	43.1	40.9
3	RAVIKUMAR	59	M	DCM	1289	1332	1321	1390	42.2	43	41.5	41
4	SATHISH	49	M	RCM	1430	1384	1361	1428	40.3	43.6	43.1	40.6
5	GOVINDARAJ	65	M	MI	1319	1141.5	1281	1192.5	41.6	31.7	44.3	38.6
6	DHANUSHKODI	54	F	DCM	1304	1409	1325.5	1326	32.9	44.9	40.9	38.4
7	SUKUMAR	39	M	RCM	1237	1230	1226	1243	39.4	41.8	45.2	43.1
8	BABU	36	M	ARVD	1251	1260	1257	1286	41.3	40.1	36.3	42.1
9	SHANKARI	44	F	NORMAL	1217	1177.2	1212.5	1230	41.4	38.5	33.2	42.1
10	SUMITHRA	45	F	NORMAL	1159	1180	1200	1134	40.6	38.2	36.8	41.1
11	KUMUDHA	48	F	HCM	1339	1300.5	1229.5	1281	39.3	38.8	34.7	42.5
12	VELU	49	M	MI	1339	1331	1237	1226	42.1	43.5	37.6	39.5
13	SELVI	48	F	RCM	1103	1343.5	1335	1258	30.1	39.4	28.2	29
14	SARADHA	55	F	DCM	1284	1290.7	1375.2	1432	42.7	45.8	45.4	42.9
15	KARTHIK	38	M	Myocarditis	1385	1472	1430	1417	41.5	42.6	43.1	43.5
16	SENTHIL MURUGAN	38	M	ARVD	1191	1247.5	1188.2	1329.7	39.3	35.9	34.5	45.7
17	SENGAMMAL	51	F	NORMAL	1124	1045	1110	1133	36.4	40.6	37.6	36.4
18	POONGAVANAM	43	F	ARVD	1320	1294	1345	1321	40.3	39.1	45.1	46.1
19	VIJAYA LAKSHMI	48	F	RCM	1242	1134	1158.6	1232.5	43.1	40.6	45.1	38.8
20	DEVI	45	F	DCM	1352	1387	1421	1365	36.5	48.1	40.6	43.2
21	NANDHINI	30	F	Myocarditis	1421	1458	1394	1427	43.1	40.9	42.7	45.1
22	VEERAMA	48	F	ARVD	1320	1310	1325	1334	41.6	38.4	40.5	41.8
23	KALLIDASS	55	M	NORMAL	1195.3	1171	1164	1176	39.1	41.3	38.2	41.4
24	MANI	41	M	HCM	1429	1432	1399	1457	47.2	46.1	42.7	48.9
25	PAVENDIRAN	25	M	NORMAL	1060.5	1143.5	1162	1066	40.6	38.4	32.8	43.6
26	SELVAKUMAR	38	M	HCM	1228	1284	1267	1301	45	41.6	46.2	44.3
27	AKBAR BASHA	52	M	MI	1212	1566.5	1176	1190	38.7	47	36.9	43.3
28	KANNIYAPPAN	45	M	ARVD	1349	1343	1361	1371	39.4	43.1	46.5	44.8
29	SIVA SHANKAR	46	M	MI	1323	1363	1216	1211.5	41.6	38.8	38.5	38.1
30	AISHWARYA	26	F	HCM	1321	1354	1253	1271	38.4	44.5	39.1	37.6
31	SELVARAJ	34	M	NORMAL	1150	1191	1041	1133	34.7	41	33.8	37.3
32	SEENUMATHIRI	55	M	RCM	1553	1467	1379	1483	36.6	39.8	42.2	38.2
33	KISHORE	55	M	RCM	1351	1362	1354	1448	35.3	40.6	40.4	39.5
34	PADMA	45	F	MI	1353	1466	1246	1230	42.8	42.5	38.6	37
35	BANU	38	F	HCM	1299	1325	1310	1294	41.9	41.6	38.5	41.1
36	THULASIRAMAN	26	M	NORMAL	1139	1158	1100.5	1181.5	39.9	35	34.1	35.4
37	SEKAR	57	M	MI	1459	1370	1473	1294	34.3	41.3	40.1	55.9
38	SUMATHI	33	F	Myocarditis	1410	1411	1413	1375	45.6	43.9	43.8	45.1
39	PUNITHA	22	F	HCM	1391	1410	1337	1386	43.6	46.1	45.1	45.3
40	SHAKIL AHAMED	55	M	NORMAL	1290	1255	1246	1171	34.9	33.8	32.9	34.2
41	PERIYADURAI	14	M	NORMAL	1271	1262	1234	1230	37.2	39.4	38.3	39.3
42	MUNIYAN	46	M	MI	1342	1362	1350	1283	38.1	35.2	36.1	33.2
43	MALLIGA	55	F	NORMAL	1070	1065	1126	1034	38.7	41	37.4	41.4
44	MOHAMMED SUHAI	19	M	DCM	1339	1367	1344	1377	40.7	40.5	41.55	39.9
45	NANDHAKUMAR	40	M	ARVD	1377	1301	1491	1392	37.4	41.6	50.2	55.7
46	THANUJA	9	F	HCM	1448	1437	1412	1492	49.6	47.2	44.2	53.2
47	KARPAGAM	40	F	DCM	1318	1340	1354	1369	41.2	42.1	43.5	41.6
48	MURUGAN	51	M	NORMAL	1149	1173	1206	1183	35.4	36.8	38.1	34.6
49	PAVENDHAN	17	M	DCM	1168	1237	1308	1186	33.9	35.6	32.3	38.8
50	SHELLA	30	F	MI	1277	1288	1249	1324	37.1	36.5	38.1	35.5
51	SANTHOSH KUMAR	24	M	NORMAL	1230.5	1221.67	1238	1261	34.9	38.9	39	42.9
52	SASIKALA	40	F	Myocarditis	1372	1424	1398	1336	45.9	45.1	43.4	45.3

ETHICS COMMITTEE APPROVAL LETTER

INSTITUTIONAL ETHICS COMMITTEE
MADRAS MEDICAL COLLEGE, CHENNAI 600 003

EC Reg.No.ECR/270/Inst./TN/2013
Telephone No.044 25305301
Fax: 011 25363970

CERTIFICATE OF APPROVAL

To

Dr.Vimal Chacko Mondy
PG in MD RD
Barnard Institute of Radiology
Madras Medical College
Chennai 600 003

Dear Dr.Vimal Chacko Mondy,

The Institutional Ethics Committee has considered your request and approved your study titled **"MYOCARDIAL MAPPING IN EVALUATION OF MYOCARDIAL DISEASES AND ASSESSING NORMATIVE VALUES IN CONTROLS" - NO.14042017**

The following members of Ethics Committee were present in the meeting hold on **04.04.2017** conducted at Madras Medical College, Chennai 3

1.Prof.Dr.C.Rajendran, MD.,	:Chairperson
2.Prof.K.Narayanasamy, MD.,DM.,Dean(FAC), MMC,Ch-3	:Deputy Chairperson
3.Prof.Sudha Seshayyan,MD., Vice Principal,MMC,Ch-3	:Member Secretary
4.Prof.B.Vasanthi,MD., Prof.of Pharmacology.,MMC,Ch-3	: Member
5.Prof.K.Ramadevi,MD., Director, Inst. of Bio-Chemistry,MMC,Ch-3	: Member
6.Prof.S.Mayilvahanan,MD,Director,Inst. of Int.Med,MMC, Ch-3	: Member
7.Tmt.J.Rajalakshmi, JAO,MMC, Ch-3	: Lay Person
8.Thiru S.Govindasamy, BA.,BL,High Court,Chennai	: Lawyer
9.Tmt.Arnold Saulina, MA.,MSW.,	:Social Scientist

We approve the proposal to be conducted in its presented form.

The Institutional Ethics Committee expects to be informed about the progress of the study and SAE occurring in the course of the study, any changes in the protocol and patients information/informed consent and asks to be provided a copy of the final report.

Member Secretary – Ethics Committee

MEMBER SECRETARY
INSTITUTIONAL ETHICS COMMITTEE
MADRAS MEDICAL COLLEGE
CHENNAI-600 003

PLAGIARISM ANALYSIS REPORT

URKUND

Urkund Analysis Result

Analysed Document:	COMPILED FOR PLAGIARISM.docx (D42281240)
Submitted:	10/8/2018 4:34:00 PM
Submitted By:	vimalchackomdy@yahoo.com
Significance:	1 %

Sources included in the report:

https://en.wikipedia.org/wiki/Cardiomyopathy

Instances where selected sources appear:

2

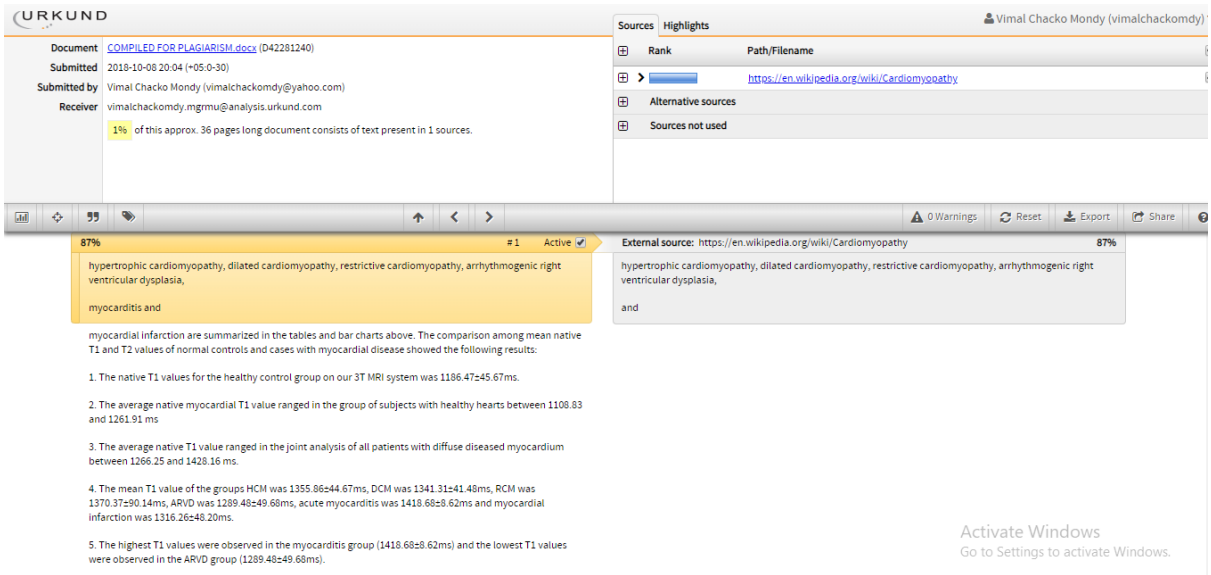

PLAGIARISM CERTIFICATE

This is to certify that this dissertation work titled **"MYOCARDIAL MAPPING IN EVALUATION OF MYOCARDIAL DISEASES AND ASSESSING NORMATIVE VALUES IN CONTROLS"** of the candidate **Dr. VIMAL CHACKO MONDY,** with registration Number **201618005** for the award of **M.D RADIODIAGNOSIS** in the branch of **VIII**. I personally verified the urkund.com website for the purpose of plagiarism check. I found that the uploaded thesis file contains from introduction to conclusion pages and result shows **0 percentage** of plagiarism in the dissertation.

Guide & Supervisor sign with Seal